

UNITED STATES NAVAL POSTGRADUATE SCHOOL



AN ANALYSIS OF A SEVERE LOCAL STORM USING ISENTROPIC TRAJECTORIES

by

Ronnie L. Alberty

and

Kenneth Lee Van Sickle

15 August 1969

This document has been approved for public release
sale; its distribution is unlimited

NAVAL POSTGRADUATE SCHOOL
Monterey, California

Rear Admiral R. W. McNitt, USN
Superintendent

R. F. Rinehart
Academic Dean

ABSTRACT:

One and one-half hour isentropic trajectories obtained from an objective computer technique for the 308K, 312K, 320K and 332K isentropic surfaces are investigated for the May 28, 1967, severe local storm case in the National Severe Storm Laboratory (NSSL) network. In conjunction with the trajectories, air parcel properties of vertical motion, acceleration, divergence, vorticity, static stability and total energy have been studied with respect to development, growth, movement and decay of the storm system. Basic assumptions are that the flow is frictionless and adiabatic over the entire grid. The results show that the observed winds do provide some skill in formulating isentropic trajectories which demonstrate the presence of storm activity in the specific region. The investigation of a mesoscale inertial-gravity wave having a wave length of 150 KM, period of 3 hours and phase speed of 14 m sec^{-1} is also presented, with its possible correlation to the onset of the severe storm.

This task was supported by: Naval Weapons Center
China Lake, California, Code 602



This report covers one aspect of the research conducted under contract to the Naval Weapons Center, China Lake, California. It is, with a few exceptions, as authored by Lieutenant Kenneth L. Van Sickle, USN. While this report is a final report, it does not indicate that studies have been completed. Other investigations are currently in progress and will be reported as warranted.

AN ANALYSIS OF A SEVERE LOCAL STORM
USING ISENTROPIC TRAJECTORIES

Kenneth Lee Van Sickle
Lieutenant, United States Navy

ABSTRACT

One and one-half hour isentropic trajectories obtained from an objective computer technique for the 308K, 312K, 320K and 332K isentropic surfaces are investigated for the May 28, 1967 severe local storm case in the National Severe Storms Laboratory (NSSL) network. In conjunction with the trajectories, air parcel properties of vertical motion, acceleration, divergence, vorticity, static stability and total energy have been studied with respect to development, growth, movement and decay of the storm system. Basic assumptions are that the flow is frictionless and adiabatic over the entire grid. The results show that the observed winds do provide some skill in formulating isentropic trajectories which demonstrate the presence of storm activity in the specific region. The investigation of a mesoscale inertial-gravity wave having a wave length of 150 KM, period of 3 hours and phase speed of 14 m sec^{-1} is also presented, with its possible correlation to the onset of the severe storm.

TABLE OF CONTENTS

	Page
Abstract	2
List of Tables	5
Acknowledgement	8
1. INTRODUCTION	9
A. Severe Storm Research	9
B. Isentropic Analysis and Trajectory Studies	11
2. OBJECTIVE ISENTROPIC TRAJECTORY COMPUTER MODEL	13
A. Basic Design	13
B. Modifications for Severe Storm Research	15
3. DATA AND STORM CHARACTERISTICS	17
A. Brief Synoptic Analysis	17
B. Storm Characteristics	19
4. DISCUSSION OF RESULTS	21
A. Severe Storm Relationships to Basic Data Analyses	21
B. Trajectory Relationships to the Severe Storm	28
C. Relationship of Associated Parameters to the Severe Storm	30
D. Inertial-gravity Wave Association to the Severe Storm	45
5. PROBLEMS ENCOUNTERED	65
6. COMPARISON WITH THEORY	76
7. CONCLUSIONS	80
8. SUGGESTIONS FOR FUTURE DEVELOPMENTS AND IMPROVEMENTS	81
References	82

APPENDIX A - Isentropic Kinematic Trajectories

85

B - Isentropic Trajectory Computer Program

101

LIST OF TABLES

Table 1 - Comparison of Predicted and Measured Changes in
Montgomery Stream Function.

Table 2 - Comparison of Composite Trajectory Properties.

LIST OF ILLUSTRATIONS

- Figure 1 - NSSL Upper Air Network Stations and Grid System.
- Figure 2a - 320K Theta Surface, 2000 GMT Montgomery Stream Function Analysis.
- Figure 2b - 320K Theta Surface, 2000 GMT Pressure Analysis.
- Figure 2c - 320K Theta Surface, 2000 GMT Relative Humidity Analysis.
- Figure 2d - 320K Theta Surface, 2000 GMT Wind Speed Analysis.
- Figure 2e - 320K Theta Surface, 2000 GMT Wind Direction Analysis.
- Figure 3a - 308K Theta Surface, 1830-2000 GMT Vertical Motions.
- Figure 3b - 312K Theta Surface, 1830-2000 GMT Vertical Motions.
- Figure 3c - 320K Theta Surface, 1830-2000 GMT Vertical Motions.
- Figure 3d - 332K Theta Surface, 1830-2000 GMT Vertical Motions.
- Figure 4a - 320K Theta Surface, 2000 GMT Horizontal Convergence.
- Figure 4b - 320K Theta Surface, 2130 GMT Horizontal Convergence.
- Figure 5 - 2000 GMT Total Energy Index.
- Figure 6 - 320K Theta Surface, 2000 & 2130 GMT Total Energy.
- Figure 7 - 320K Theta Surface, 2000 GMT Specific Humidity.
- Figure 8 - 2145 GMT Simplified Streamline and Isotach Pattern.
- Figure 9 - 320K Theta Surface, 1830-2000 GMT Kinematic Trajectories Relative to the Storm.
- Figure 10 - 320K Theta Surface, 1830-2000 GMT Accelerations.
- Figure 11 - 320K Theta Surface Composite Trajectories (1700-2300).
- Figure 12 - 2045 GMT Storm Position.
- Figure 13 - 2030-2130 GMT Surface Microbarograph Traces.
- Figure 14 - Mesoscale Pressure Tendency.
- Figure 15 - Time Section Station Distribution.

Figure 16a - Time Section, Station LTS.

Figure 16b - Time Section, Station FSI.

Figure 16c - Time Section, Station CHK.

Figure 16d - Time Section, Station TIK.

Figure 17a - Time Section, Station LTS.

Figure 17b - Time Section, Station FSI.

Figure 17c - Time Section, Station CHK.

Figure 17D - Time Section, Station TIK.

Figure 18 - 332K Theta Surface Air Parcel Conditions.

Figure 19 - 332K Theta Surface Adjusted Montgomery Stream Function Field.

Figure 20a - 320K Theta Surface, 2000 GMT Montgomery Stream Function Re-analysis.

Figure 20b - 320K Theta Surface, 2000 GMT Pressure Re-analysis.

Figure 20c - 320K Theta Surface, 2000 GMT Relative Humidity Re-analysis.

Figure 20d - 320K Theta Surface, 2000 GMT Wind Speed Re-analysis.

Figure 20e - 320K Theta Surface, 2000 GMT Wind Direction Re-analysis.

Figure 21 - 320K Theta Surface, 2000-2130 GMT Re-analysis Comparison.

Figure 22 - 320K Theta Surface, 2000 GMT Montgomery Stream Function Adjustment.

ACKNOWLEDGEMENT

The author wishes to express his deepest gratitude to Dr. R. L. Alberty for the initial stimulation for this research and the many hours of personal concern, guidance and discussions in both this study and the course of instruction at the U. S. Naval Postgraduate School. Additionally, the same gratitude goes to Dr. J. D. Mahlman for the initial idea to investigate the severe local storm through isentropic trajectories, for use of his isentropic trajectory program, for suggestions concerning the investigation of the mesoscale wave, and the most considerate interest in sharing advice and thoughts with which to build the case study. Having both professors with such willingness to teach enabled the author to have many pleasurable hours of work on this project and an invaluable supplement to his education.

Thanks also go to the Meteorology Department staff for their assistance rendered in this project.

1. INTRODUCTION

The severe local storm is an extremely complex meteorological phenomenon which can lend itself to interesting and challenging research. The approaches one can take for extensive studies are almost unlimited as evidenced by the wealth of literature on various aspects of the severe storm. Yet there are many questions on the formation, movement, growth and decay of these systems which remain unanswered. Similar synoptic conditions may seem to exist during two separate time periods, and yet storms may be forecasted to develop and then not form, or vice-versa. In particular, the extent to which an individual storm may evolve is not reasonably understood or predictable.

A. SEVERE STORM RESEARCH

In 1947 a comprehensive study was undertaken in the Thunderstorm Project which was perhaps the beginning of extensive scientific efforts into the study of severe local storms. From this project Byers and Braham (1949) provided new concepts on the structural features of such storms. The National Severe Storms Project, initiated in 1961, was an effort designed to study Great Plains convective storms and the environment in which they form. More recently the Barbadoes Experiment, which has provided data for study of tropical cumulus convection, and Project Storm Fury, for the study of hurricanes, have enabled investigators to carry on detailed research into severe storm characteristics.

Mesoscale networks located in various regions, with instrumentation positioned at specified spacing, have provided for collection

of data for certain research objectives.' In particular, the National Severe Storms Laboratory (NSSL), Norman, Oklahoma, has a systematic network of surface and upper air reporting stations and radar facilities.

There have been several studies involving kinematic properties which have given insights into storm characteristics. Williams (1962) investigated small-scale kinematic properties of surface horizontal velocity divergence, horizontal stretching deformation, and the vertical component of horizontal shearing deformation for isolated thunderstorms. He found the intensity and rate of change of these properties for small scale systems were 2 to 3 orders of magnitude greater than those normally measured on the gross synoptic scale. Endlich and Mancuso (1968) investigated a number of kinematic quantities using objective analysis procedures and compared them with storm developments. They found vorticity production in low levels and horizontal divergence in the upper troposphere to be good objective indicators of severe storm activity. Fankhauser (1964) used a statistical and observational approach to propose that the translation of convective complexes is related in a systematic way to the mean wind through the tropospheric layer in which the clouds are imbedded, and that this relationship is dependent on the unique character of the mean wind field. Hammond (1967) investigated an isolated airmass storm, which moved rapidly northeastward across central Oklahoma where its movement was to the left of all winds in the middle and upper troposphere. He concluded that the same environmental wind field can account for the characteristic organization and structure of either right or left moving storms,

depending on storm velocity. Studies by Browning and Fujita (1965), Newton and Fankhauser (1964) and Browning and Ludlum (1962) have shown that large thunderstorms normally travel to the right of the winds in the lower and middle level of the troposphere. Matsumoto, Ninomiya and Akiyama (1967) studied the relations of cumulus convections and the mesoscale convergence field over the coastal area of Japan and found that well developed cumuli exist only in the area of surface convergence of more than 10^{-4} sec^{-1} .

B. ISENTROPIC ANALYSIS AND TRAJECTORY STUDIES

The use of isentropic analysis to study the physical processes at work in the atmosphere is well known since Rossby (1937) introduced the technique. The analysis and its uses are well described by Namias (1940). Tongues of dry and moist air from specific humidity analysis on isentropic surfaces show moisture sources and instability regions for thunderstorm activity.

Calculations of isentropic trajectories for the study of moisture sources, vertical motions, velocity accelerations, type of air and circulations within systems, vorticity sources, and for investigations of transports of pollutants and trace substances has long been appealing since non-precipitating motions in the free atmosphere may be assumed to be isentropic for limited periods of time. Many investigators have used graphical calculations from isotach and streamline analysis to determine the trajectories (Danielsen, 1959; Reiter and Danielsen, 1960; Reiter, 1963). The use of isentropic trajectories in thunderstorm studies (Bradley and Feteris, 1966; Feteris and Stout, 1966; Carlson and Ludlum, 1968) can provide useful information in the study of these mesoscale systems.

It is intended in this research to investigate, by the use of isentropic trajectories, meteorological properties of air parcels and their relationship to severe local storms. Several questions will be considered:

1. Do isentropic trajectories over a short period of time describe flow patterns which adequately show the formation, growth, movement, and decay of the severe storm?

2. Do associated parameters computed along isentropic trajectories describe motions directly related to the dynamics of the severe storm?

3. Does a combination of any computed parameters correlate well with the storm?

4. Is there an oscillation or wave phenomenon, in particular a gravity-inertial wave, that can be detected from the data and/or computed parameters which might relate to the local severe storm?

It is intended to deal with these specific questions in the ensuing sections by conducting a case study of a specific severe storm system. The isentropic trajectories will be computed from an objective computer technique in order that a sufficient number of trajectories and isentropic surfaces can be studied for the severe storm case.

2. OBJECTIVE ISENTROPIC TRAJECTORY COMPUTER MODEL

Danielsen (1961) introduced an objective method for computing isentropic trajectories based on the total energy equation. This provided the foundation for the technique for which Mahlman (1968) developed a computer method for an objective computation of adiabatic three-dimensional trajectories.

A. BASIC DESIGN

Utilizing the graphical method by Danielsen (1961), the computer program applies an objective method which confines the computed trajectory from deviating too far laterally from its true position. The concept of the system emanates from the horizontal equation of motion in isentropic coordinates, which is

$$\frac{d\mathbf{W}}{dt} = -f \mathbf{k} \times \mathbf{W} - \nabla_{\theta} M + \mathbf{F} \quad (1)$$

where \mathbf{W} is the two dimensional horizontal wind vector, f the Coriolis parameter, \mathbf{k} the unit vector in the vertical, ∇_{θ} the two dimensional gradient operator on a surface of constant potential temperature θ , M the Montgomery stream function, and \mathbf{F} the friction force.

The basic model utilizes variables of true wind direction, wind speed, pressure and Montgomery stream function at each point in a four-dimensional (x, y, θ, t) grid. The first step in the program is to obtain u and v components of the velocity field, with the effects of latitude/longitude type gridding included in the calculations over the data area. Then, the u and v fields are linearly interpolated to give values at twelve time step intervals.

The first approximation of the trajectory is using a straightforward kinematic approach. Beginning at a grid point, a parcel is displaced for one time step using the initial values of u and v to determine the length and direction of the displacement. This displacement is determined by:

$$S = \bar{W}\Delta t \quad (2)$$

where S is the displacement and \bar{W} is the average wind velocity along the trajectory over a Δt interval. Then the time interpolated u and v values are spatially interpolated from the four nearest grid points to the parcel to obtain new u and v wind components at the parcel's new position. These new values are then used to extrapolate the parcel for the next time step. This process is repeated until twelve time steps are reached. At each point along the trajectory a test is made to determine if the trajectory remains within the original grid. If not, then the trajectory is terminated at the point where it leaves the field and a new trajectory is begun at the next grid point. These isentropic kinematic trajectories can provide a valid result as long as the original wind fields have been adequately specified, and the time interpolations are satisfactory.

It is important to note that for inclusion of changes in the Montgomery stream function, Mahlman (1968) indicated that the corrections were sensitive to analysis errors in the M field, rapid changes of wind direction perpendicular to the estimated trajectory path, and for cases where the wind speed is less than 10 m sec^{-1} . Since preliminary studies of the data indicated cases where the wind flow was perpendicular to isolines of Montgomery stream function and wind speeds less than 10 m sec^{-1} , the subsequent research was thus

conducted from the isentropic kinematic trajectories. The incorporation of adjustments for changes in Montgomery stream function is a separate subroutine in the program so, if only kinematic trajectories are desired, the subroutine can be left out. The programming is included in Appendix B.

B. MODIFICATIONS FOR SEVERE STORM RESEARCH

An additional field of relative humidity was added in order to include a moisture constituent. Routines to compute certain meteorological parameters were incorporated so that initial conditions and variations along the kinematic isentropic trajectories could be studied. These routines include calculations of:

$$\zeta_{\theta} = \left(\frac{\partial v}{\partial x} - \frac{\partial u}{\partial y} \right)_{\theta} + f \quad (3)$$

$$D_{\theta} = \left(\frac{\partial u}{\partial x} + \frac{\partial v}{\partial y} \right)_{\theta} \quad (4)$$

$$A_{\theta} = \left(\frac{\partial u}{\partial x} - \frac{\partial v}{\partial y} \right)_{\theta} \quad (5)$$

$$B_{\theta} = \left(\frac{\partial v}{\partial x} + \frac{\partial u}{\partial y} \right)_{\theta} \quad (6)$$

$$\sigma = - \frac{\partial \theta}{\partial p} \quad (7)$$

where ζ_{θ} is the absolute vorticity, D_{θ} the horizontal divergence, A_{θ} the stretching deformation, B_{θ} the shearing deformation, and σ the static stability. Also the height (z), specific humidity (q), saturated specific humidity (q_s) and temperature (T) fields for each isentropic surface and data time were determined. Along each kinematic trajectory the initial and final values of specific humidity, saturated specific humidity, divergence, absolute vorticity, Montgomery stream function, kinetic energy, total energy, static stability, and

potential vorticity were computed. Total energy, in units of 10^7 ergs gm^{-1} , was defined as:

$$\text{TE} = C_p T + gZ + Lq + \frac{v^2}{2} \quad (8)$$

where C_p is the specific heat at constant pressure and L the latent heat. Potential vorticity was computed as:

$$\mathcal{P} = \sigma \zeta_\theta \quad (9)$$

where \mathcal{P} is in units of $10^{-10} \text{K sec cm gm}^{-1}$.

The latitude and longitude positions, u and v components, and interpolated height at each of the twelve time steps of the trajectory were obtained. The average vertical motion ($\bar{\omega}$) along the trajectory was calculated using the procedure:

$$\bar{\omega} = \frac{P_f - P_i}{\Delta t} \quad (10)$$

with $\bar{\omega}$ in mb hr^{-1} and where the i and f refer to initial and final pressure over the interval Δt . The acceleration of the parcel over the trajectory was also calculated. Finally, the pressure at which the air parcel would become saturated (P_s) and the time of saturation (t_s) were determined by:

$$P_s = P_i \left[1.0 + \left(\frac{q_i - q_{si}}{q_{si}} \right) \left(\frac{L}{C_p T} - 1 \right)^{-1} \right] \quad (11)$$

$$t_s = \frac{P_s - P_i}{P_f - P_i} \Delta t \quad (12)$$

where the i and f refer to initial and final points on the trajectory and P , q and q_s are as previously defined.

A routine to utilize the CALCOMP plotter with the IBM OS/360 computer was included in order to graphically display the computed trajectories on a x, y grid system. The data generated by the program was displayed such that subsequent studies could be made.

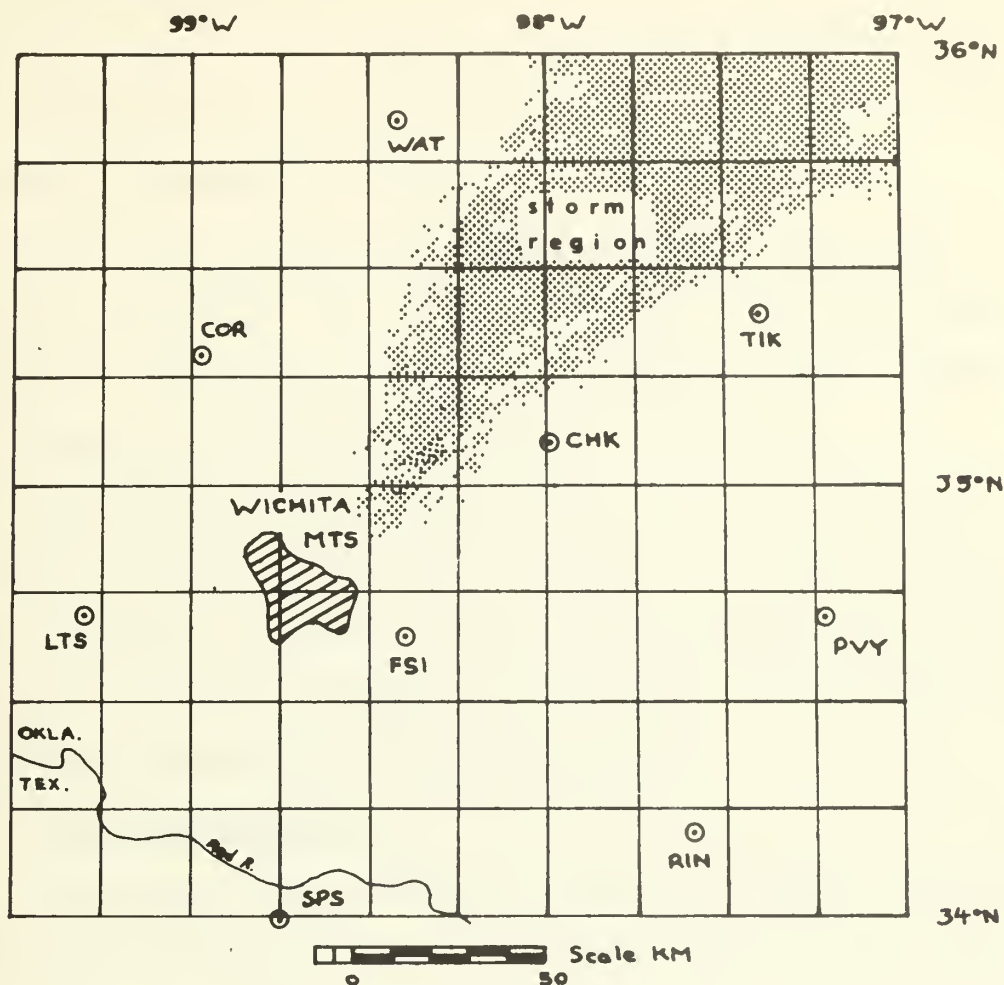
3. DATA AND STORM CHARACTERISTICS

Data that was considered in the case study are from observations in the NSSL mesoscale network on May 28, 1967. Upper air data from nine radiosonde stations systematically spaced over the network region (Fig. 1) provided data at 1700, 1830, 2000, 2130 and 2300 GMT.

Utilizing computer processing of mesoscale rawinsonde data (Kreitzberg and Brockman, 1961), fields of Montgomery stream function (10^7 erg gm^{-1}), wind direction (deg from north), wind speed (m sec^{-1}), pressure (mb) and relative humidity (%) from the isentropic plane section were hand analyzed over the network area. Allowances for balloon drift and non-simultaneous releases were not taken into account. However, a comparison was made between the original analysis and a re-analysis taking into account balloon drift and storm location. These results are reported on in later sections. A 9×11 latitude-longitude grid (Fig. 1), with grid separation of .25 degrees, was established (southeastern boundary -34°N , 97°W). Analyzed data were then interpolated to the nearest grid point. Theta surfaces 308K, 312K, 320K and 332K were those selected for the analysis levels. The 308K theta surface was the lowest level for which data were available at most stations over the time periods. The 332K theta surface was selected as being representative of the upper level of storm influence. This surface was located at a height of about 300 mb.

A. BRIEF SYNOPTIC ANALYSIS

The surface synoptic situation over Oklahoma at 1800 GMT on May 28, 1967 indicated a weak high pressure (1018 mb) over the Oklahoma Panhandle, with low pressure areas located over NW Missouri



CHK - Chickasha, Oklahoma
 COR - Cordell, Oklahoma
 FSI - Ft. Sill, Oklahoma
 LTS - Altus, Oklahoma
 PVY - Pauls Valley, Oklahoma
 RIN - Ringling, Oklahoma
 SPS - Sheppard AFB, Texas
 TIK - Tinker AFB, Oklahoma
 WAT - Watonga, Oklahoma

Figure 1, NSSL upper air network and latitude-longitude grid system, Stippled area represents storm region,

(1010 mb) and in central New Mexico (1005 mb). A weak cold front lay between the two low areas, passing through central Oklahoma. The front remained nearly stationary during the period under consideration, but began to dissipate and become a warm front by 2400 GMT.

The 1800 and 2400 GMT 500 mb height synoptic analyses showed straight southwesterly flow of about 15 kt. The 300 mb height chart indicated westerly flow of 20-30 kt at 1200 GMT with winds shifting to southwesterly and increasing slightly by 2400 GMT.

As reported by Fankhauser (1968), the characteristics were only marginally conducive to thunderstorm formation, with slightly negative stability indexes on morning soundings. The stationary front provided sufficient low-level convergence to set off weak convective storms over the northwest portion of the network by midday.

B. STORM CHARACTERISTICS

The initial radar presentation available for study was at 1817 GMT. Small echoes were present in the western grid area about 30-50 nautical miles from station TIK at this time. Larger and more intense echoes were present by 2000 GMT. Storm tops to the northwest of station TIK exceeded 11 KM in height, and the storm system was oriented SW-NE across the grid area. The 2100 GMT radar reflection indicated the system to the west of station TIK had decreased in intensity and size, with tops reaching to about 9 KM.

Storm motions used for calculating the relative trajectories were obtained from viewing surface radar presentations of similar echoes. These velocities were determined as:

<u>TIME DIFFERENTIAL</u>	<u>COURSE (deg from)</u>	<u>SPEED (m sec⁻¹)</u>
1700-1830 GMT	---	0.0 (no echo)
1830-2000	268	1.5
2000-2130	274	2.1
2130-2300	272	4.1

Fankhauser (1968) indicated that echo velocity was 247 (deg from) at a speed of 8 m sec⁻¹. Also this course and speed were remarkably constant throughout the lifetime of the storm. The mean wind direction through the atmospheric layer for the 1700-2300 GMT period was 247 (deg from) and had a mean wind speed of 8 m sec⁻¹.

4. DISCUSSION OF RESULTS

A. SEVERE STORM RELATIONSHIPS TO BASIC DATA ANALYSES

There were five basic fields which were analyzed on the isentropic surfaces in the mesoscale network. No objective smoothing was performed on these fields. Part of the research was to investigate these basic fields and to determine if they provide an indication of storm development, growth, movement and decay.

The mesoscale analysis over the NSSL network disclosed that a region of lower Montgomery stream function values was maintained near the middle of the grid area and to the southwest of the storm region. This prevailing pattern was consistent on each theta surface. Values were generally larger at the initial data time of 1700 GMT and then decreased in value over the entire grid as time progressed. However, the predominant contour pattern remained the same (values on the 308K theta surface at 1700 GMT ranged from 310.40 joules gm^{-1} to 310.62; at 2130 GMT values ranged from 310.17 to 310.45). The horizontal gradient ($\nabla_{\theta} M$) was stronger to the SE of the storm area. A stronger gradient existed at 2300 GMT on the theta surfaces than for previous times. It was noted that the thunderstorm had almost dissipated by this time. A dome of colder temperatures was associated with the low stream function values. This low M value and strong gradient region could be associated with the stationary front which existed over central Oklahoma and would indicate the thunderstorm was occurring northwest of the front. Figure 2a is an example of the Montgomery stream function pattern.

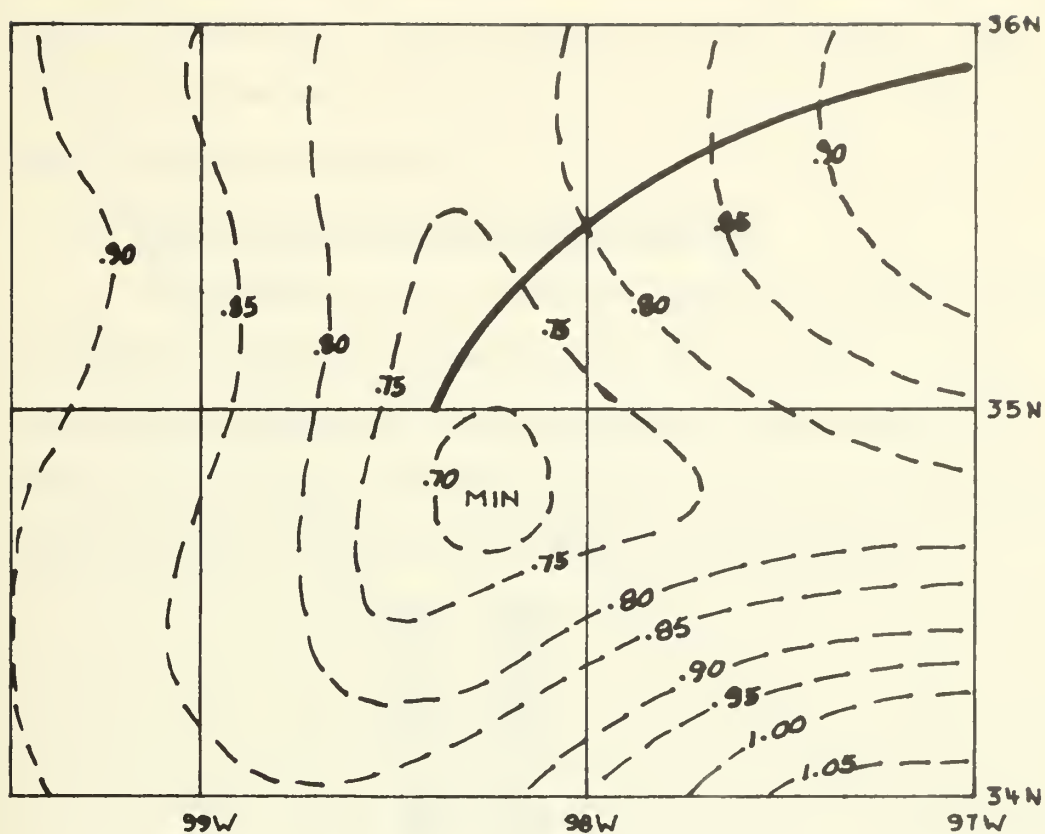


Figure 2a, 320K Theta surface, 2000 GMT Montgomery stream function analysis (add 320,00 to each value), Heavy solid line represents region of storm activity, Values in joules gm^{-1} ,

conducted from the isentropic kinematic trajectories. The incorporation of adjustments for changes in Montgomery stream function is a separate subroutine in the program so, if only kinematic trajectories are desired, the subroutine can be left out. The programming is included in Appendix B.

B. MODIFICATIONS FOR SEVERE STORM RESEARCH

An additional field of relative humidity was added in order to include a moisture constituent. Routines to compute certain meteorological parameters were incorporated so that initial conditions and variations along the kinematic isentropic trajectories could be studied. These routines include calculations of:

$$\zeta_{\theta} = \left(\frac{\partial v}{\partial x} - \frac{\partial u}{\partial y} \right)_{\theta} + f \quad (3)$$

$$D_{\theta} = \left(\frac{\partial u}{\partial x} + \frac{\partial v}{\partial y} \right)_{\theta} \quad (4)$$

$$A_{\theta} = \left(\frac{\partial u}{\partial x} - \frac{\partial v}{\partial y} \right)_{\theta} \quad (5)$$

$$B_{\theta} = \left(\frac{\partial v}{\partial x} + \frac{\partial u}{\partial y} \right)_{\theta} \quad (6)$$

$$\sigma = - \frac{\partial \theta}{\partial p} \quad (7)$$

where ζ_{θ} is the absolute vorticity, D_{θ} the horizontal divergence, A_{θ} the stretching deformation, B_{θ} the shearing deformation, and σ the static stability. Also the height (z), specific humidity (q), saturated specific humidity (q_s) and temperature (T) fields for each isentropic surface and data time were determined. Along each kinematic trajectory the initial and final values of specific humidity, saturated specific humidity, divergence, absolute vorticity, Montgomery stream function, kinetic energy, total energy, static stability, and

Pressure analyses on each theta surface exhibited sporadic patterns. There was no real evidence of vertical consistency with regions of high or low pressure, and no time dependency as to movement or preservation of any defined center. There were large pressure ranges in the grid area on the 308K and 312K theta surfaces at 2130 and 2300 GMT (748-865 mb for 308K and 649-753 mb for 312K). These pressure ranges were a result of the decrease in height of the 308K and 312K surfaces in the SW corner of the grid at 2130 GMT and extending into the center of the grid by 2300 GMT. Pressure analyses on the 320K theta surface shows that a strong gradient existed to the SE of the storm. An example of the pressure pattern is given in Figure 2b.

An analysis of relative humidity revealed a region in the S-SE area of the network which was a minimum value area on all theta surfaces at all times (Fig. 2c). Since the storm activity occurred between upper air network stations, there was no clear indication of a region of high relative humidity. A moist or dry tongue was not evident from the relative humidity analyses.

There was a region of higher wind speed in the NW corner of the grid area and lower wind speeds in the SE corner (Fig. 2d) on all theta surfaces. This wind maximum propagated toward the east with time and increased in intensity until 2300 GMT when the speed began to decrease.

Wind direction was generally anticyclonic in the SE area and cyclonic in the NW region with a shear line along the thunderstorm activity (Fig. 2e). Time sections at stations LTS, FSI, CHK and TIK, along with the theta surface analyses of wind direction, indicated

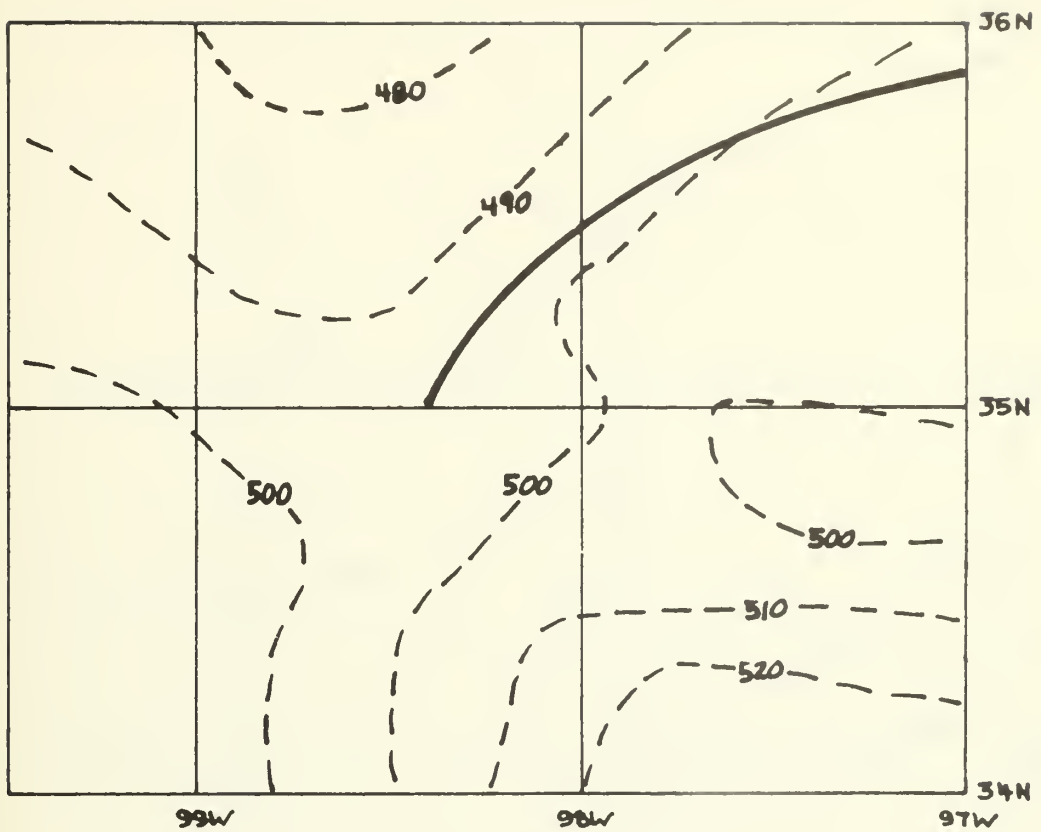


Figure 2b, 320K Theta surface, 2000 GMT pressure (mb) analysis,
Heavy solid line represents region of storm activity,

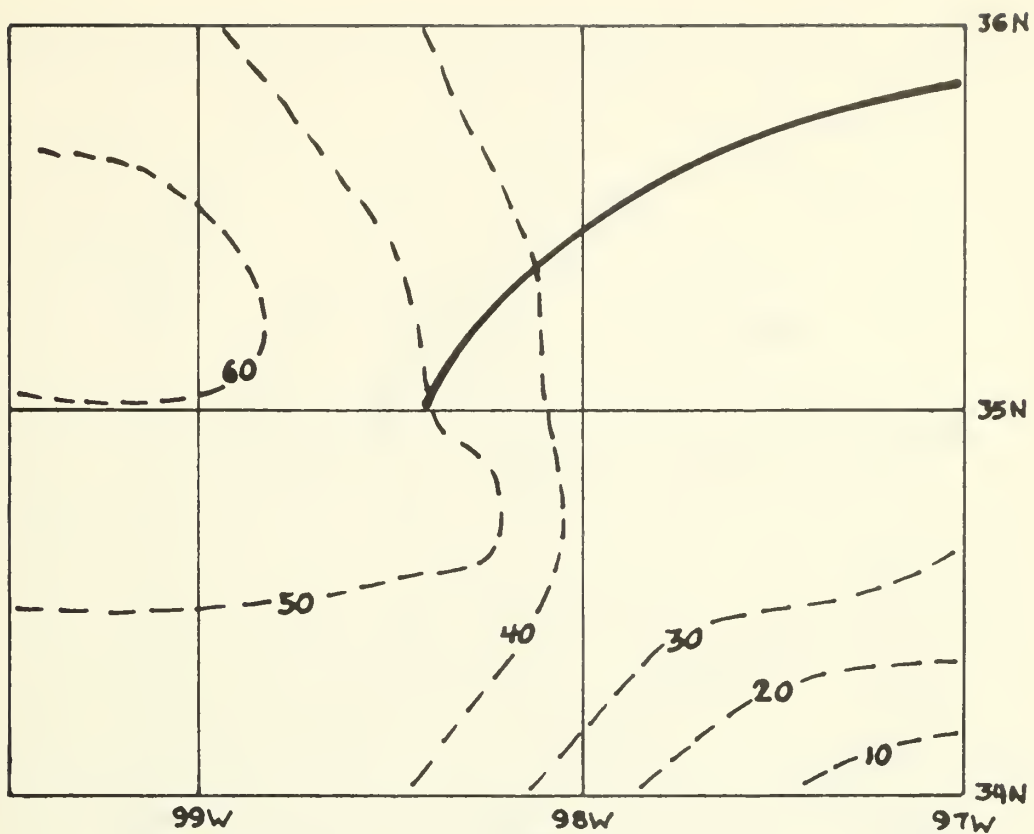


Figure 2c, 320K Theta surface, 2000 GMT relative humidity (%) analysis, Heavy solid line represents region of storm activity,

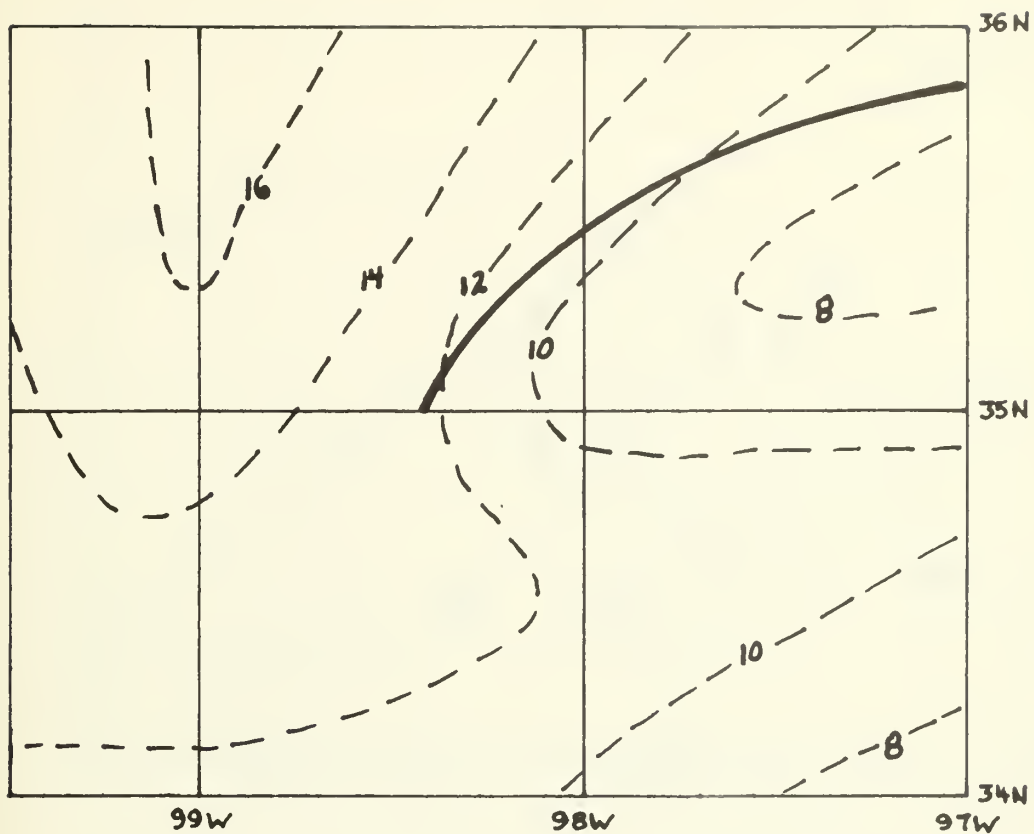


Figure 2d, 320K Theta surface, 2000 GMT wind speed (m sec^{-1}) analysis, Heavy solid line represents region of storm activity,

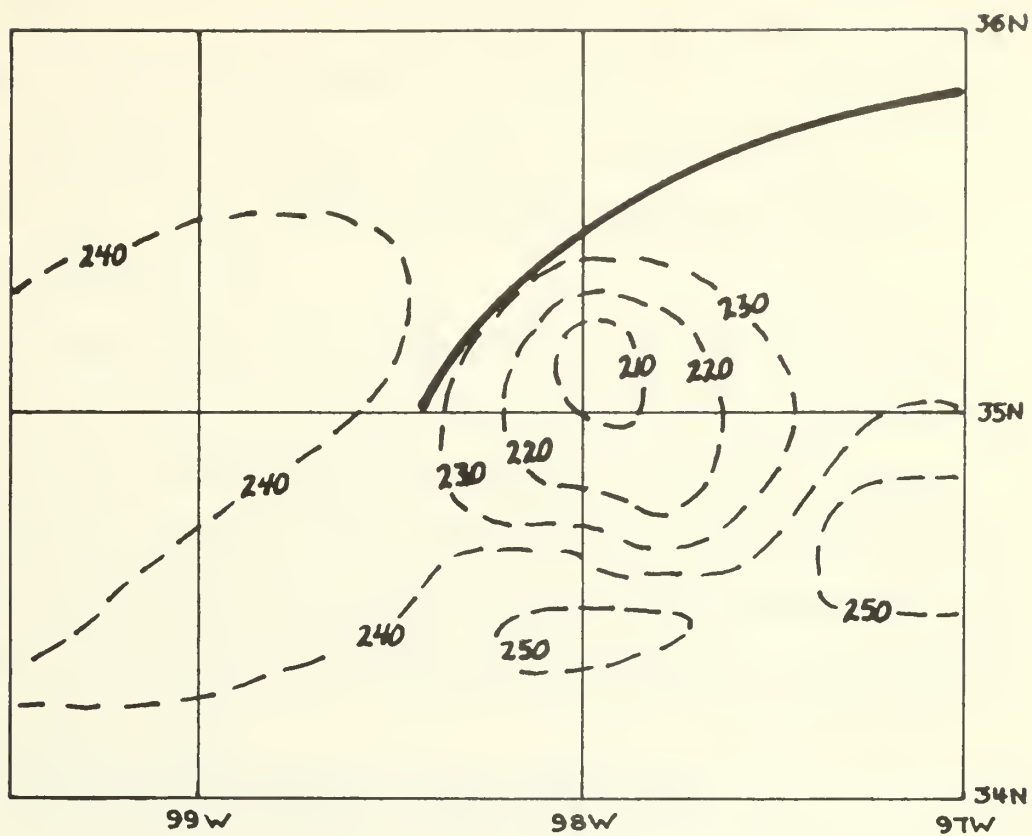


Figure 2e, 320K Theta surface, 2000 GMT wind direction (degs from north) analysis, Heavy solid line represents region of storm activity,

the wind veered with height and with time on the 308K, 312K and 320K theta surfaces. The time sections indicated the wind began to back with height above the 320K surface. This backing was evident by 1830 GMT at station LTS, by 2000 GMT at FSI, by 2130 GMT at CHK and by 2130 GMT at TIK. Wind speed at these stations generally increased with time and with height.

Data from stations LTS and FSI, which are toward the SW of the storm area, indicated the low level wind speed increased until about 2015 GMT and then began to decrease. Stations CHK and TIK, located in the SE edge of the storm region, show the wind speed continues to increase over the whole time period (1700-2300 GMT). Both the veering with height and speed increase have been correlated with severe storm activity (Miller, 1967).

B. TRAJECTORY RELATIONSHIPS TO THE SEVERE STORM

The kinematic isentropic trajectories were computed for one and one-half hour time periods at each grid point and on each theta surface. For reference to the trajectories that are discussed, see Appendix A.

The 1700-1830 GMT trajectories clearly show veering with height and time in the wind field. The 308K and 312K trajectories indicate anticyclonic flow over the whole grid, whereas the 320K and 332K trajectories have cyclonic flow in the W-NW corner and anticyclonic flow in the S-SE area. This is the flow pattern just prior to the storm formation, since the thunderstorm did not appear on radar until about 1817 GMT.

The 1830-2000 GMT trajectories imply changes in the wind field that are significant. On the 308K surface, the trajectories are beginning to have cyclonic flow in the W-NW, with a shear line almost

along the line of thunderstorm activity. The 312K trajectories specify anticyclonic flow over the whole area. The 320K surface flow pattern exhibits cyclonic flow along the south edge of the storm area, anticyclonic flow to the north, and straight flow along the center line of the storm activity. The 332K trajectory pattern denotes cyclonic flow to the SW and along the southern edge of storm activity, with anticyclonic flow in the NW and SE grid area. The storm appears to be oriented along the 320K trajectory flow pattern over this 1830-2000 GMT time frame.

During the time interval 2000-2130 GMT, the storm was in its most intense stages. It appears to be more oriented along the 308K flow pattern, which is from the south and cyclonic over most of the grid. The area to the west of the storm is strongly cyclonic. The 312K trajectories indicate straight SW flow. The 320K trajectories give evidence of a cyclonic area just to the south of the more intense regions of the storm. The 332K trajectories display anticyclonic flow over the entire grid. There is a veering of 70 degrees or more between the 308K and 320K trajectories over this period and pronounced backing in the NW region between the 320K and 332K surfaces.

Radar presentations indicate the dissipation of the storm over the 2130-2300 GMT period. The 312K trajectories are from the SW and show slight anticyclonic turning. The 320K and 332K trajectories indicate a slight cyclonic turning in the western portion of the grid and anticyclonic turning in the eastern portion. Strong backing of 45 degrees or more with height is evident between the 320K and 312K trajectory patterns.

Selected composite trajectories were obtained from each time interval in order to investigate air parcel flow over the whole time period .

These trajectories and associated parameters are discussed in the following section.

C. RELATIONSHIP OF ASSOCIATED PARAMETERS TO THE SEVERE STORM

One of the most important parameters to be computed from the kinematic isentropic trajectory program was the average vertical motion distribution for each theta surface and each 1.5 hour time interval. When used alone, these average vertical motion patterns are not sufficient to describe the storm activity. However, they do provide very definite clues to the storm dynamics when used in conjunction with other properties.

During the time interval 1700-1830 GMT, the vertical distribution of vertical motions over the NSSL network indicated lower level air parcel sinking in the western half of the grid of about 8 mb hr^{-1} and rising motions of $10\text{-}20 \text{ mb hr}^{-1}$ in the eastern half of the grid. Upper level patterns were reversed, with rising motions in the western half and sinking motions in the eastern half. In addition, there was very strong rising motion ($20\text{-}30 \text{ mb hr}^{-1}$) in the western half of the grid at a height of about 10 KM. It is possible that the high level vertical motion pattern is the initial indication of an upper level formation of supporting vertical motions for the storm.

The 1830-2000 GMT vertical motion patterns (Fig. 3a-3d) clearly delineate and support the storm system. At each level there is strong rising motion as air parcels come into the storm area, with sinking motions over the remaining grid area. The 320K isentropic surface vertical motion pattern indicates the region of maximum rising motion. The storm is also oriented parallel to the 320K trajectory flow pattern over this period. It would appear the 320K (i.e. approximately 500 mb) flow is responsible for maintaining the storm at this time.

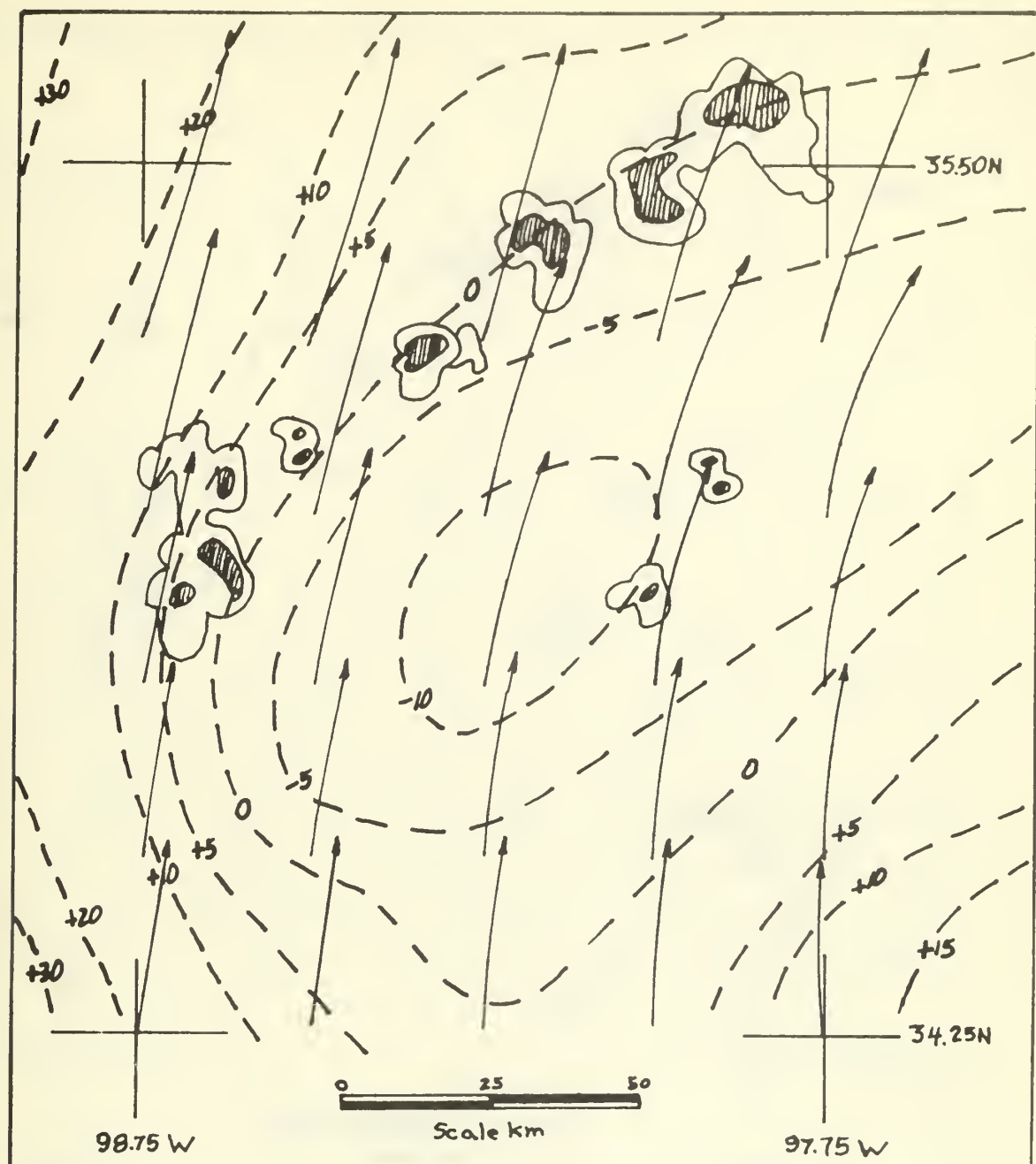


Figure 3a, 308K Theta surface, 1830-2000 GMT average vertical motions (mb hr⁻¹) and kinematic isentropic trajectories, Storm position as of 1915 GMT,

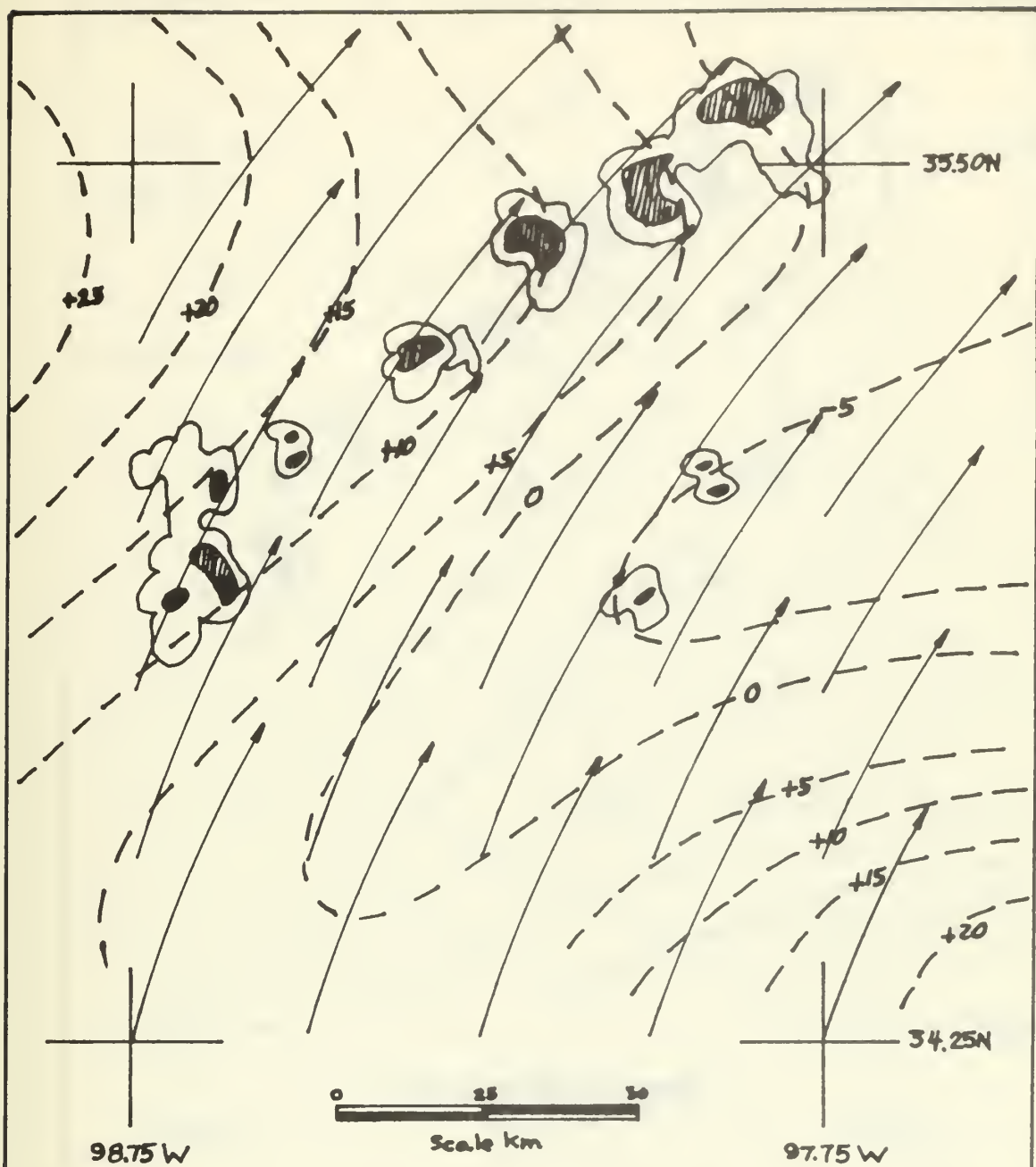


Figure 3b, 312K Theta surface, 1830-2000 GMT average vertical motions (mb hr^{-1}) and kinematic isentropic trajectories, Storm position as of 1915 GMT,

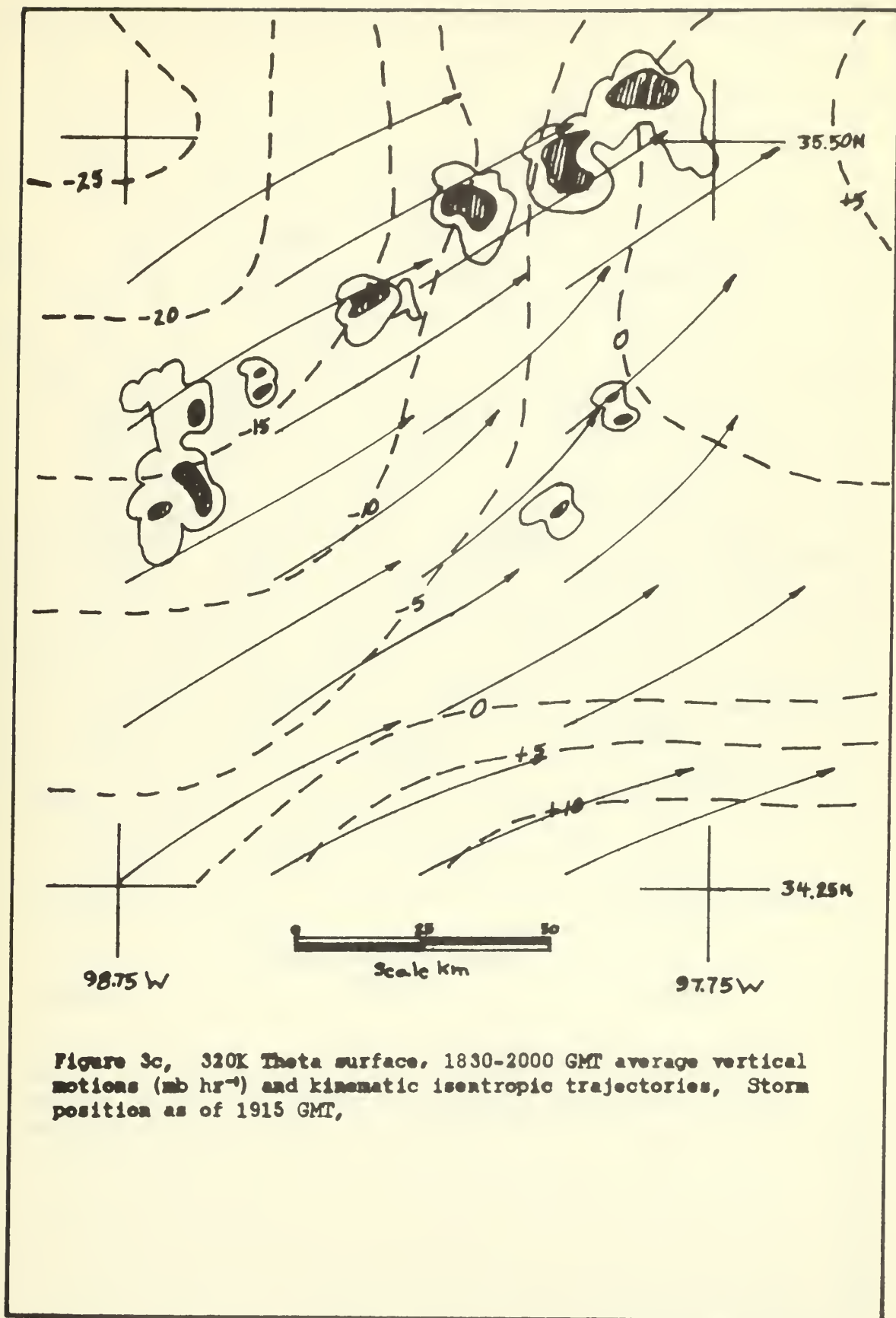


Figure 3c, 320K Theta surface, 1830-2000 GMT average vertical motions (mb hr^{-1}) and kinematic isentropic trajectories, Storm position as of 1915 GMT,

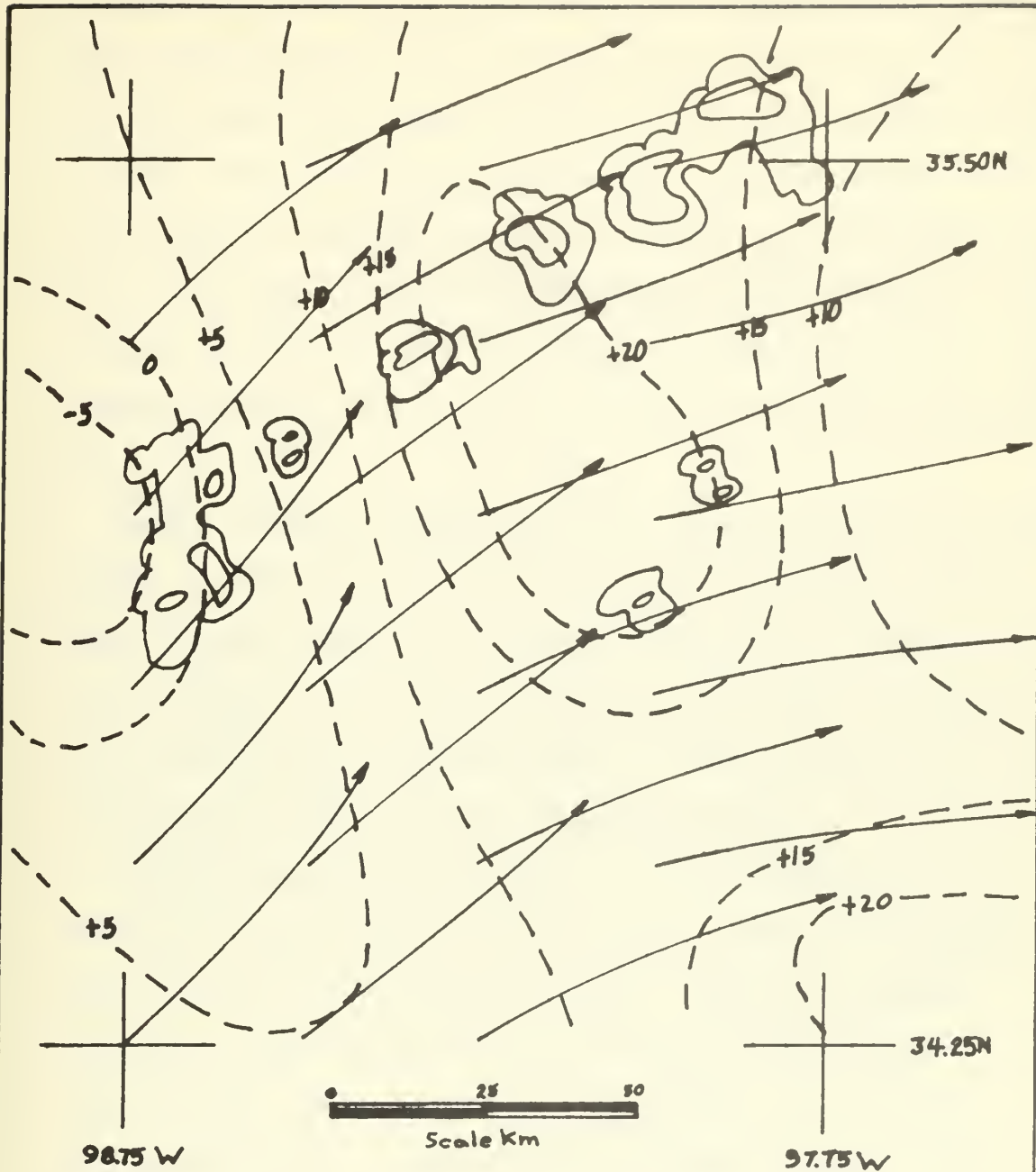


Figure 3d, 332K Theta surface, 1830-2000 GMT average vertical motions (mb hr⁻¹) and kinematic isentropic trajectories, Storm position as of 1915 GMT,

Over the 2000-2130 GMT period the 308K and 312K isentropic surfaces vertical motion patterns present sinking motion over most of the grid, with larger values ($25-30 \text{ mb hr}^{-1}$) in the northern half of the grid. The 320K and 332K theta surfaces vertical motions still show rising in front and into the storm system, but the patterns are not as well defined. The 2000-2130 GMT convergence fields on the 320K isentropic surface are well correlated with the storm system and show strong convergence of $1.0 \text{ to } 1.5 \times 10^{-4} \text{ sec}^{-1}$ in the system (Figs. 4a, 4b).

Darkow (1968) has examined the total energy environment of severe storms on the synoptic scale of motion and has determined a "Total Energy Index". This index is computed as the difference between the "total energy" ($c_p T + gz + Lq$) at 500 mb and the total energy at 850 mb. Index values more negative than -2.0 cal gm indicate severe storms and associated tornado activity are highly probable.

The NSSL isentropic plane section computer output for the nine radiosonde stations gives the static energy. This data was investigated in terms of a "Total Energy Index". Values at 1700 GMT indicated a region of -2.0 in the area where the thunderstorms began to occur. Values in the same region were -4.0 or larger by 2000 GMT (Fig. 5). Values over the remaining grid area were slightly negative or positive.

Total energy, defined by equation (8), was investigated for storm evolution. The 312K and 320K isentropic surfaces for the 2000 and 2130 GMT analyses show a region of maximum total energy in the storm vicinity, with decreasing values toward the NW and SE. This region is seen in Figure 6. As shown by Figure 7, the contour pattern of total energy closely resembles the specific humidity distribution, which

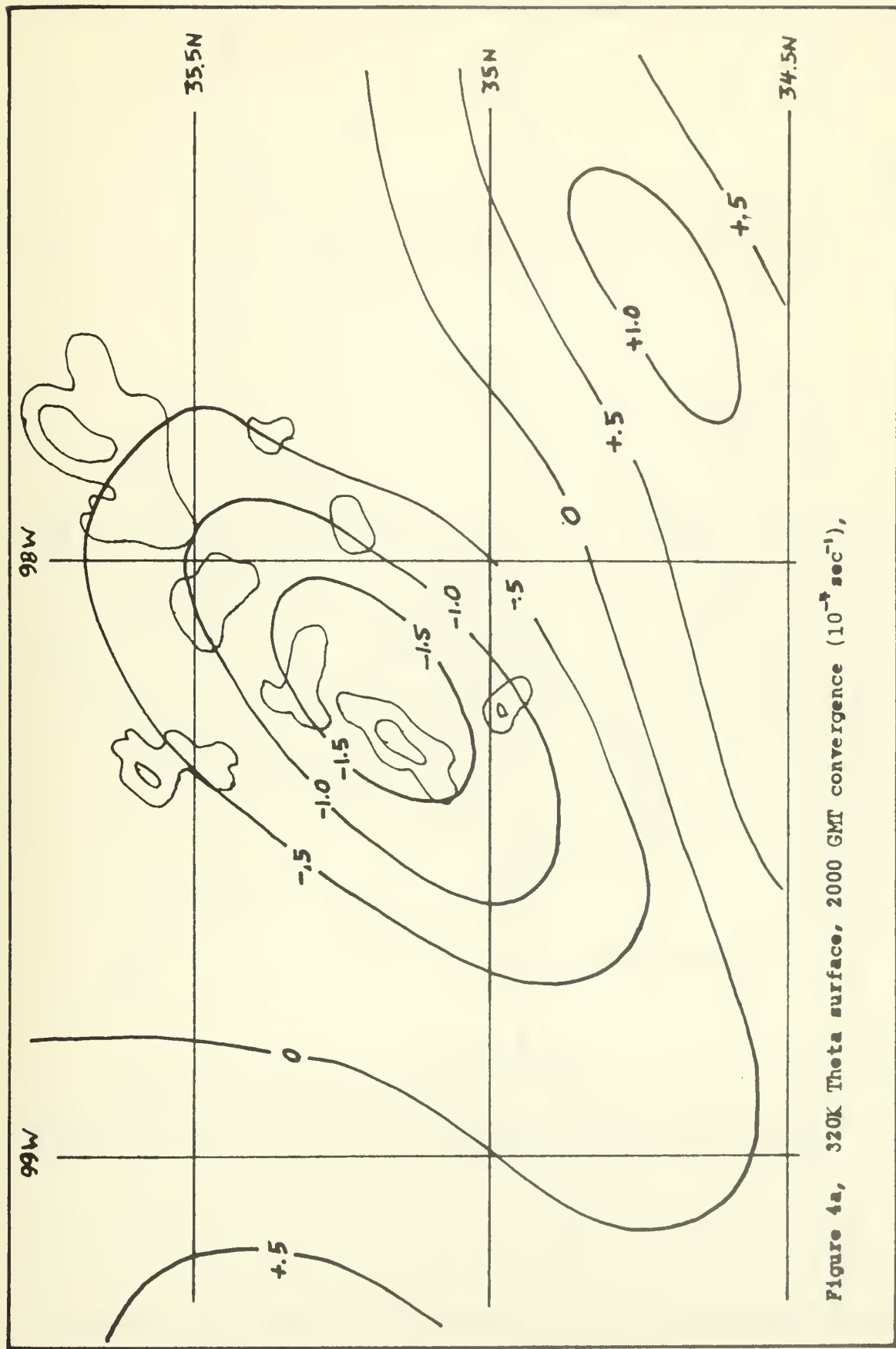


Figure 4a, 320K Theta surface, 2000 GMT convergence (10^{-3} sec^{-1}),

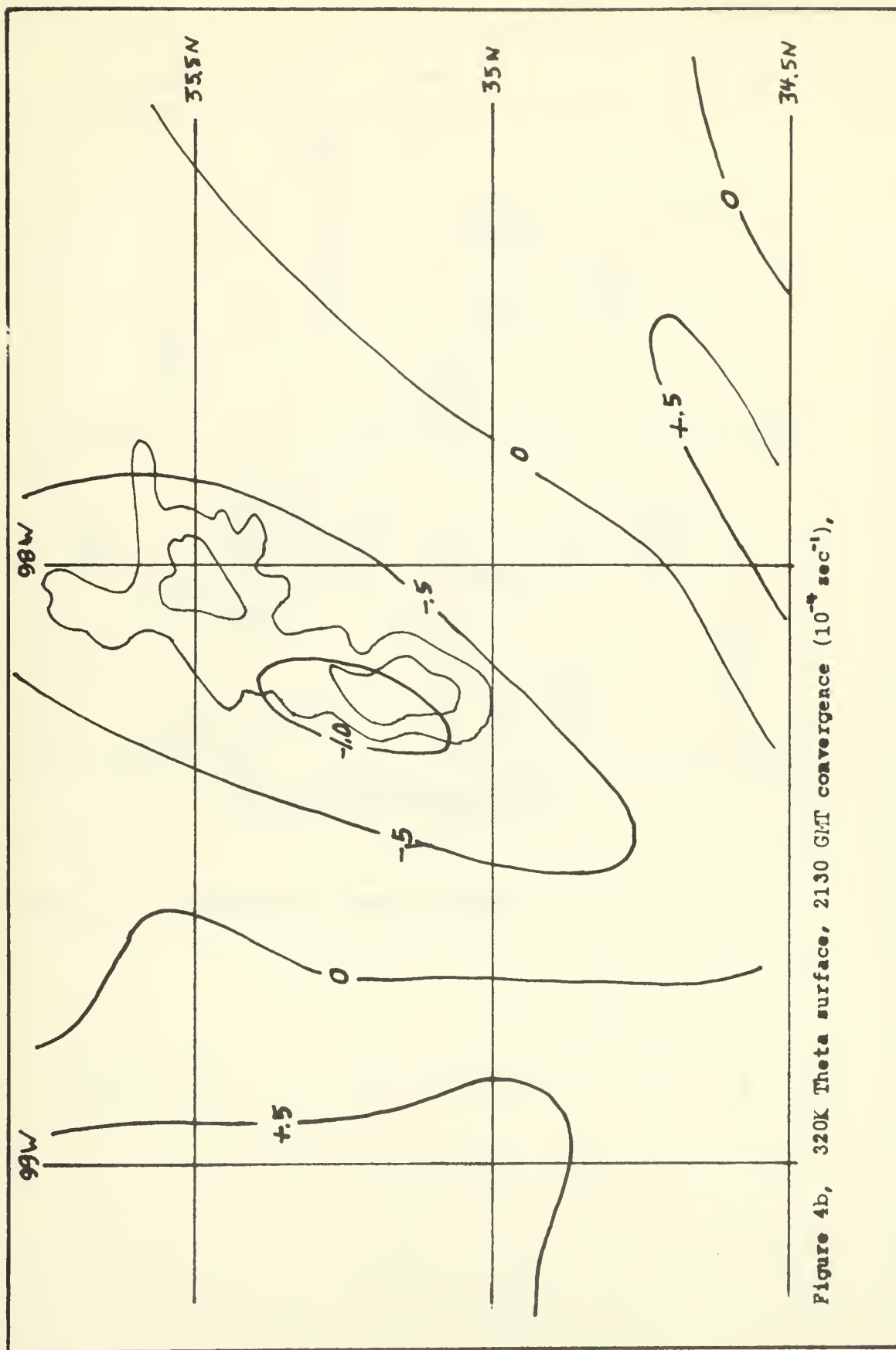


Figure 4b, 320K Theta surface, 2130 GMT convergence (10^{-4} sec^{-1}),

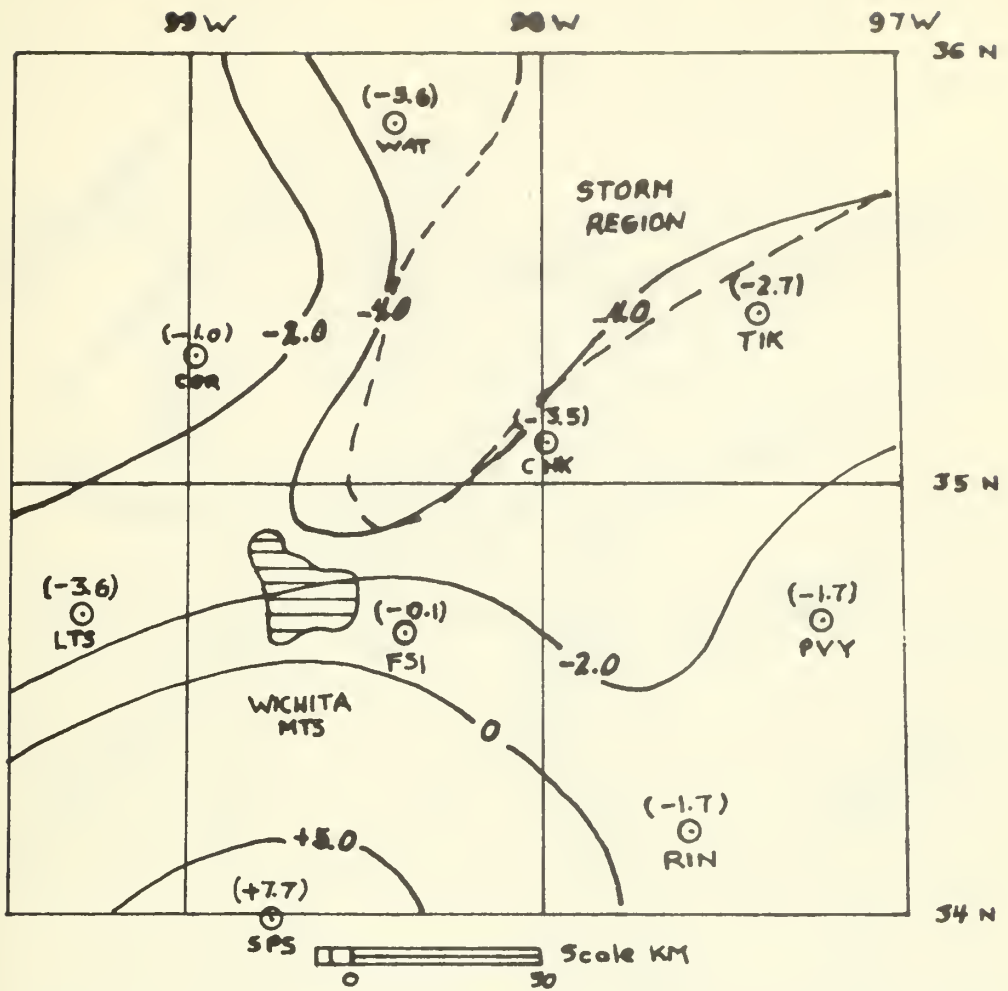


Figure 5, 2000 GMT Total energy index,

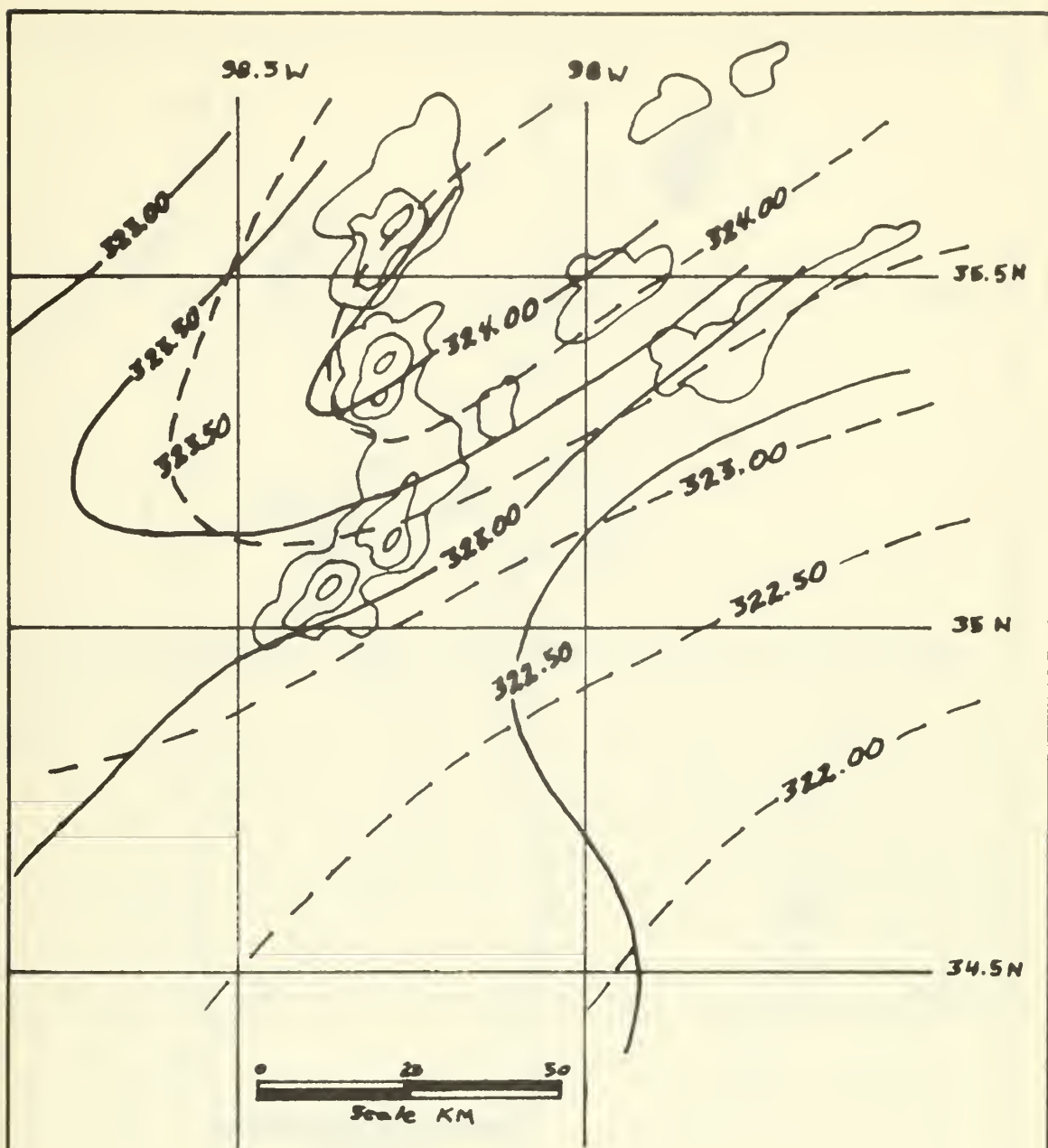


Figure 6, 320K Theta surface total energy (joules gm^{-1}) analysis, Solid lines are 2000 GMT pattern and dashed lines are 2130 GMT pattern, Storm position as of 2045 GMT,

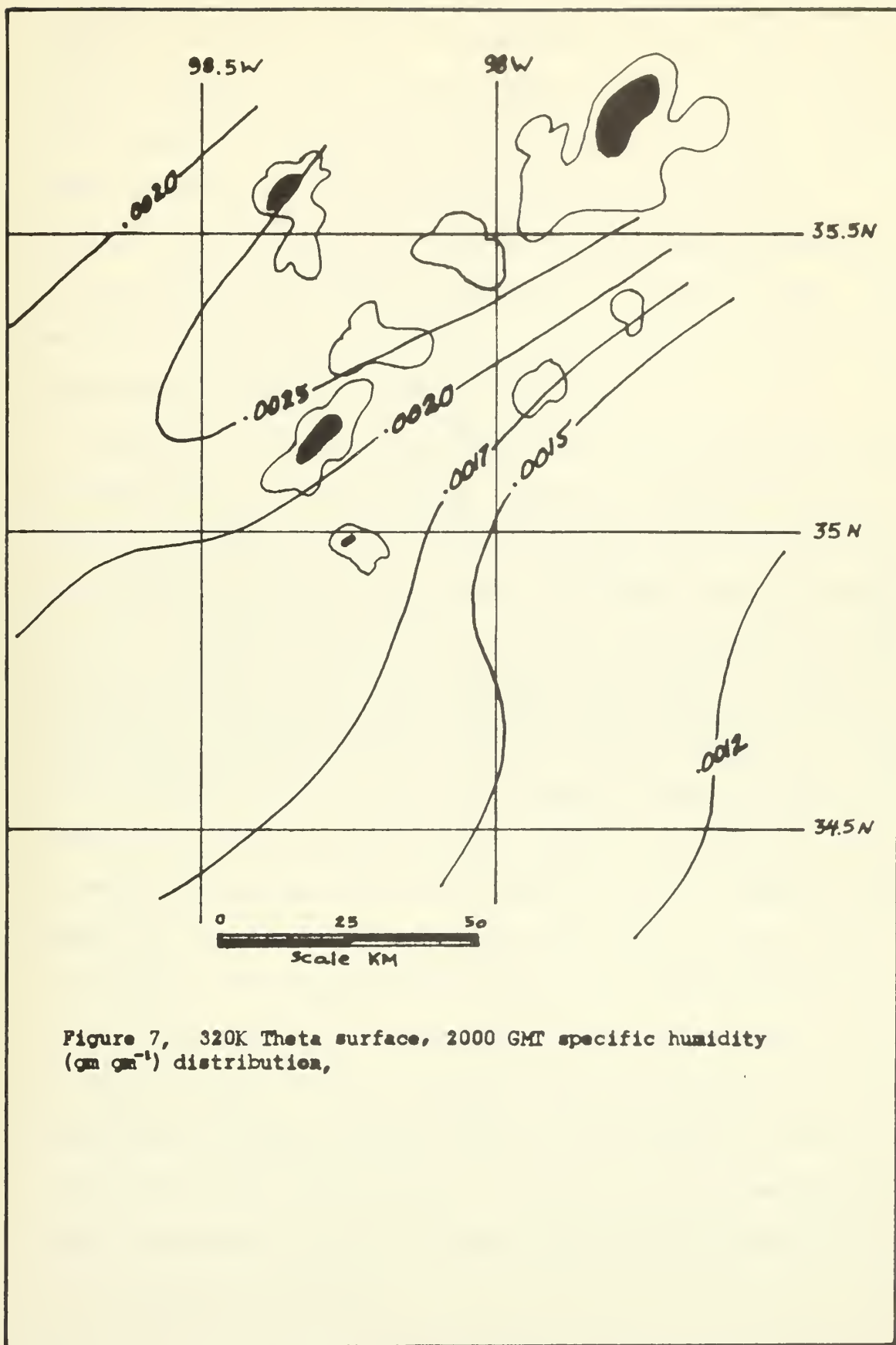


Figure 7, 320K Theta surface, 2000 GMT specific humidity (gm gm^{-1}) distribution,

indicates the L_q term dominates the pattern. Thus the relative humidity analysis is a critical factor in determining the total energy. The relative humidity is not the most reliable information from a radiosonde sounding, particularly at higher altitudes. Since the L_q term seems to dominate the total energy contours, unless the relative humidity field is adequately specified, the total energy computations will not provide good information with which to study the storm. There are also inaccuracies in the Montgomery stream function field which may amplify the error in total energy computations.

Fankhauser (1968) has demonstrated the wind field relationship for this same May 28, 1967 storm system. Using chaff trajectories and aircraft measurements, the streamline and isotach pattern of the composite relative wind field with respect to the storm echo are presented (Fig. 8). The 320K isentropic surface almost corresponds with the 500 mb isobaric surface, thus a good comparison can be made. In Figure 9 the isentropic trajectories show that flow is being deviated around the storm, convergence into the storm and divergence behind the storm. The acceleration field (Fig. 10) also shows maxima to the right and left of the storm and minima in front of and behind the storm. Fankhauser has demonstrated the flow for an isolated storm echo and the fields are instantaneous. The isentropic trajectories show average conditions for the larger storm system, and yet the results are strikingly similar. The comparison times are also different, which may indicate this wind distribution is present throughout the storm cycle for both isolated cells and the entire storm complex. Thus the 1.5 hour kinematic isentropic trajectories correlate very well with the chaff trajectories that Fankhauser has obtained.

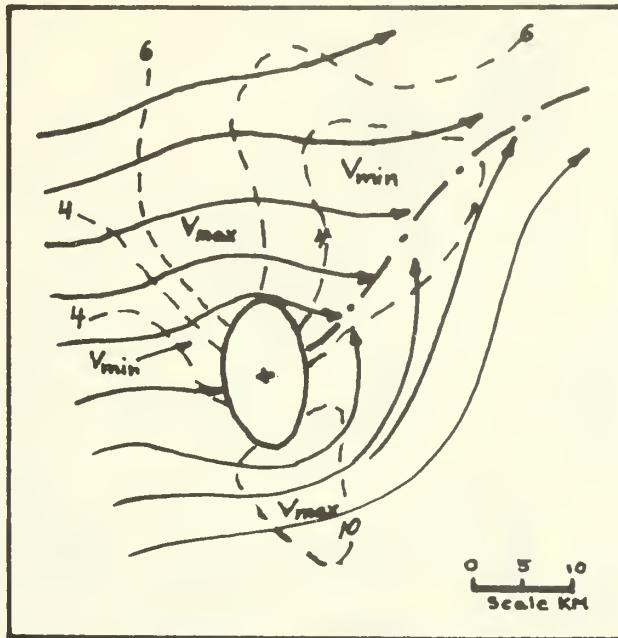


Figure 8, 2145 GMT simplified streamline and isotach pattern relating the composite relative wind field with respect to storm echo centered on cross, (after Fankhauser, 1968, fig, 8), Wind speeds in m sec^{-1} ,

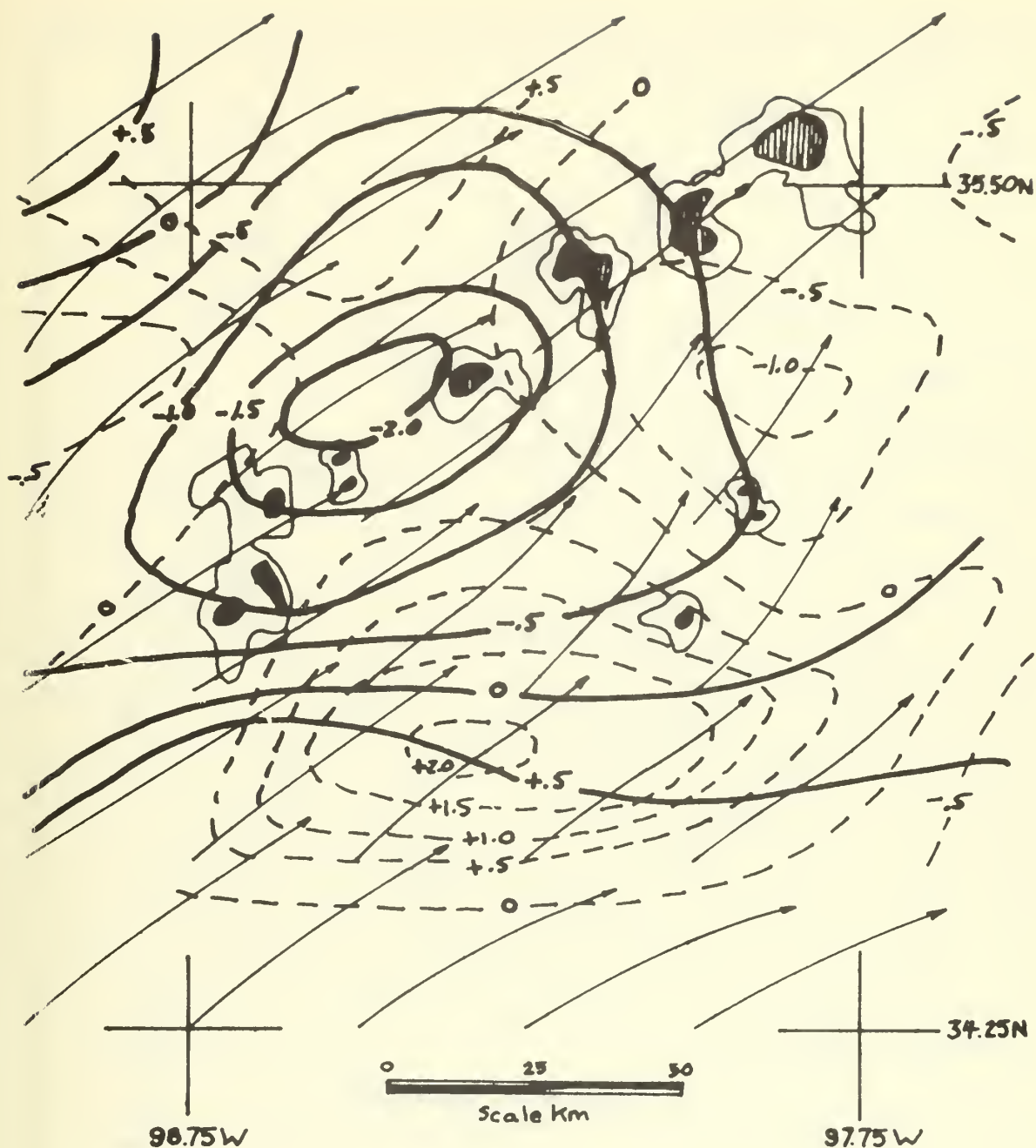


Figure 9, 320K Theta surface, 1830-2000 GMT kinematic isentropic trajectories relative to the storm, Dashed lines represent changes in absolute vorticity (10^{-4} sec^{-1}) computed along the trajectory, Heavy solid lines represent changes in divergence (10^{-4} sec^{-1}) computed along the trajectory, Storm position as of 1915 GMT,

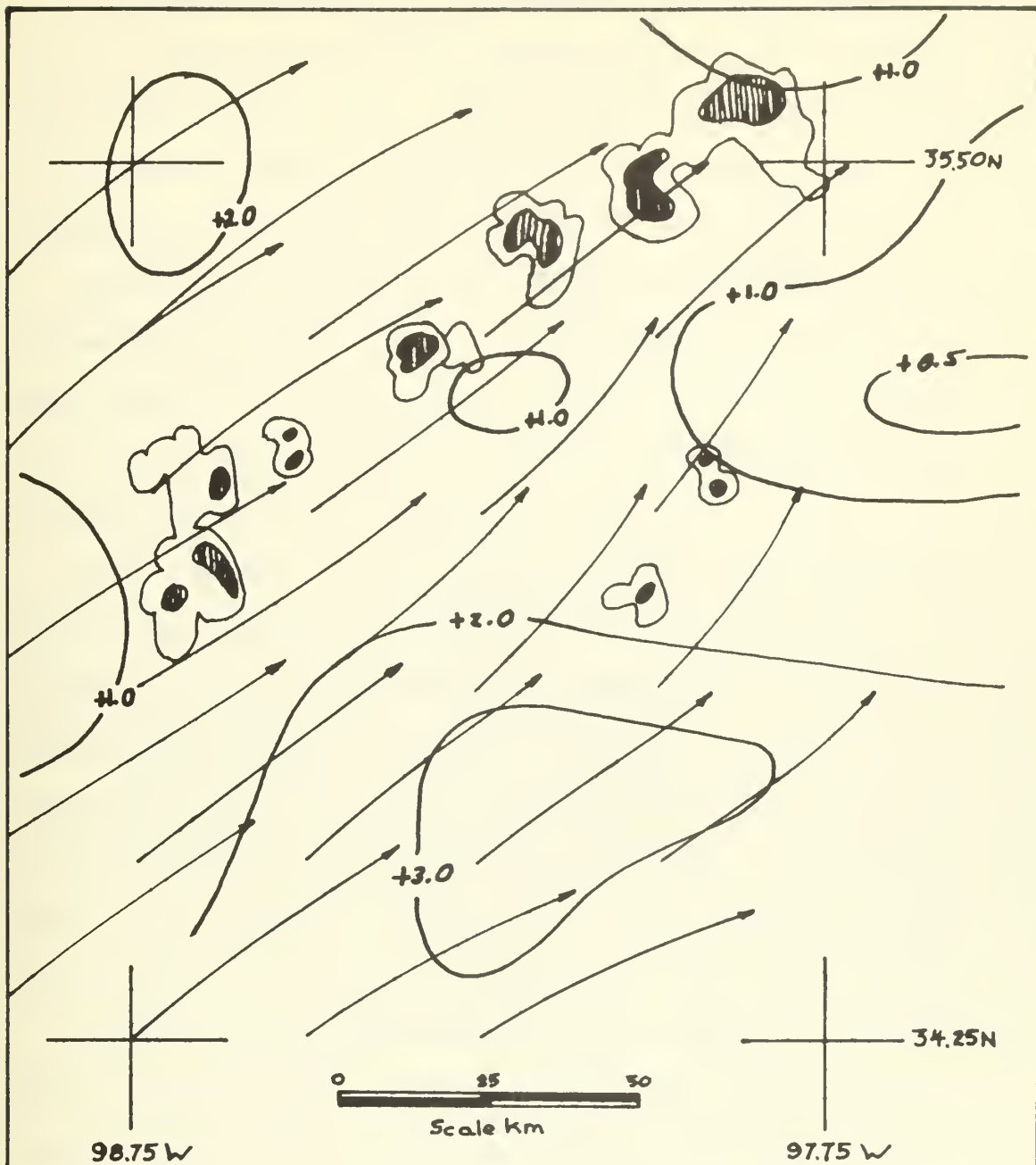


Figure 10, 320K Theta surface, 1830-2000 GMT accelerations ($\text{m sec}^{-1} \text{hr}^{-1}$), Storm position as of 1915 GMT,

D. INERTIAL-GRAVITY WAVE ASSOCIATION TO THE SEVERE STORM

A close look at various analyses seems to imply an oscillation present in the network area. Thus an investigation into the possibility of a wave like phenomenon present over the data area was considered as a possible source of the storm activity and storm movement.

An oscillatory tendency can be observed on the 320K theta surface composite trajectories (Fig. 11). Measurements in the center of the grid region show a wave length of about 150 KM and period of about 3 hours. Radar presentations of the most intense storm activity also indicate a wave length of about 150 KM (Fig. 12).

Surface pressure tendencies over the network area were studied to determine if the oscillation could be detected at the surface. Micro-barograph traces were available at 35 stations over the data area. The pressure tendencies indicated falling pressures of about 0.03 inches of Hg per 1.5 hours over the grid during the entire life cycle of the storm. Figure 13 illustrates this tendency over the area. A noticeable fluctuation was not apparent at most stations. Even the presence of the storm was difficult to detect (see stations 3A, 3C, 4B and 4C on Fig. 13).

Synoptic pressure tendency patterns were obtained for 1800 and 2400 GMT, and a mean synoptic pressure tendency over the grid area was calculated. This value was then subtracted from the network stations pressure tendency at each time frame in order to calculate a "meso-scale pressure tendency". The results, as seen in Figure 14, indicate both rise and fall areas. The rise and fall areas show a half wave length of about 100 KM along the mean low level wind field, and a 150 KM wave length between two negative centers along a line of mean wind direction.

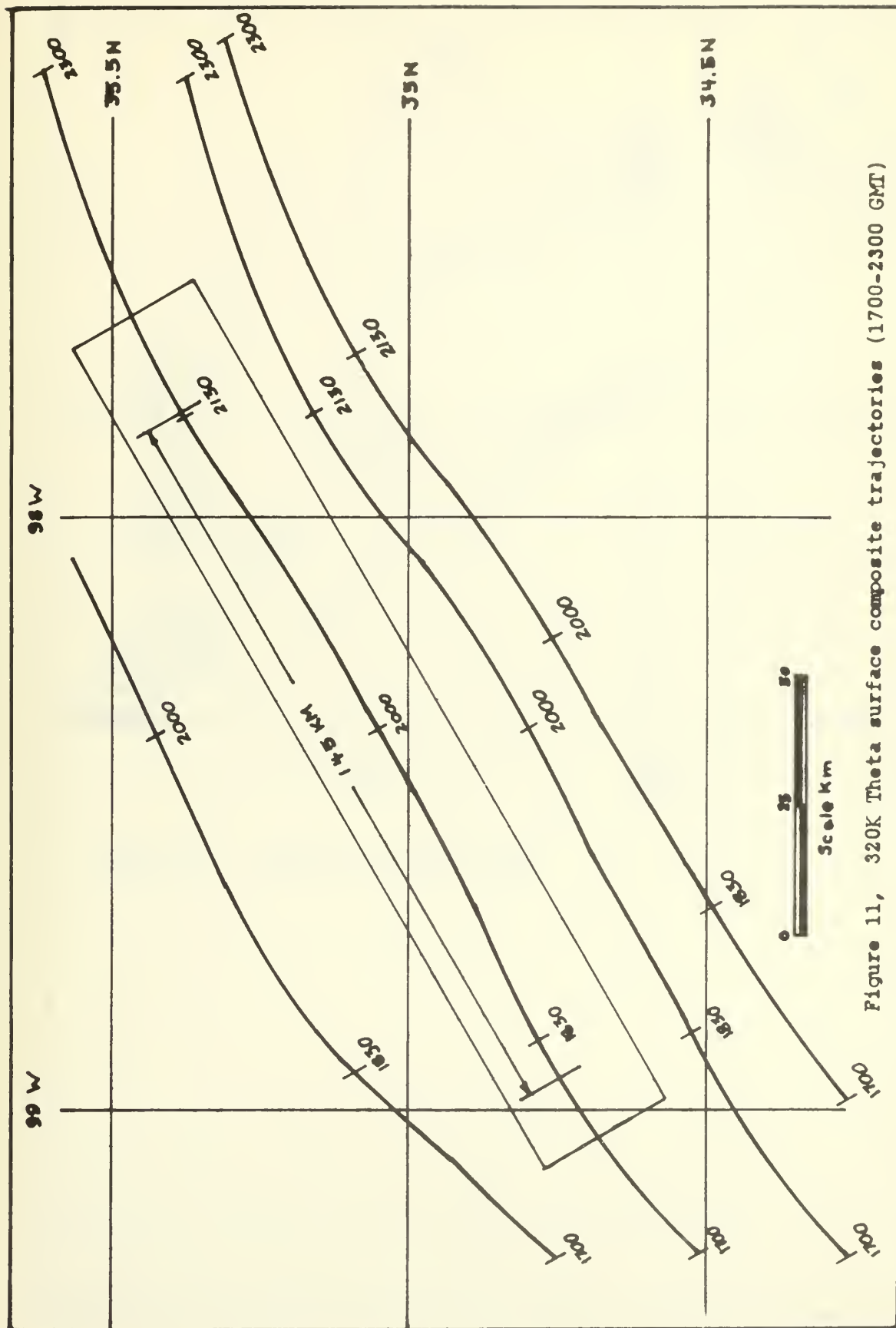


Figure 11, 320K Theta surface composite trajectories (1700-2300 GMT)

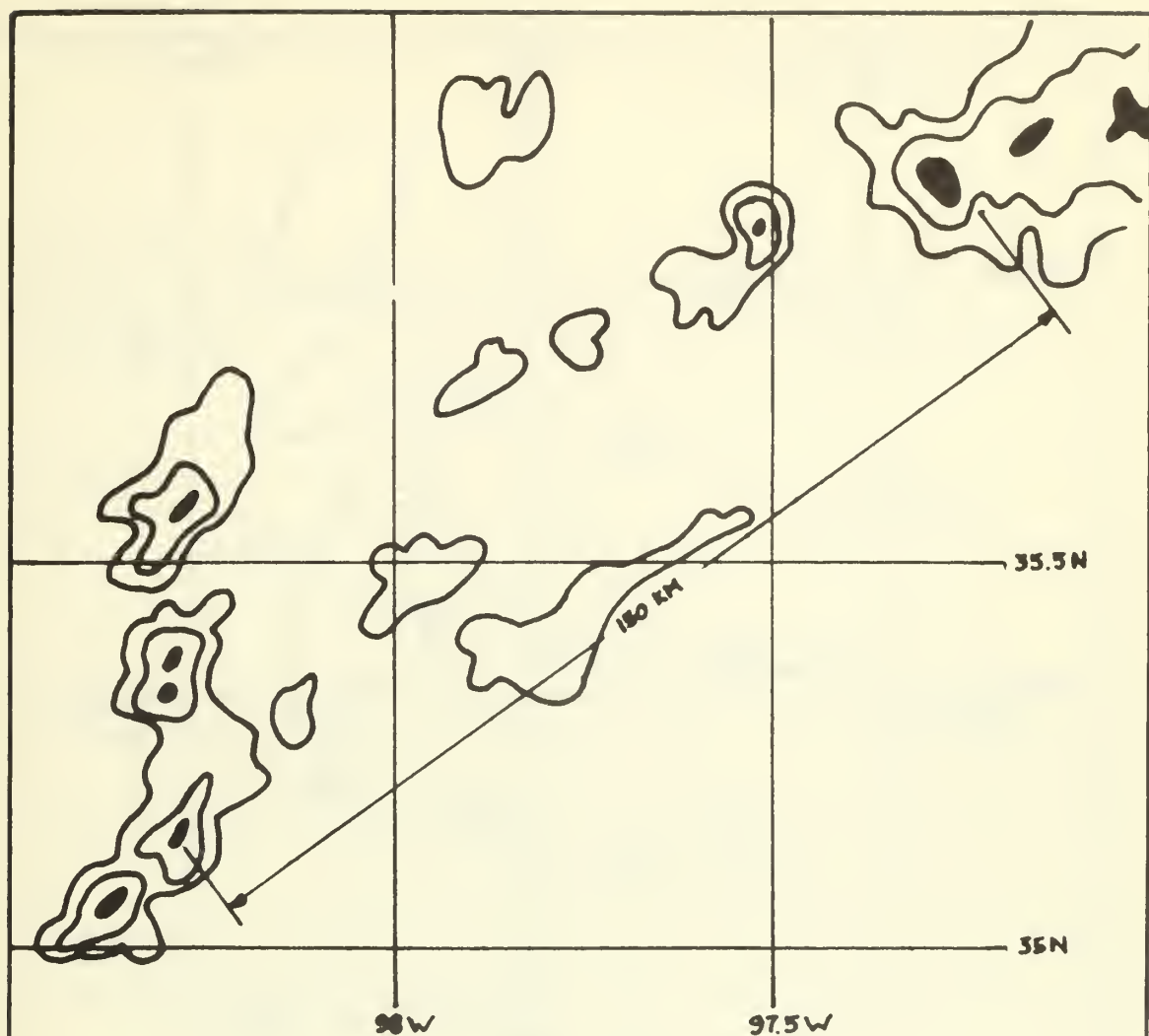


Figure 12, 2045 GMT storm position,

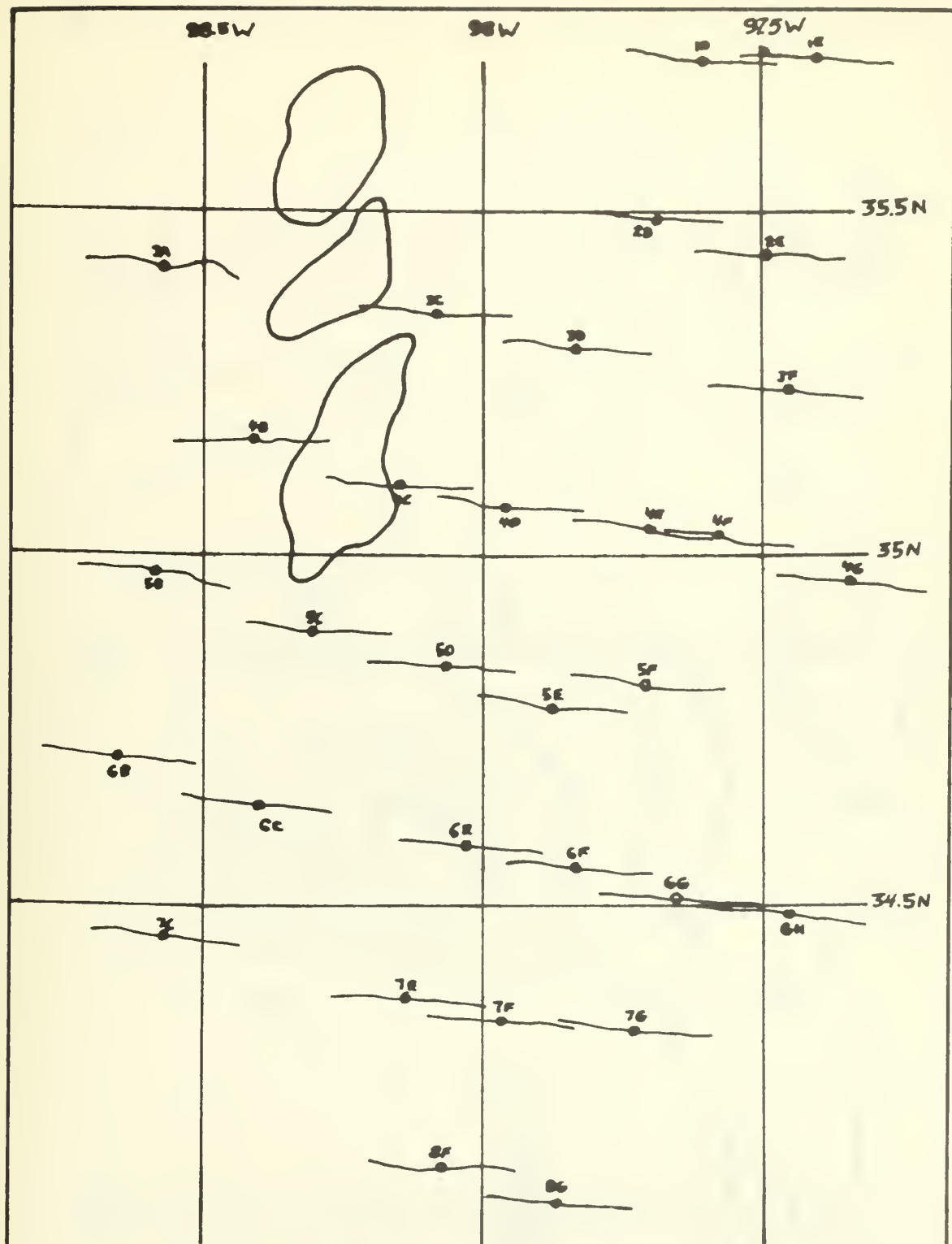
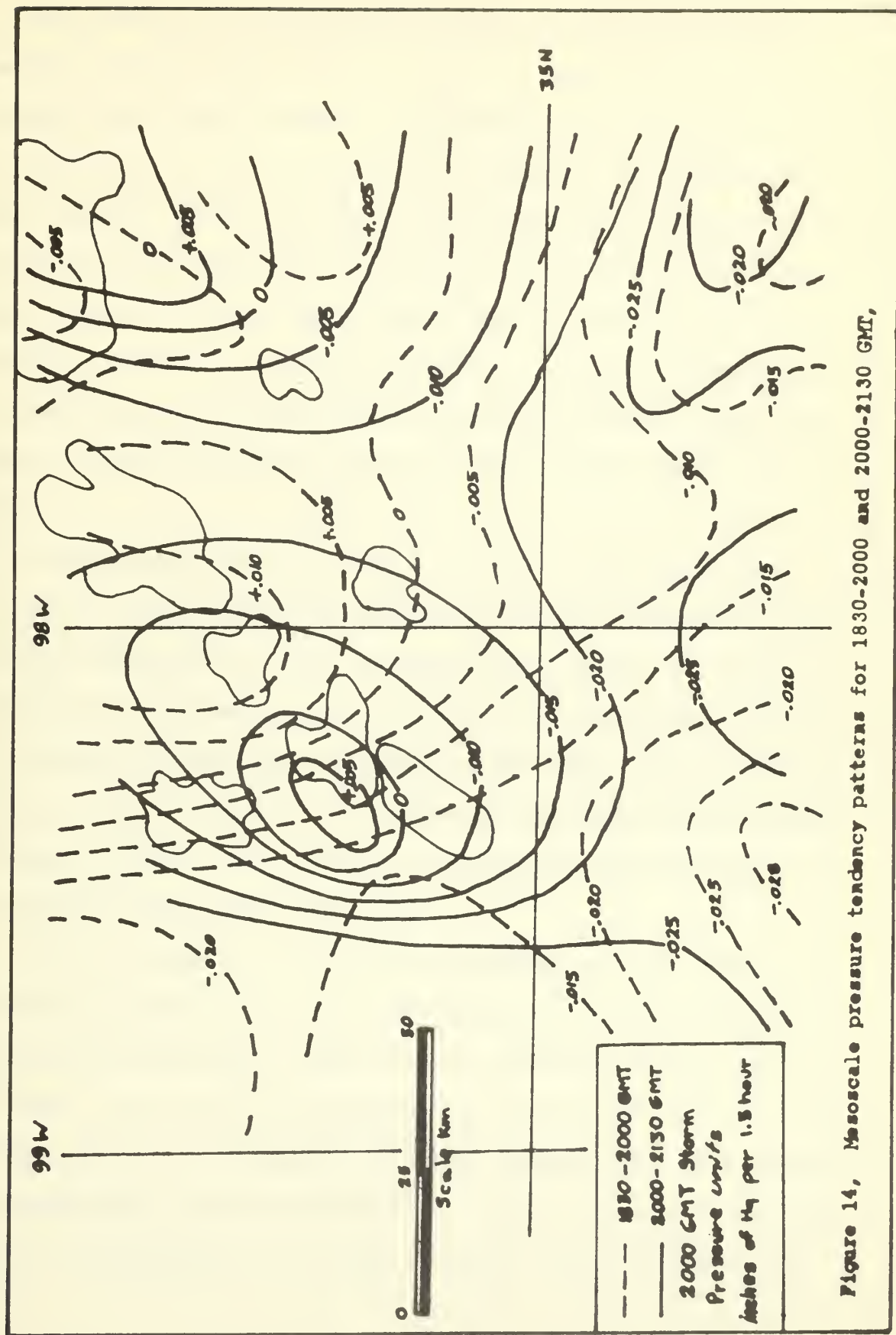


Figure 13, 2030-2130 GMT surface microbarograph traces centered at 2100 GMT on each station, Measurements in inches of Hg, 2100 GMT storm position,



Time sections at selected stations along the mean wind direction (see Fig. 15) were made in order to study the time variations of vertical motion, static stability, relative humidity, wind speed and wind direction. The time sections at stations LTS, FSI, CHK and TIK (Figs. 16a-16d) indicate an apparent periodicity in the vertical motion and static stability patterns. The vertical motions are the average omega obtained by the trajectory method, and the static stability is the value centered between two adjacent theta surfaces. Measurements on these time sections, from the vertical motion patterns, give a wave length of about 150 KM, wave period of 3 hours and wave speed of 14 m sec^{-1} .

It can be seen in Figure 16a that a region of vertical motion of $+30 \text{ mb hr}^{-1}$ is occurring at station LTS at 1915 GMT, between the 308K and 312K theta surfaces. With the measured wave speed of 14 m sec^{-1} (50 KM hr^{-1}), a propagating wave without change in amplitude, constant wave length and moving in the direction of the mean wind would produce a region of about $+30 \text{ mb hr}^{-1}$ at station FSI about 2045 GMT and station CHK about 2145 GMT. This condition is verified at these stations for the specified times (Figs. 16b & 16c).

With the assumption of a wave-like phenomenon present, a study was conducted to determine if such a wave phenomenon and other supporting dynamic and thermodynamic forces could be correlated with the onset of the storm. The earliest radar presentation at 1817 GMT indicated small cumulus activity in the western portion of the grid area. Time sections at stations LTS, FSI, CHK and TIK (Figs. 17a-17b) show that at 1700 GMT there is a pronounced shift in wind direction between the stations on

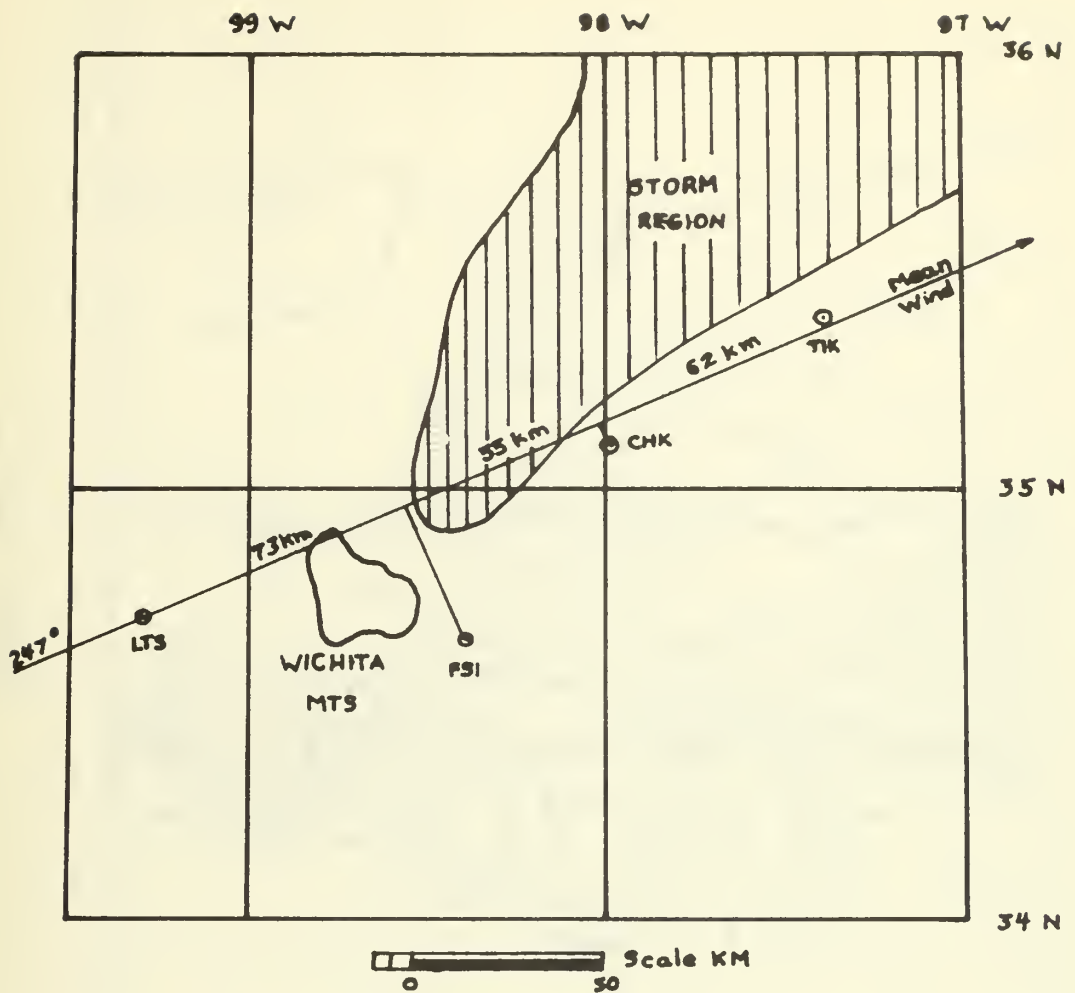


Figure 15, Station cross-section distribution for time sections,

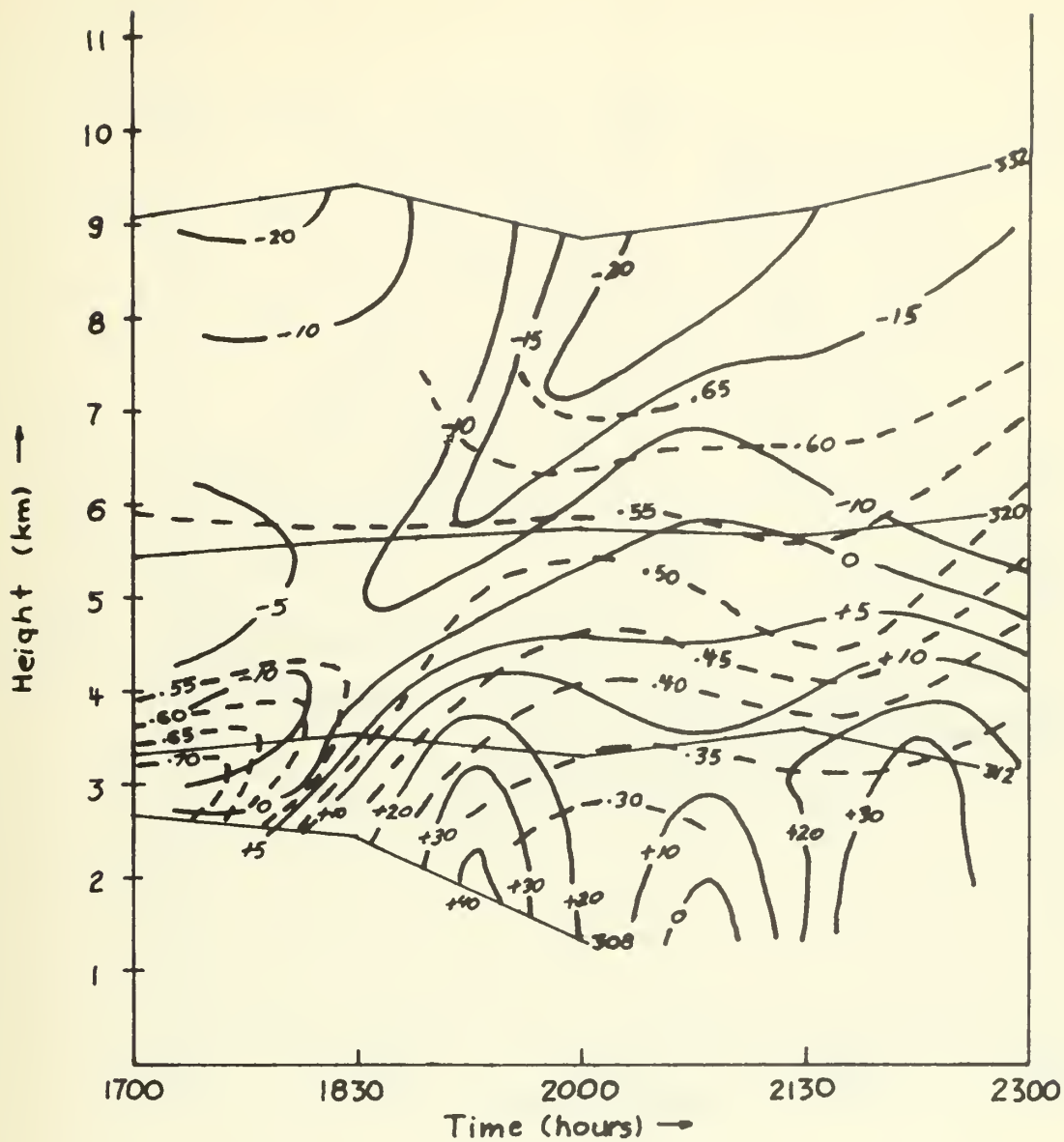


Figure 16a, Time section at station LTS, Heavy solid lines represent vertical motions (mb hr^{-1}), Dashed lines represent static stability (K mb^{-1}), Thin solid lines represent theta surface positions,

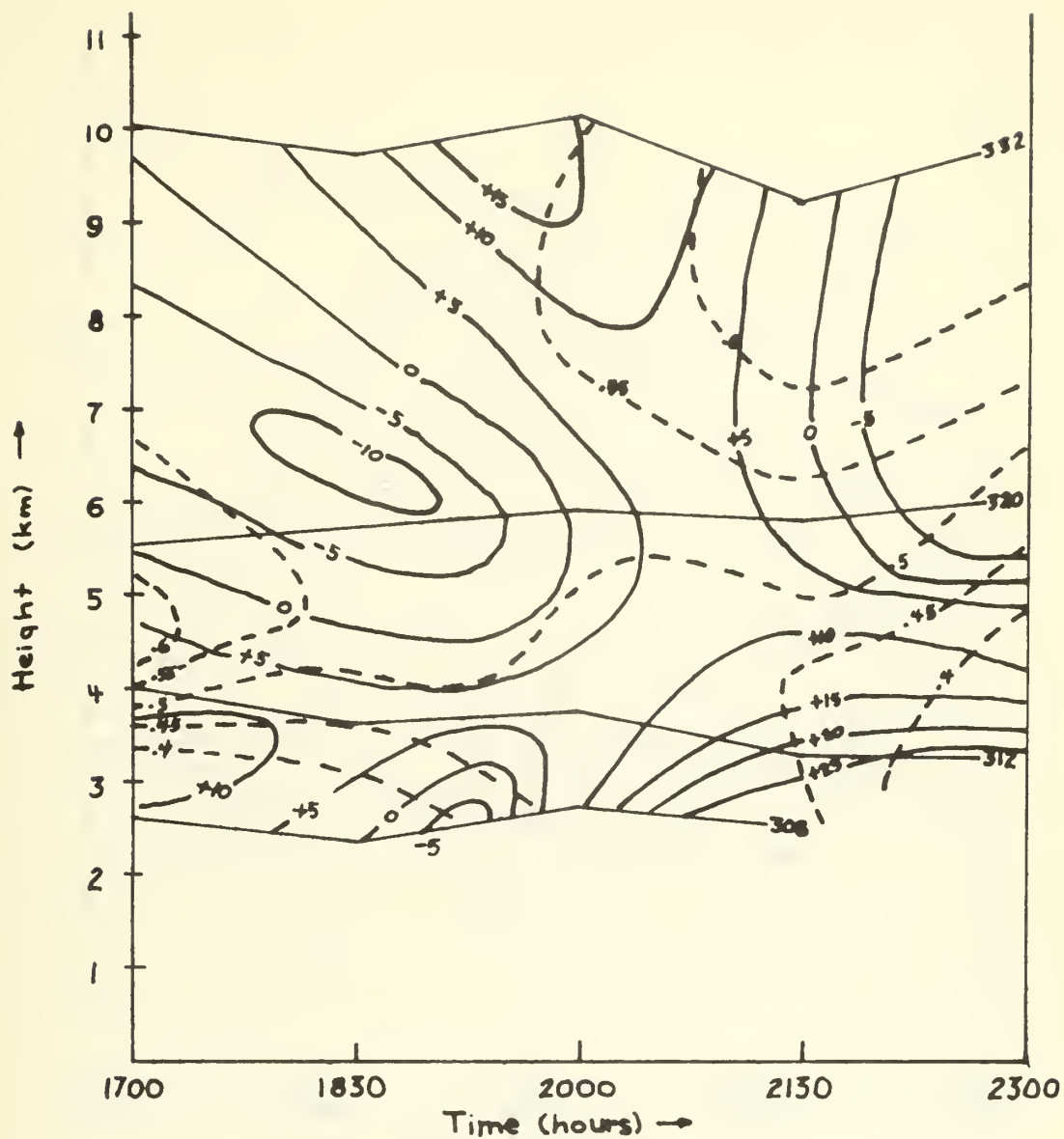


Figure 16b, Time section at station FSI, For explanation see fig, 16a,

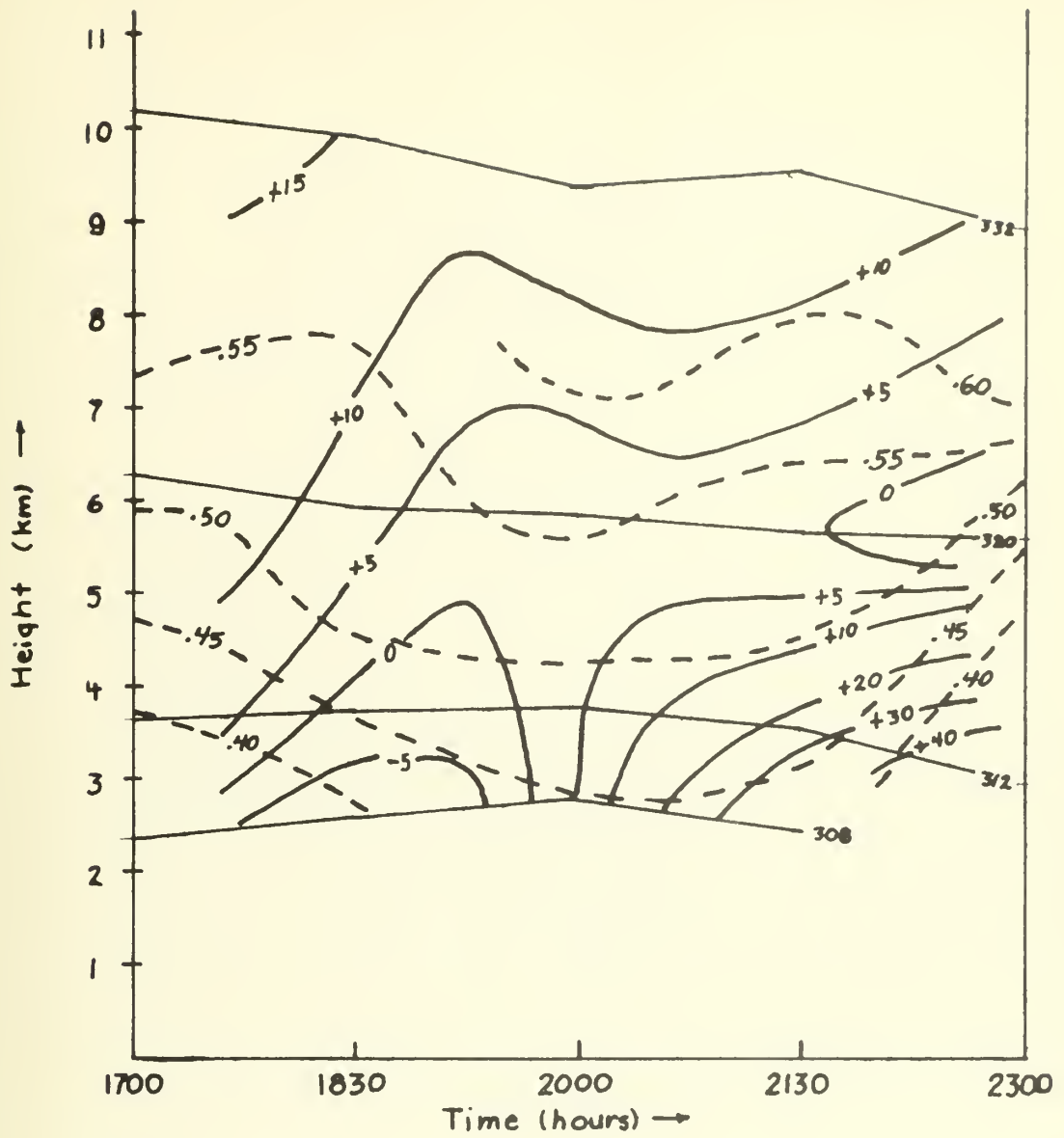
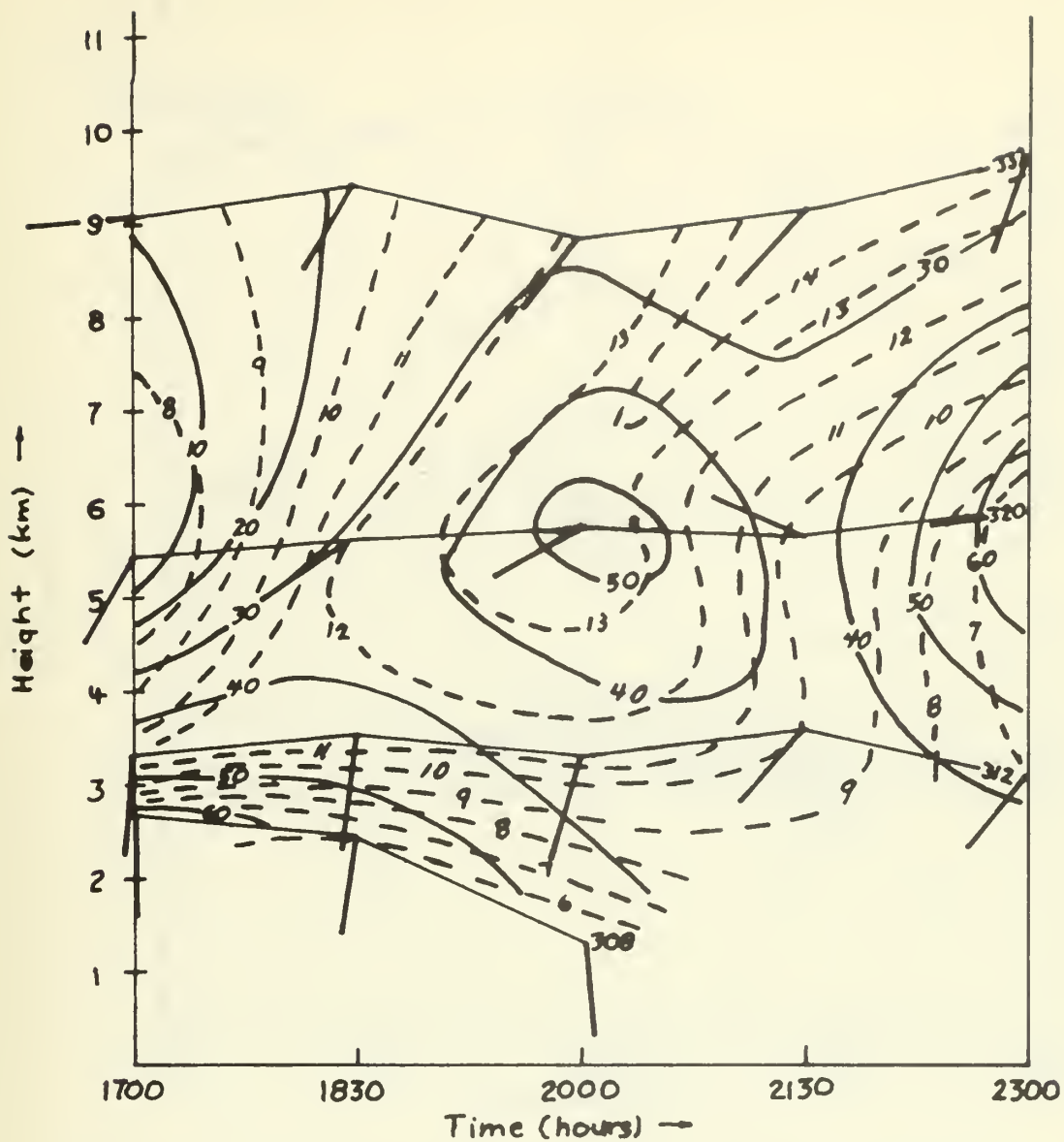


Figure 16c, Time section at station CHK, For explanation see fig, 16a,



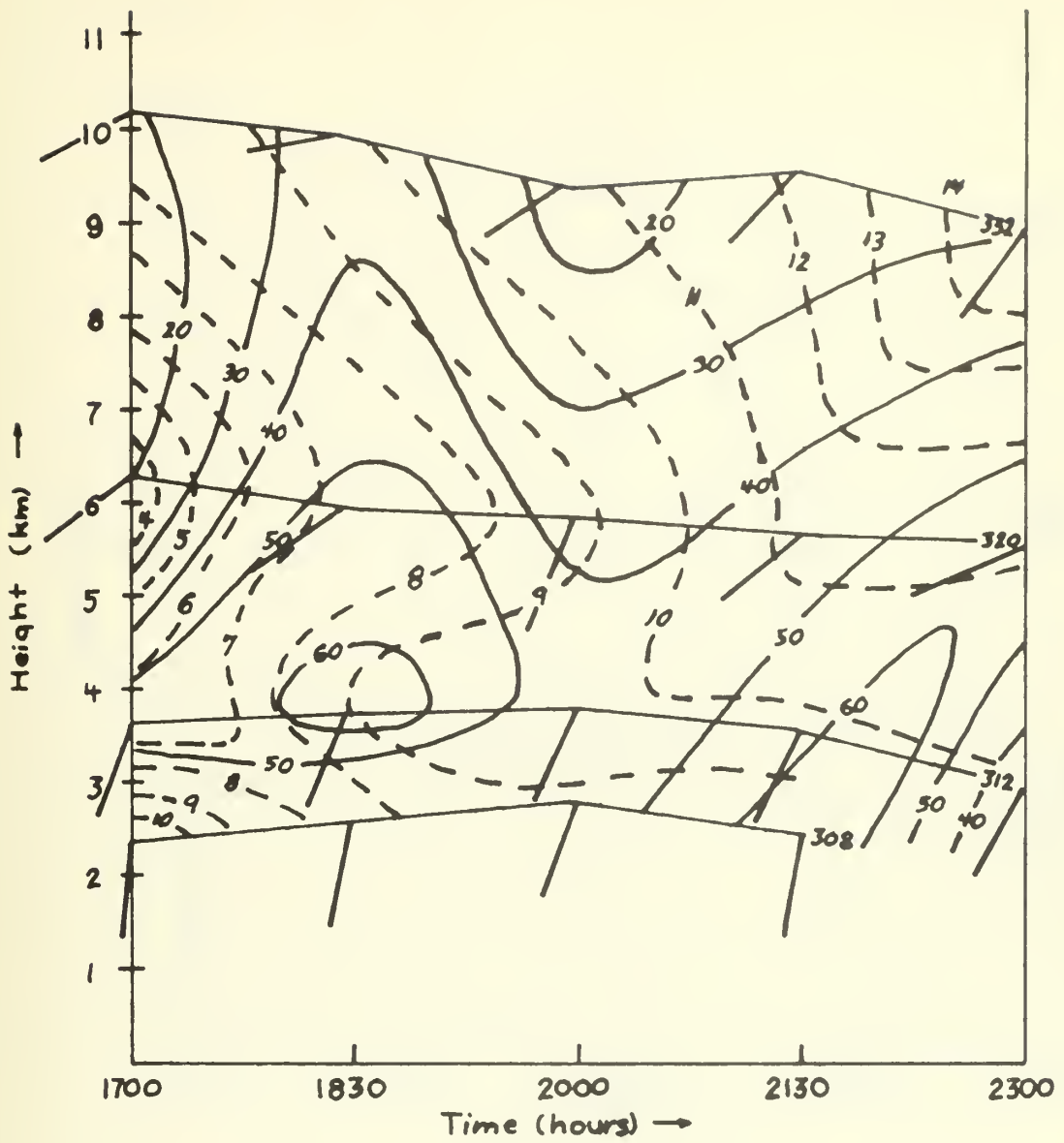


Figure 17c, Time section at station CHK, For explanation see fig, 17a,

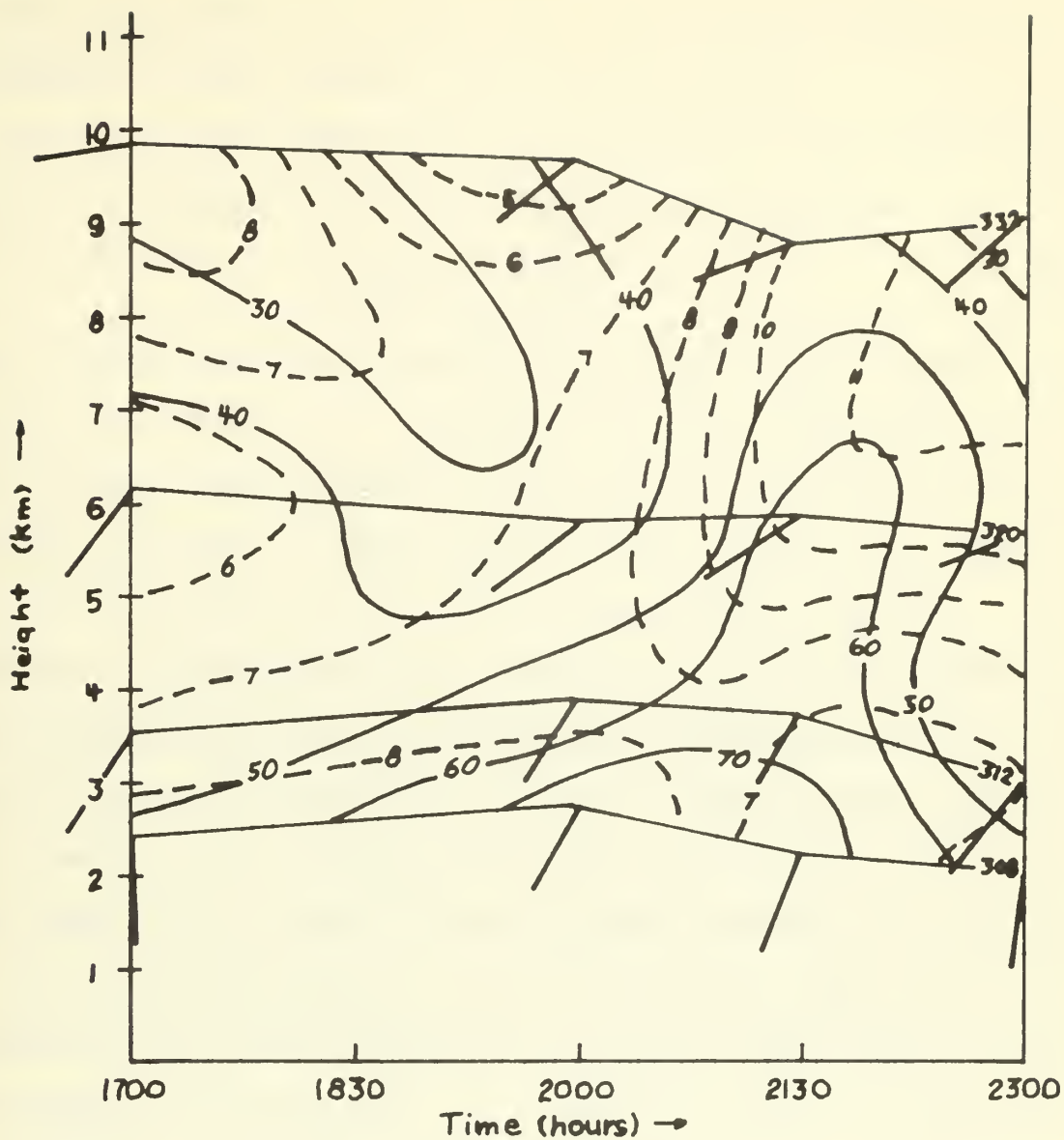


Figure 17d, Time section at station TIK, For explanation see fig, 17a,

the 332K theta surface. This wind shift could be further evidence of the passage of a wave through the area around 1700 GMT.

The relationship between the horizontal curvature of the trajectory (K_H) and the streamline (K_S) can be related by Blaton's equation:

$$K_H = K_S + \frac{1}{V_S} \frac{\partial ff}{\partial t} \quad (13)$$

where V_S is in the wind speed and $\frac{\partial ff}{\partial t}$ is the local rate of turning of the horizontal wind direction. At station FSI (Fig. 17b) $\frac{\partial ff}{\partial t}$ is positive, thus K_H should be greater than K_S , which is what is observed (Fig. 18). At station CHK (Fig. 17c) $\frac{\partial ff}{\partial t}$ is negative, thus K_H should be less than K_S , which is also the case (Fig. 18). If the streamlines are wave-shaped and if the wave moves with a speed greater than the mean wind speed, the curvature of the streamlines and trajectories may be of opposite sign and the trajectories will have a curvature greater than the streamlines. This approach implies that a wave having a phase speed greater than the mean wind speed is indeed present in the region.

The 1700-1830 GMT vertical motion, 1700 GMT static stability and divergence patterns were superimposed upon the 1700 GMT streamline flow on the 332K theta surface (Fig. 18). A parcel of air, with respect to a wave that is traveling faster than the mean wind speed, is actually moving toward the west. Thus the air parcels are experiencing convergence, sinking motions and entering a stability minimum area in the western portion of the grid.

From the conservation of potential vorticity on an isentropic surface, which is given by:

$$\frac{d}{dt} (\zeta_\theta \sigma) = 0 \quad (14)$$

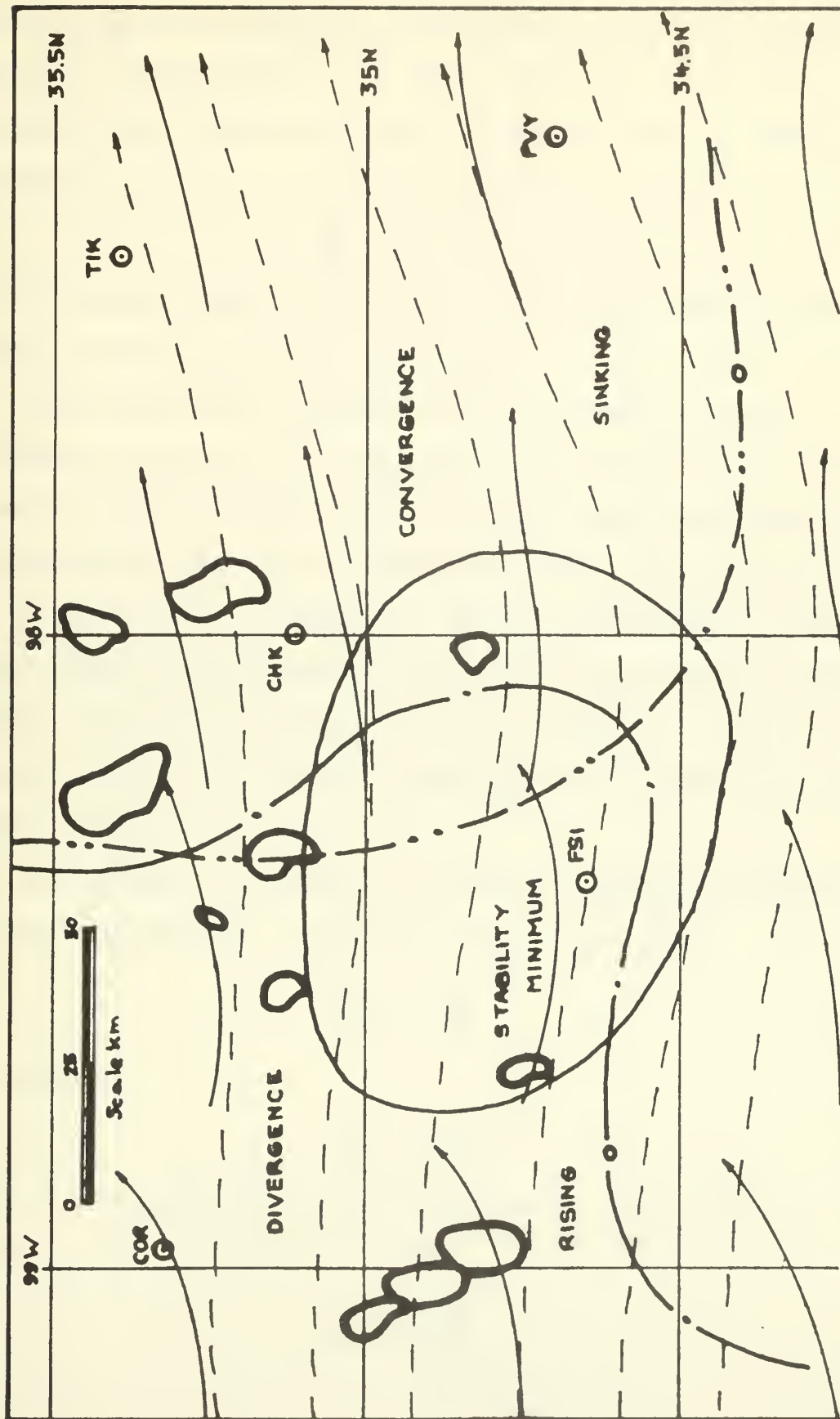


Figure 18, 332K. Theta surface, 1700 GMT streamlines (—), static stability (---), 1830 GMT storm position, 1700-1830 GMT trajectories, (— · —), 1700-1830 GMT vertical motion (— · — · —), 1830 GMT storm position, 1700-1830 GMT trajectories,

where ζ_θ and σ are defined as in equations (3) and (7), an air parcel entering a trough region would normally experience an increase in vorticity, thus requiring a decrease in static stability. From the continuity equation in isentropic coordinates in the form:

$$\frac{d\sigma}{dt} - \sigma \nabla_\theta \cdot V = 0 \quad (15)$$

it is seen that, where σ is positive, a parcel experiencing convergence must have a decrease in static stability.

There thus appears good evidence of the presence of a wave phenomenon in the region in the early stages of storm activity. There also is a good indication that the wave has a phase speed greater than the mean wind speed. The 1700 GMT model on the 332K isentropic surface gives evidence that the parameters can only be consistent for a wave speed greater than the mean wind speed. With this dynamically consistent model there has been established a region conducive to convective activity for the 1700-1830 GMT period which could initiate the severe storm activity.

For adiabatic, frictionless flow along a streamline, the equation of motion in isentropic coordinates reduces to the form:

$$\frac{dV_s}{dt} = - \frac{\partial M}{\partial S} \quad (16)$$

By assuming:

$$\frac{\partial}{\partial t} = - C \frac{\partial}{\partial s} \quad (17)$$

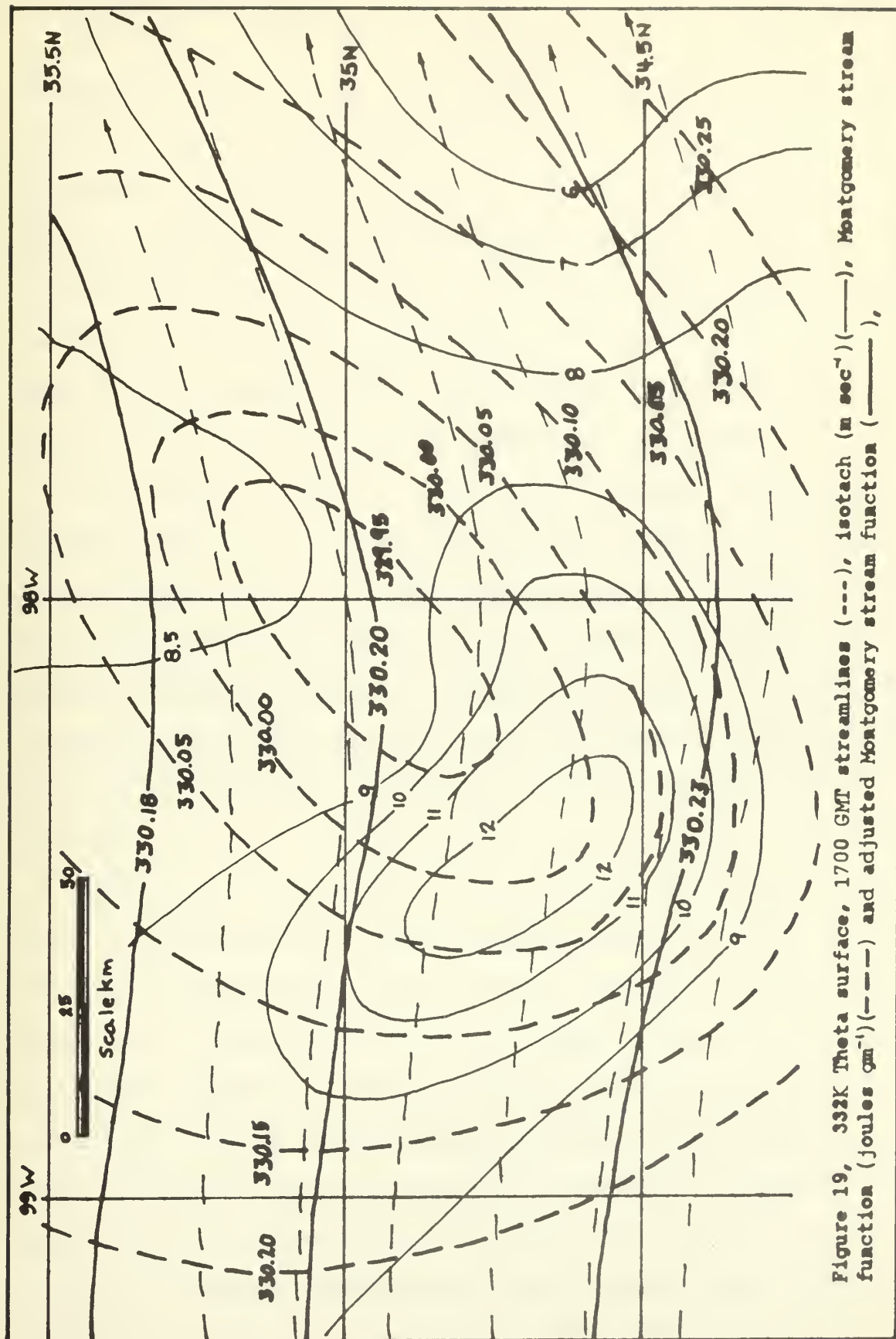
where C is the phase speed, equations 16 and 17 can be reduced to the form:

$$C = V_s + \frac{\frac{\partial M}{\partial S}}{\frac{\partial V_s}{\partial S}} \quad (18)$$

where V_s is the mean wind speed. Now by assuming a phase speed of twice the mean wind speed, a relationship for adjusting the mass field to the wind field can be obtained in the form:

$$\frac{\partial M}{\partial S} = V_s \frac{\partial V_s}{\partial S} \quad (19)$$

such that $\Delta M = \Delta V_s$ along the streamline for the same Δs . Figure 19 illustrates the adjustment that is necessary in the Montgomery stream function field. This adjusted field is dynamically consistent with the model that has been established on the 332K theta surface at 1700 GMT. Air parcels, moving with respect to the wave, which are experiencing an acceleration are also experiencing a decrease in Montgomery stream function. Thus knowledge of the wave in the region can be helpful in adjusting the mass and wind fields such that they are dynamically consistent.



5. PROBLEMS ENCOUNTERED

One of the most demanding and important parts of the research are the initial analyzed fields. The problem has required the analysis of 100 data fields. Proper analysis involves both spatial and time considerations, as well as dynamical and thermodynamical relationships between variables. The horizontal gradients are very important as interpolations are made between network stations. Subjective smoothing can destroy the very detail that may well be important, but at the same time under smoothing may produce anomalies that invalidate subsequent studies. Station bias must be carefully considered.

On the synoptic scale, the normal concern of changes in a certain parameter that must be detected over a specified distance or time will usually be expressed in, say, whole numbers. However, for mesoscale work one must detect changes that amount to tenths or hundredths for a specified distance or time. The instrumentation for data collecting is the same for both scales of motion, thus the sensitivity of the instruments and the magnitude of instrument error and measurements is very critical.

Engelmann and Davis (1968) have found that the standard observational error in radiosonde data will give a computational error of $0.04 \times 10^7 \text{ cm}^2 \text{ sec}^{-2}$ in the Montgomery stream function. These errors result from errors in the instruments and receiving equipment, baseline check and in the mean temperature. The M fields were analyzed for each $0.05 \times 10^7 \text{ cm}^2 \text{ sec}^{-2}$ interval, which is about the value of the computational error. Thus the M values and analyses fields contain inaccuracies which effect calculations using these fields. It was seen in section 4D that the Montgomery stream function fields required rather large adjustments in order to be dynamically consistent with the winds.

Figures 20a-20e indicate the changes in the analyses for the 320K isentropic surface at time 2000 GMT when balloon displacement, location of the storm at analysis time, and a conscientious effort toward spatial and time continuity were made. The 320K surface was selected as a comparison for the re-analysis since its height fluctuations were minimal over the entire grid and between each data time. Isolines of Montgomery stream function were oriented along streamlines and rapid changes perpendicular to the flow were minimized. Pressure isolines were also oriented along the flow, as were relative humidity values. Also larger values of relative humidity were analyzed for, in the vicinity of the storm. Wind direction and speed considerations were carefully matched, particularly with respect to time continuity.

The effects of the re-analyses on the trajectories and values of the associated parameters were investigated to determine if any significant changes resulted. Figure 21 shows the comparison between the initial analysis (IA) and the re-analysis (RA) for selected trajectories and their associated parameters. Vertical motion (VM) (mb hr^{-1}), acceleration (A) (m sec^{-1}), vorticity change (V CHG) (sec^{-1}), divergence change (D CHG) (sec^{-1}), total energy change (TE CHG) (10^7 erg gm^{-1}), static stability change (SS CHG) ($^{\circ}\text{K mb}^{-1}$) and potential vorticity change (PV CHG) ($10^{-10} ^{\circ}\text{K sec cm gm}^{-1}$) are given for each of the trajectories. Vertical motions and accelerations are smaller for the re-analyzed case and there are two cases which have sign changes. The re-analyzed trajectories have more cyclonic curvature in the vicinity of the storm, and trajectory 1 has more anticyclonic curvature. Other parameters show little difference.

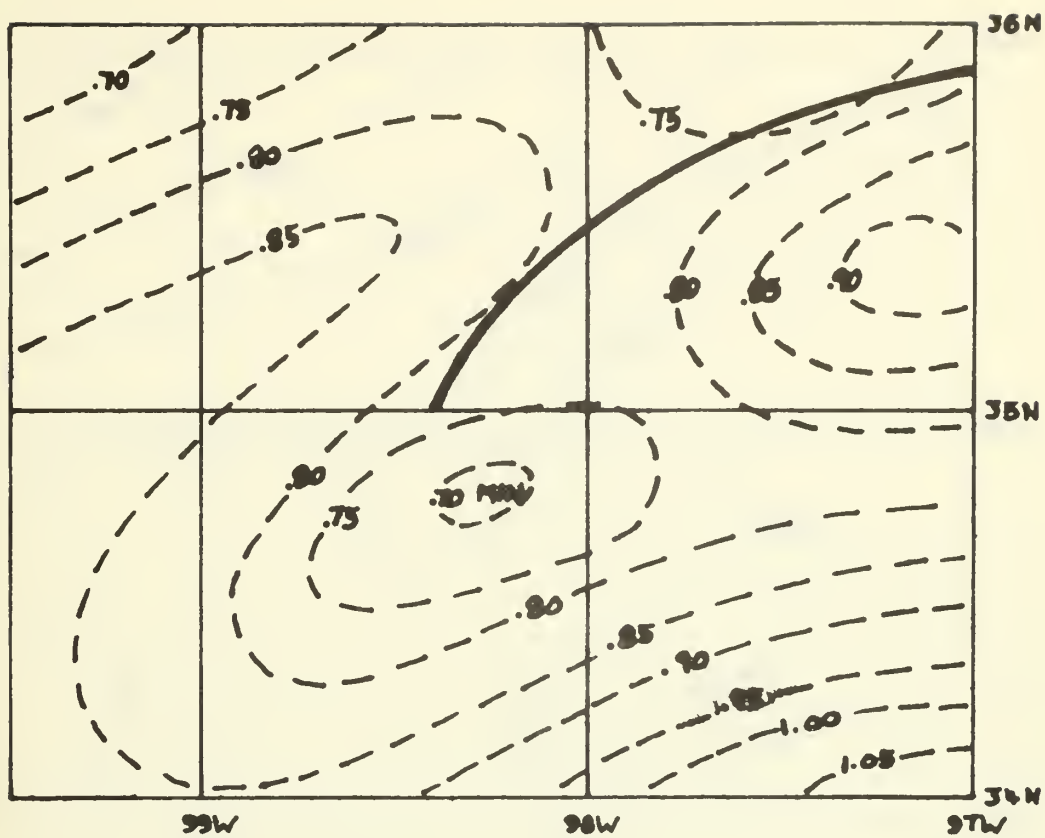


Figure 20a, 320K Theta surface, 2000 GMT Montgomery stream function re-analysis, See fig, 2a for explanation,

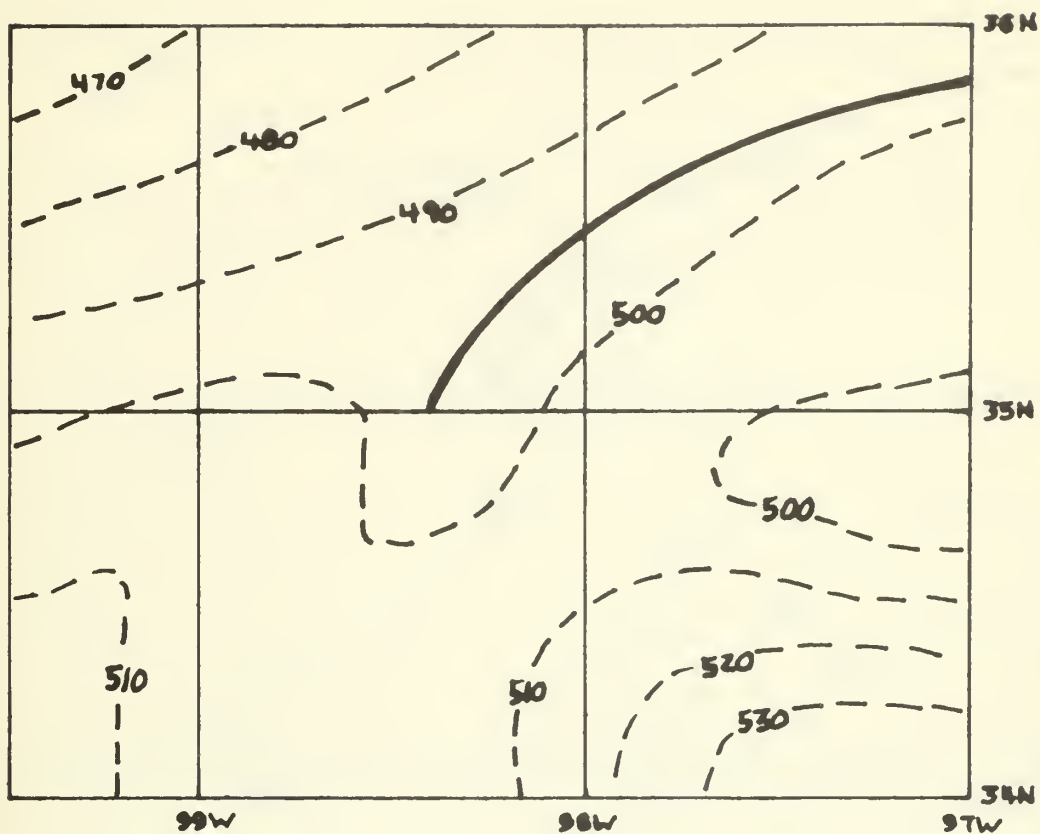


Figure 20b, 320K Theta surface, 2000 GMT pressure (mb)
re-analysis,

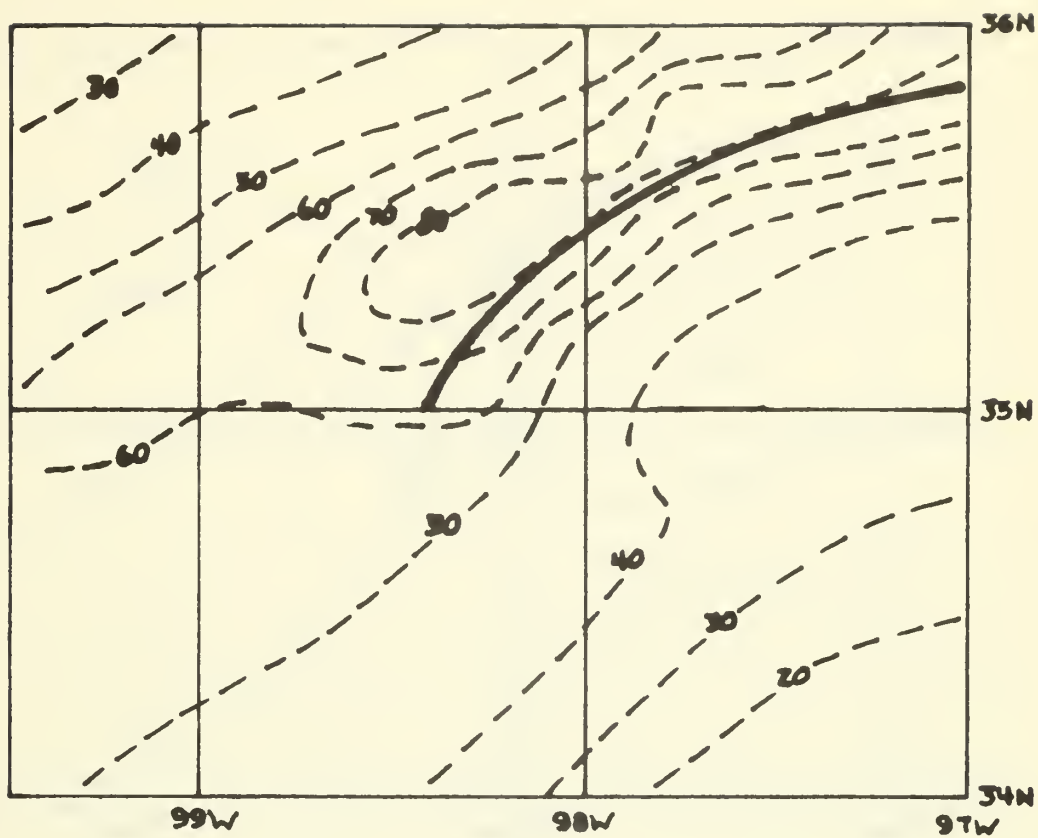


Figure 20c, 320K Theta surface, 2000 GMT relative humidity (%) re-analysis,

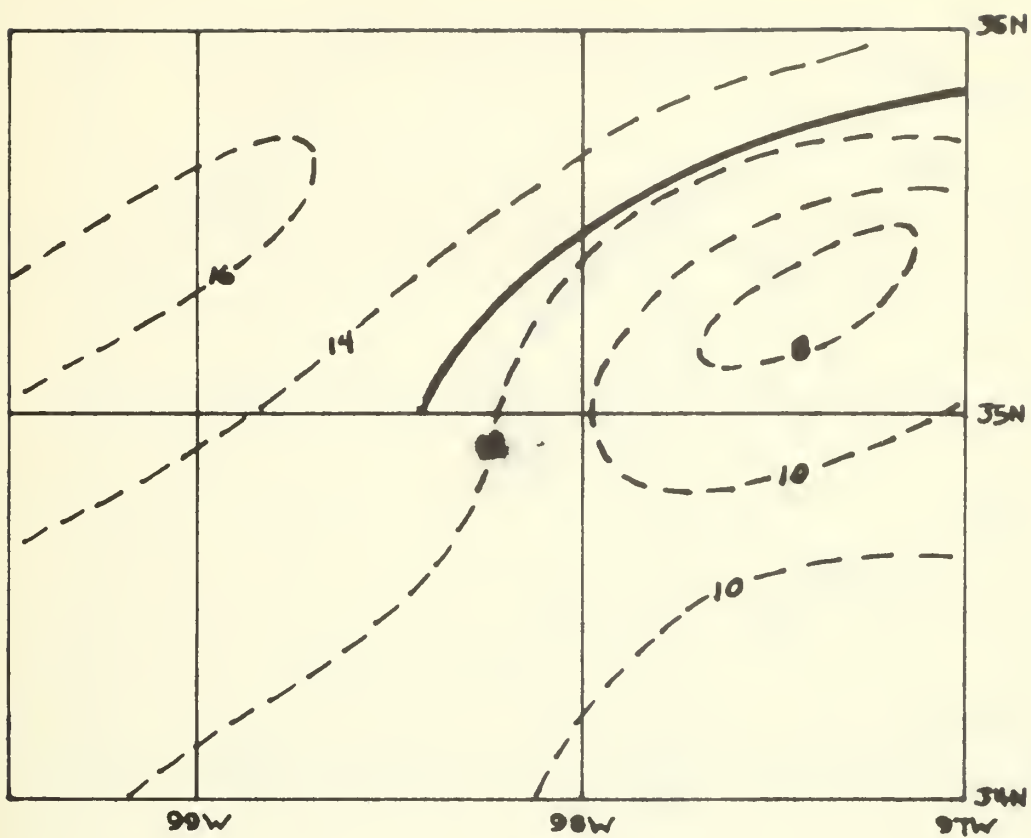


Figure 20d, 320K Theta surface, 2000 GMT wind speed (m sec⁻¹) re-analysis,

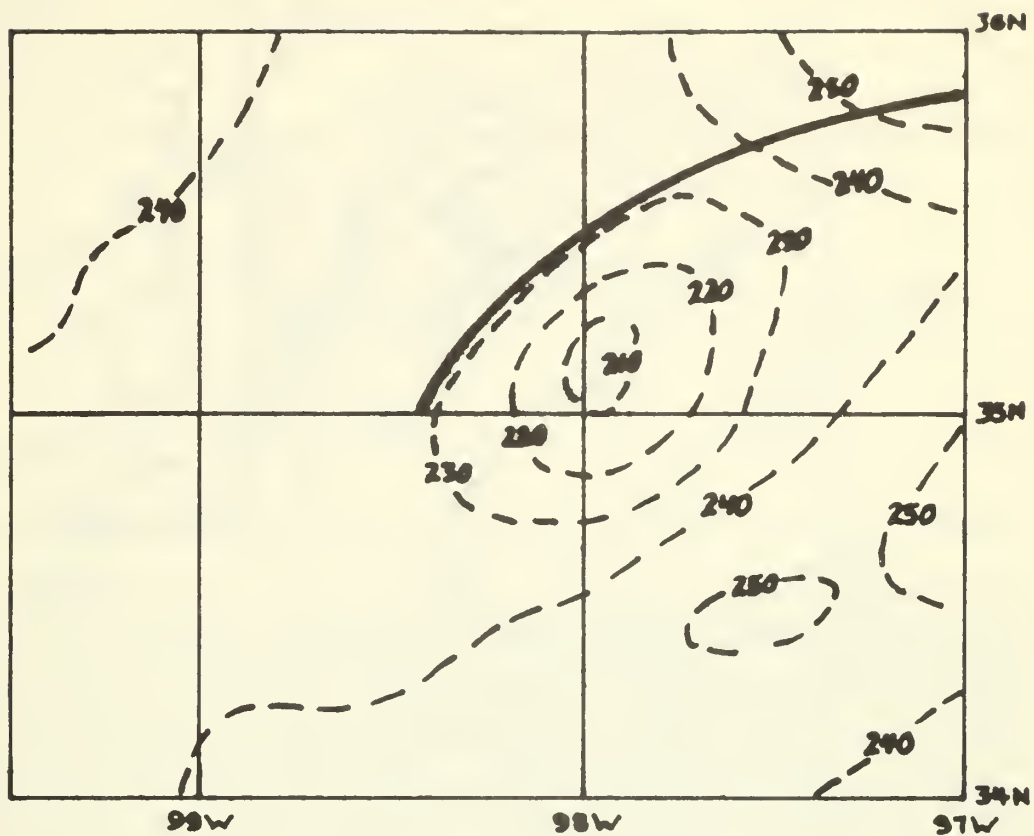
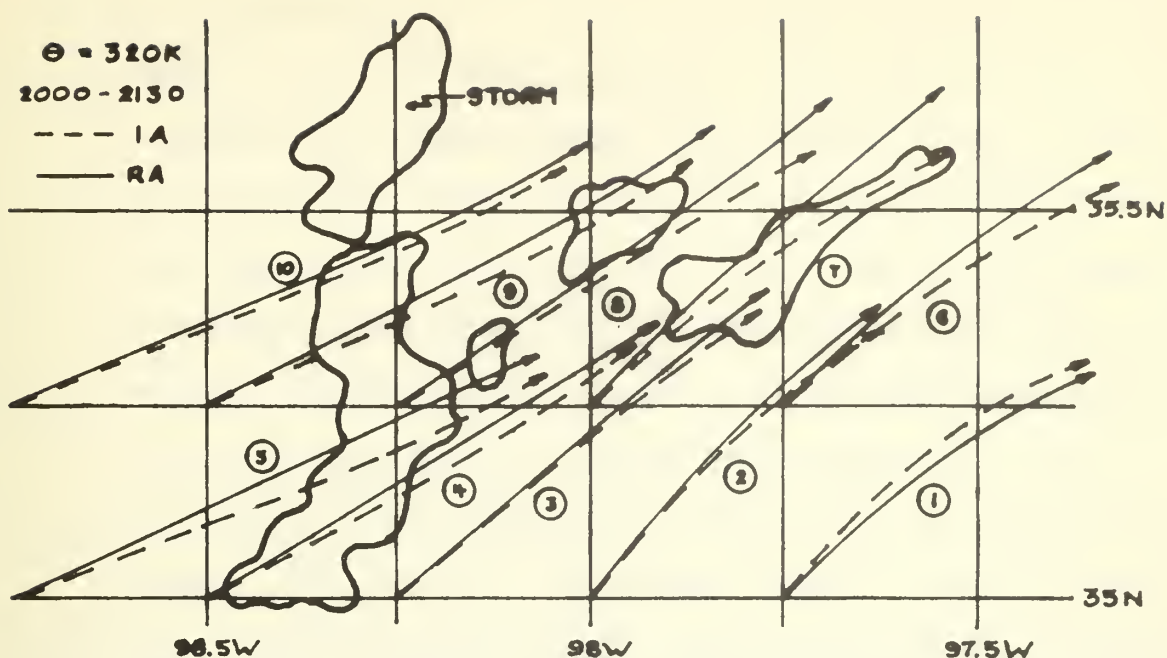


Figure 20e, 320K Theta surface, 2000K wind direction (degs from north) re-analysis,



TRAJ	VE	A	V CHG	D CHG	TE CHG	SS CHG	PV CHG
1	IA	2.0	1.2	- 0.23	0.19	0.74	.001
	RA	1.4	1.3	- 0.58	0.34	0.55	0.0
2	IA	2.0	1.2	- 0.88	0.55	0.81	-.001
	RA	- 0.1	0.9	- 0.43	0.73	0.87	- .002
3	IA	4.9	0.2	- 0.71	1.46	0.58	- .001
	RA	2.5	- 0.3	- 0.21	1.32	0.43	- .001
4	IA	7.1	- 0.7	- 0.45	0.79	0.17	.002
	RA	2.5	- 0.6	- 0.01	0.37	0.44	0.0
5	IA	6.7	- 1.2	0.51	- 0.23	- 0.23	.003
	RA	2.2	- 0.9	0.58	- 0.33	0.42	.002
6	IA	- 5.3	1.8	1.21	0.10	0.95	- .006
	RA	- 4.5	2.3	0.76	0.17	1.27	- .003
7	IA	- 5.4	1.2	0.63	1.12	0.95	- .008
	RA	- 3.1	0.9	0.14	1.83	1.15	- .003
8	IA	0.6	0.0	- 0.08	1.61	0.86	- .004
	RA	- 0.1	- 0.1	- 0.58	1.48	0.41	- .001
9	IA	4.8	- 1.0	0.02	0.12	0.58	- .001
	RA	1.7	- 0.6	0.22	0.02	0.10	.002
10	IA	5.9	- 1.5	0.14	- 0.39	0.15	.001
	RA	2.6	- 0.9	0.95	- 0.50	0.87	.003

Figure 21, Initial and re-analysis comparison,

Using equation 16 and the 2000-2130 GMT accelerations that were computed from the kinematic isentropic trajectories, the expected changes in the Montgomery stream function values along a selected ΔS of 50 KM were computed at various areas over the grid on the 320K theta surface (Fig. 22). The solid black lines are the analyzed M field based on the data at the nine NSSL upper air stations at 2000 GMT. The values are given in units of $10^7 \text{ cm}^2 \text{ sec}^{-2}$. The dashed black lines represent the 2000-2130 GMT accelerations ($\text{m sec}^{-1} \text{ hr}^{-1}$) and the short green lines are the position of ΔS over the area. In Table 1 a comparison of the predicted value and measured value for the M values are given. In many cases there is almost an order of magnitude difference, with the predicted values having a much lower absolute value. Using these predicted changes and approximate values at each station, an adjustment to the M field was made (Fig. 22 - red dashed lines). This new M field is now dynamically consistent with the winds. It would thus seem that the Montgomery stream function and hence the temperature and height fields are in error. It is not conclusive however, but along with the adjustments in the M field discussed in Section 4D there appears to be unacceptable errors in the initial data fields of Montgomery stream function. From this point of view, therefore it appears the wind data is more accurate.

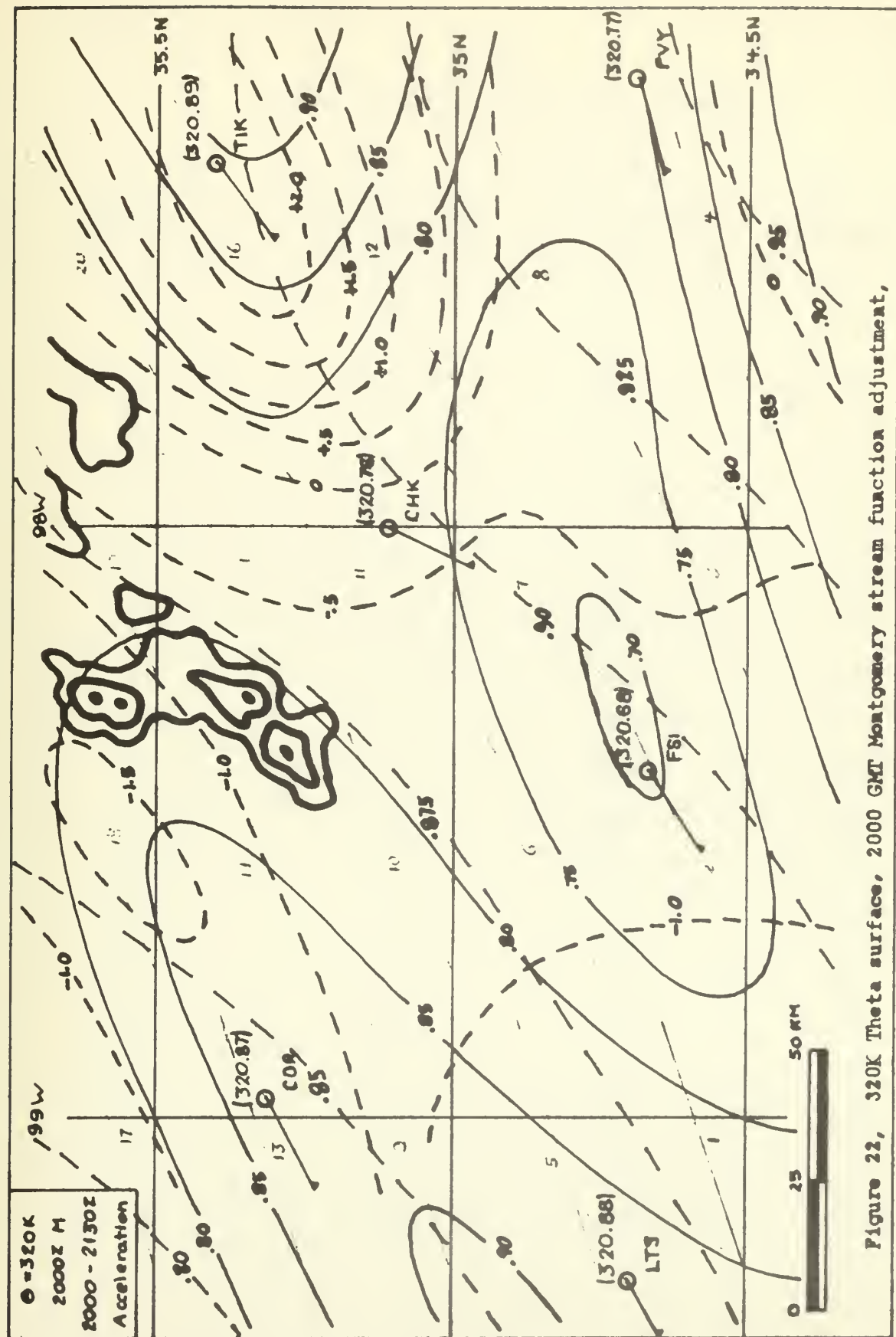


TABLE 1

Predicted and Measured M Value Comparison

Calculation Point	Acceleration (m sec ⁻¹ hr ⁻¹)	M Predicted (cm ² sec ⁻²)	M Measured (cm ² sec ⁻²)
1	-1.4	+0.020	-.08
2	-0.9	+0.013	-.07
3	-0.5	+0.007	0.03
4	-0.1	+0.001	0.01
5	-1.3	+0.018	0.05
6	-0.9	+0.013	-.01
7	-0.6	+0.008	+0.06
8	-0.2	+0.003	+0.05
9	-1.0	+0.014	-.05
10	-0.8	+0.011	-.03
11	-0.4	+0.006	+0.03
12	+1.1	-.016	+0.14
13	-1.2	+0.017	+0.01
14	-1.0	+0.014	-.04
15	-0.4	+0.006	-.01
16	+2.0	-.028	+0.05
17	-0.9	+0.013	+0.01
18	-1.5	+0.021	-.04
19	-0.7	+0.010	-.03
20	+1.0	-.014	0.0

6. COMPARISON WITH THEORY

In the basic assumption of frictionless, adiabatic flow along an isentropic surface, on which the study was based, there are three parameters which should be conserved for an air parcel moving in the flow. These parameters are potential temperature (θ) ($^{\circ}\text{K}$), specific humidity (q) (gm gm^{-1}) and potential vorticity (P) ($10^{-10} \text{ }^{\circ}\text{K sec cm gm}^{-1}$). The initial input fields into the computer program were analyzed on constant theta surfaces, thus the program constrained theta to be conserved for each trajectory. However, specific humidity and potential vorticity were allowed to vary.

Selected composite trajectories were studied in order to determine both short (1.5 hour) and long (6 hour) term variations. In Figure 22 and Table 2 the deviations are shown for the 320K theta surface. Vertical motions (w) (mb hr^{-1}), accelerations (A) ($\text{m sec}^{-1} \text{ hr}^{-1}$), static stability (σ) ($^{\circ}\text{K mb}^{-1}$) and total energy (TE) (10^7 erg gm^{-1}) were also studied in conjunction with the conserved properties to determine if any correlations exist. Trajectories labeled 1A-1F are for 1700-1830 GMT; 2A-2F for 1830-2000 GMT; 3A-3F for 2000-2130 GMT; and 4A-4F for 2130-2300 GMT. Both initial (i) and final (f) values for each of the properties are given.

With the exception of 1A-1F trajectories, the specific humidity was somewhat conserved for each trajectory. Changes are random and do not appear to be associated with vertical motions or accelerations. Trajectories 2E and 3F indicate their deviations may be from the storm effects, since their initial point is outside the storm and final point inside the storm region.

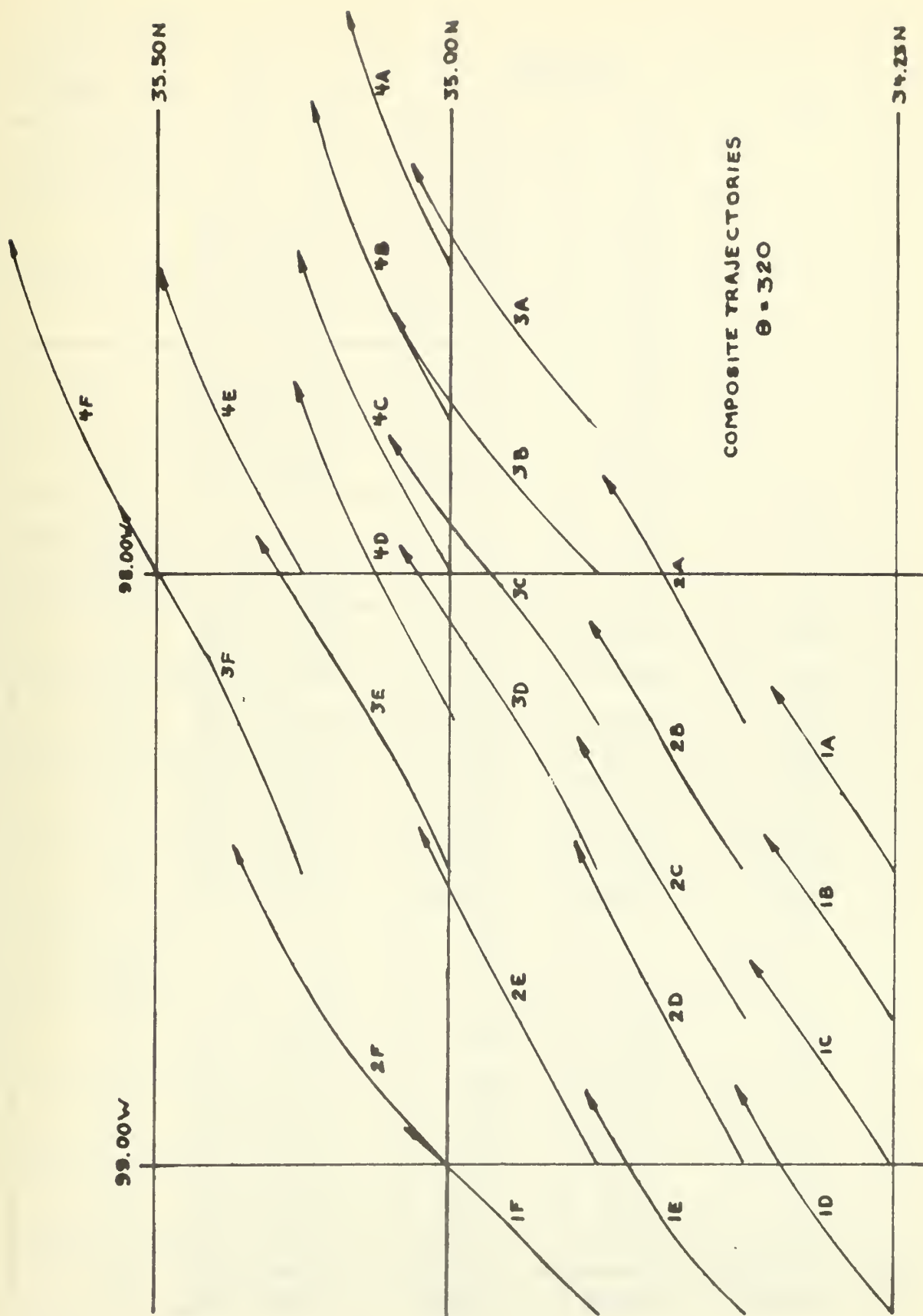


Figure 23, 320K Theta surface composite trajectories,

THETA = 320		TRAJECTORY			
		1A	2A	3A	4A
ω		-7,5	-1,1	+7,4	
A		-0,3	+3,2	-0,9	
q	i	,0007	,0012	,0012	
	f	,0011	,0012	,0014	
σ	i	,051	,051	,050	
	f	,051	,051	,055	
p	i	60,56	48,51	94,05	
	f	49,62	106,34	29,63	
TE	i	321,64	322,12	322,11	
	f	322,09	322,15	322,40	
		1B	2B	3B	4B
ω		-6,7	-3,8	+5,6	+5,3
A		-0,2	+3,1	-0,7	-0,1
q	i	,0005	,0013	,0013	,0015
	f	,0013	,0015	,0016	,0019
σ	i	,051	,052	,052	,053
	f	,052	,052	,055	,042
p	i	51,49	27,33	134,37	25,09
	f	33,58	116,73	26,67	25,25
TE	i	321,51	322,27	322,25	322,48
	f	322,25	322,39	322,56	323,06
		1C	2C	3C	4C
ω		-6,1	-8,3	+8,7	-1,1
A		+0,3	+2,2	-0,6	-0,8
q	i	,0004	,0014	,0018	,0017
	f	,0013	,0018	,0017	,0018
σ	i	,049	,052	,051	,051
	f	,052	,051	,052	,038
p	i	28,19	16,97	92,65	38,11
	f	21,01	81,67	25,83	45,73
TE	i	321,37	322,35	322,77	322,66
	f	322,32	322,71	322,65	322,79

Table 2

		TABLE 2 (Continued)			
		1D	2D	3D	4D
ω		-6,7	-9,5	+9,3	-5,5
A		+1,1	+1,3	-0,8	-1,8
q	i	,0002	,0013	,0017	,0016
	f	,0013	,0017	,0017	,0018
σ	i	,048	,052	,049	,049
	f	,052	,048	,050	,035
ρ	i	33,81	28,46	37,53	84,93
	f	23,14	48,51	34,34	45,99
TE	i	321,18	322,33	322,70	322,58
	f	322,34	322,70	322,69	322,71
		1E	2E	3E	4E
ω		-5,4	-14,7	+7,1	+3,1
A		+1,7	+1,1	-0,7	-2,5
q	i	,0003	,0013	,0017	,0018
	f	,0042	,0016	,0018	,0019
σ	i	,050	,053	,044	,047
	f	,053	,045	,046	,036
ρ	i	19,39	40,21	45,17	34,47
	f	34,25	41,42	26,46	40,29
TE	i	321,26	322,34	322,72	322,77
	f	322,36	322,60	322,89	322,98
		1F	2F	3F	4F
ω		-3,0	-20,7	+4,8	+10,1
A		+2,4	+1,9	-1,0	-1,5
q	i	,0004	,0013	,0016	,0020
	f	,0013	,0014	,0021	,0019
σ	i	,050	,056	,041	,040
	f	,057	,041	,040	,035
ρ	i	19,84	62,96	16,73	18,60
	f	25,51	15,33	17,18	27,46
TE	i	321,42	322,36	322,59	323,03
	f	322,37	322,45	323,17	322,98

7. CONCLUSIONS

The research has demonstrated the critical nature of mesoscale data both in instrumentation and analysis errors. It was found that the wind data were perhaps the most reliable for use in the study. Subsequently the 1.5 hour kinematic isentropic trajectory relationship to the severe local storm warranted considerable exploration. It was further noted that the 320K theta surface (approximately 500 mb) showed the trajectory and air parcel properties which were more closely associated with the life cycle of the storm.

The trajectories indicated that prior to storm development the wind veered with height at all levels, flow was anticyclonic with the exception of cyclonic flow in the NW corner in upper levels, and a wind maximum region existed in the NW corner of the network. With the presence of an inertial-gravity wave at the 332K theta surface at 1700 GMT, the dynamically consistent vertical motions, static stability, convergence, trajectories, streamlines and adjusted Montgomery stream function fields support conditions which could initiate convective activity. It was also noted that the storm is to the NE of the Wichita mountains, and the existence of a lee wave supporting the inertial-gravity wave is worthy of additional studies.

The study of various air parcel properties on the isentropic surfaces has provided insights into the storm dynamics. The 1830-2000 GMT vertical motions indicated supporting rising motions for storm growth. The 2000-2130 GMT, 320K theta surface convergence patterns help to illustrate the intensity of the storm during this period. The lack of supporting vertical motions, and the anticyclonic flow in each level tended to provide the response necessary for decay of the storm over the 2130-2300 GMT period.

The orientation of the storm along the upper level trajectories in the early stages and along the low level trajectories in the latter stages may be indicative of storm movement. When the storm orientation is considered along with the inertial-gravity wave, there exists the possibility the storm formed at high levels and propagated downward into the lower levels. It is concluded that the kinematic isentropic trajectories, over short periods of time, do provide an effective method for studying local severe storm activity in the mesoscale range.

8. SUGGESTIONS FOR FUTURE DEVELOPMENTS AND IMPROVEMENTS

Since the initial data fields are critical to the success of the computer model, it would be of benefit to investigate the application of error analysis techniques in order to improve the initial data. Further studies are necessary when corrections for Montgomery stream function changes can be made, in order to improve the final trajectories. Incorporation of diabatic effects in regions where air parcels are becoming saturated prior to the final trajectory point can be included in the model. Further studies of different storm systems is encouraged in order to test the short period kinematic isentropic trajectories, and to determine if they can be utilized as a forecasting aid. Since there existed deviations in conservation of specific humidity and potential vorticity along the trajectories, additional research will be necessary to investigate the conservation of these properties. With the supporting evidence of an inertial-gravity wave in the region, a theoretical approach is recommended in order to study the phenomenon in the range of wave length and wave speed encountered in this case study.

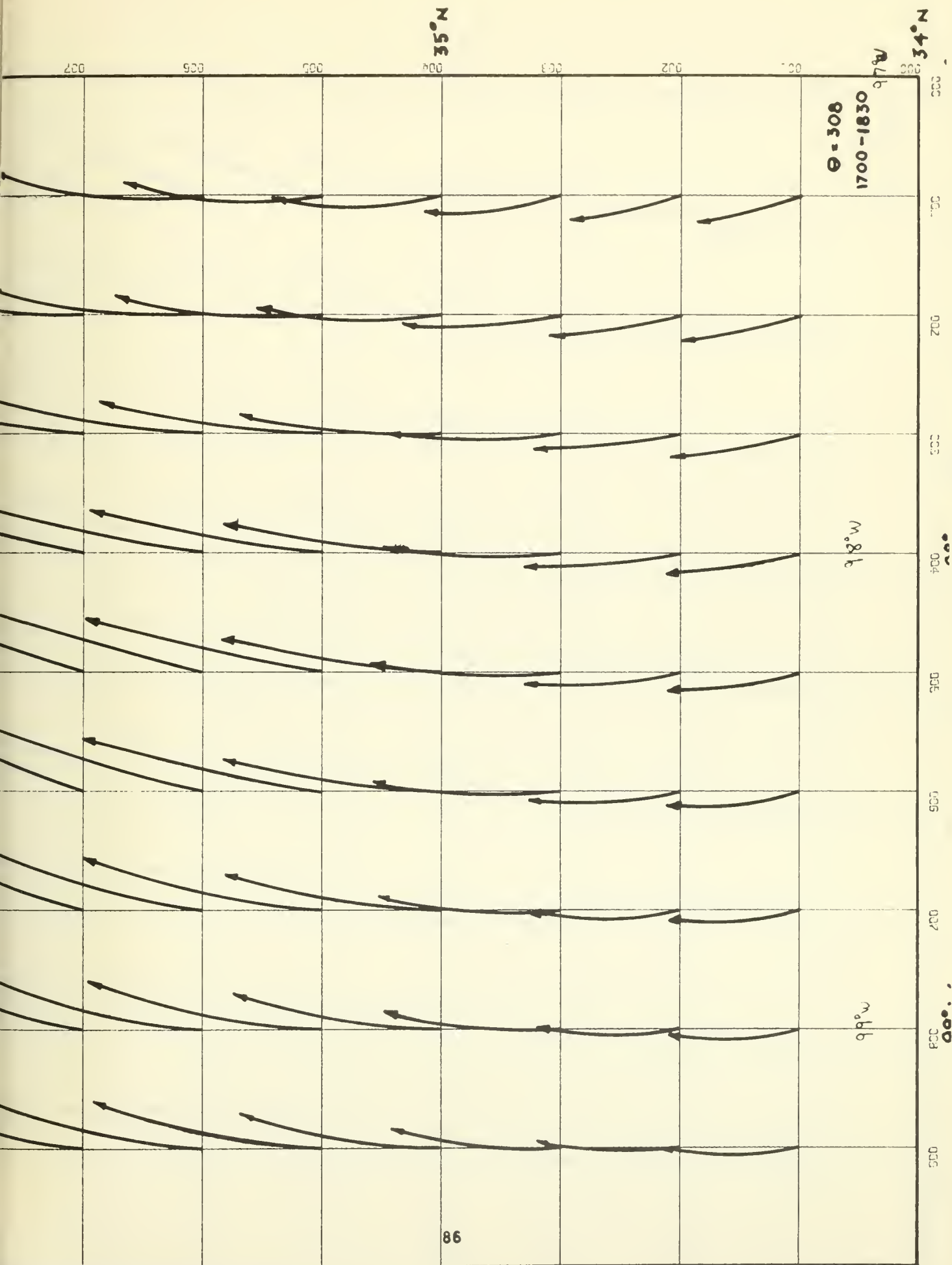
REFERENCE LIST

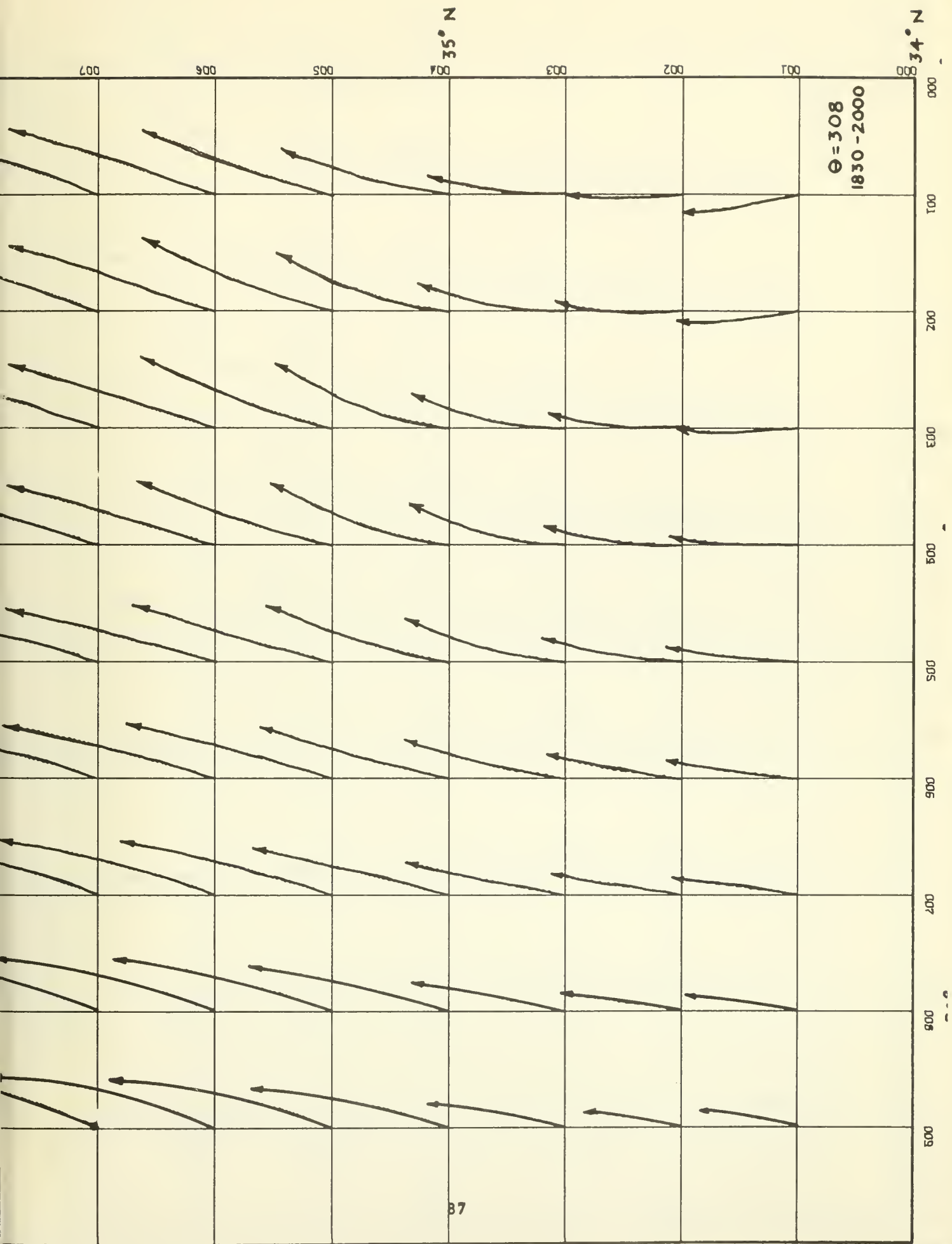
- BRADLEY, W. E. and P. J. FETERIS, 1966: Study of rainout of radioactivity in Illinois. Fifth Progress Report, AEC Contract No. AT (11-1)-1199.
- BROWNING, K. A. and T. FUJITA, 1965: A family outbreak of severe local storms - a comprehensive study of the storms in Oklahoma on 26 May 1963, part I. AFCRL Report No. AFCRL-65-695(1), Special Report No. 32.
- _____, and F. H. LUDLAM, 1962: Airflow in convective storms. Quarterly Journal of the Royal Meteorological Society, Vol. 88, 117-135.
- BYERS, H. and R. BRAHAM, 1949: The Thunderstorm. U. S. Government Printing Office, Washington, D. C., 287 pp.
- CARLSON, T. N. and F. H. LUDLAM, 1968: Conditions for the occurrence of severe local storms. Tellus, Vol. XX, pp 203-226.
- DANIELSEN, E. F., 1959: The laminar structure of the atmosphere and its relation to the concept of a tropopause. Archiv fur Meteorologie, Geophysik und Bioklimatologie, All, 293-332.
- _____, 1961: Trajectories: isobaric, isentropic and actual. Journal of Meteorology, Vol. 18.
- DARKOW, G. L., 1968: The total energy environment of severe storms. Journal of Applied Meteorology, Vol. 7, pp 199-205.
- ENDLICH, R. M. and R. L. MANCUSO, 1968: Objective analysis of environmental conditions associated with severe thunderstorms and tornadoes. Monthly Weather Review, Vol. 96, No. 6, pp 342-350.
- ENGELMANN, R. J. and W. E. DAVIS, 1968: Low-level isentropic trajectories and the midas computer program for the Montgomery stream function. U. S. Atomic Energy Commission Contract AT (45-1)-1830.
- FANKHAUSER, J. C., 1964: On the motion and predictability of convective systems. NSSP Report No. 21, U. S. Weather Bureau.
- _____, 1968: Thunderstorm-environment interactions revealed by chaff trajectories in the mid-troposphere. NSSL Tech. Memo. No. 39, U. S. Weather Bureau.
- FETERIS, P. J. and G. E. STOUT, 1966: Relation of lightning, rainfall, and hail to the properties of mesoscale meteorological patterns. First Progress Report, NSF Contract No. GP-5196.
- HAMMOND, G. R., 1967: Study of a left moving thunderstorm of 23 April 1964. NSSL Tech. Memo. No. 31, U. S. Weather Bureau.

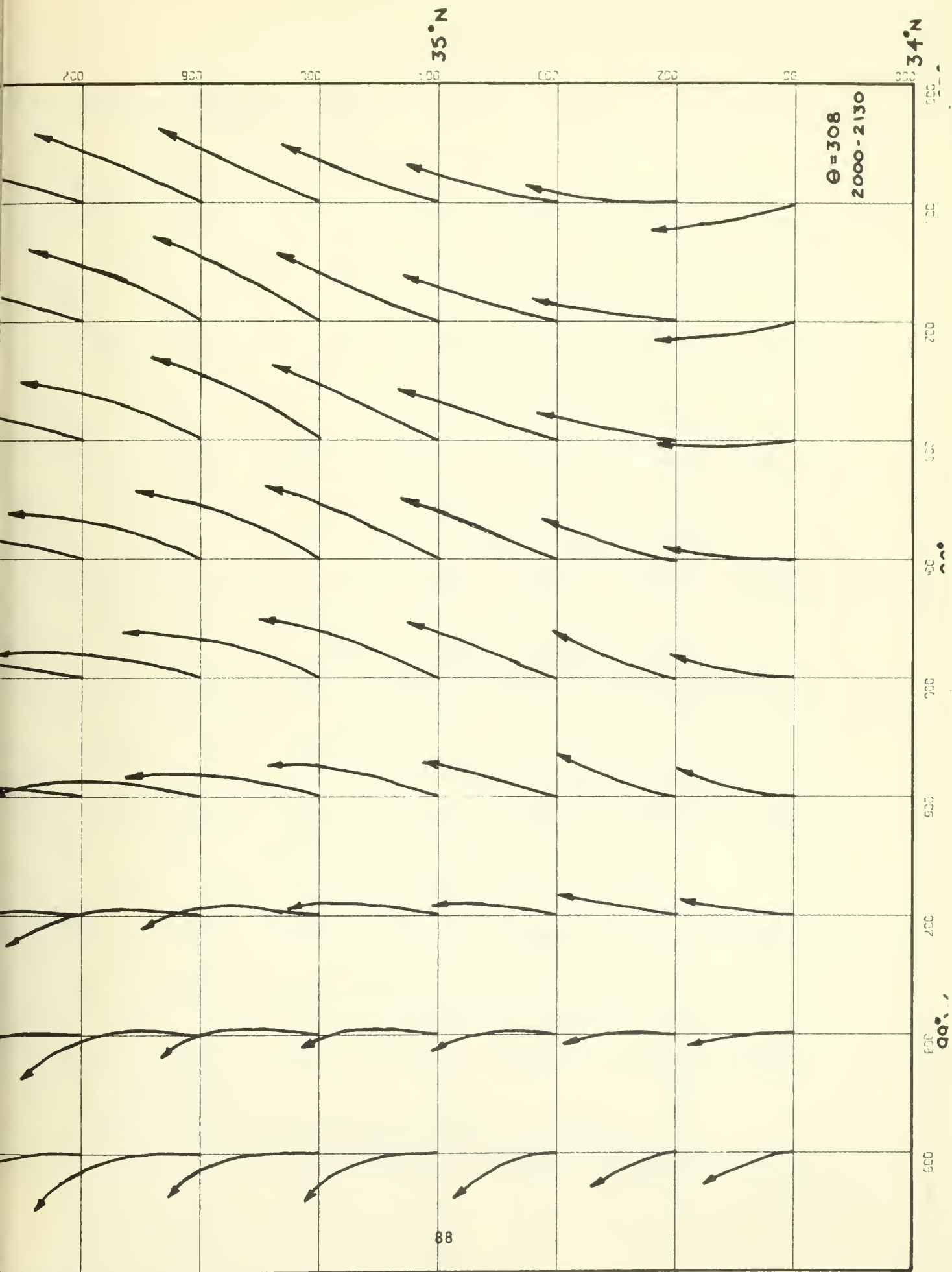
- KREITZBERG, C. W. and W. E. BROCKMAN, 1966: Computer processing of mesoscale rawinsonde data from project stormy spring. AFCRL Special Report No. 41.
- MAHLMAN, J. D., 1968: Numerical methods of computing three-dimensional trajectories for adiabatic and diabatic flows. AFCRL Report No. 68-0357.
- MATSUMOTO, S., K. NINOMIYA and T. AKIYAMA, 1967: Cumulus activities in relation to the mesoscale convergence field. Journal of Meteorological Society of Japan, Vol. 45, No. 4, pp 292-304.
- MILLER, R. C., 1967: Semi-objective evaluation of the relative importance of parameters favoring production of severe local storms. Fifth Conference on Severe Local Storms, 1967.
- NAMIAS, J., 1940: Air Mass and Isentropic Analysis. The American Meteorological Society, Milton, Mass.
- NEWTON, C. W. and J. C. FANKHAUSER, 1964: On the movements of convective storms, emphasis on size discrimination in relation to water-budget requirements. Journal of Applied Meteorology, Vol. 3, pp 651-668.
- REITER, E. R. and E. F. DANIELSEN, 1960: Bemerkungen zu E. Kleinschmidt: Nicht-adiabatische Abkühlung im Bereich des jet stream. Beiträge zur Physik der Atmosphäre, 32, 265-273.
- _____, 1963: A case study of radioactive fallout. Journal of Applied Meteorology, 2, 691-705.
- ROSSBY, C. G. and Collaborators, 1937: Isentropic analysis. Bulletin of the American Meteorological Society, Vol. 18, pp 201-209.
- WILLIAMS, D. T., 1962: A study of the kinematic properties of certain small-scale systems. NSSP Report No. 11, U. S. Weather Bureau.

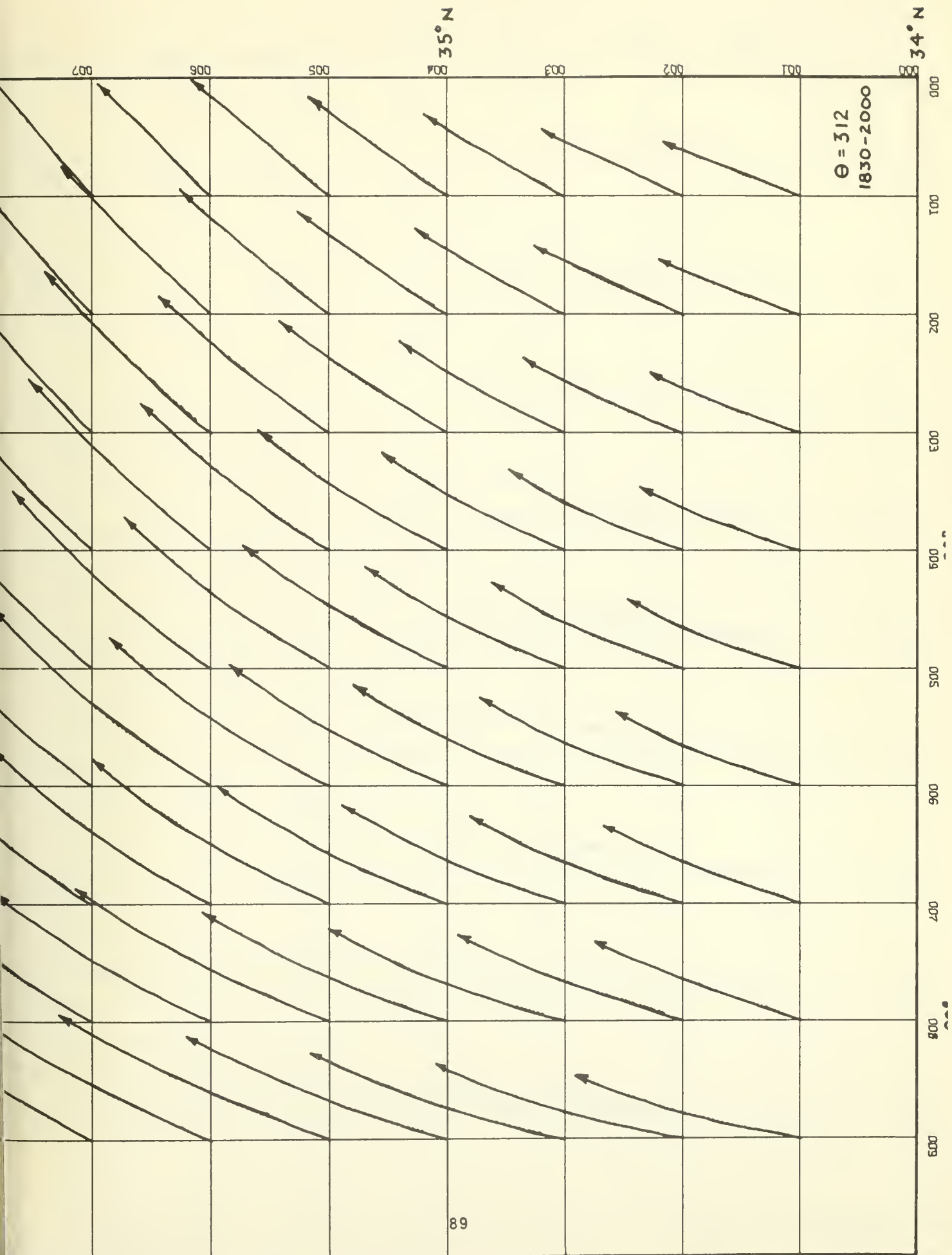
APPENDIX A - ISENTROPIC KINEMATIC TRAJECTORIES

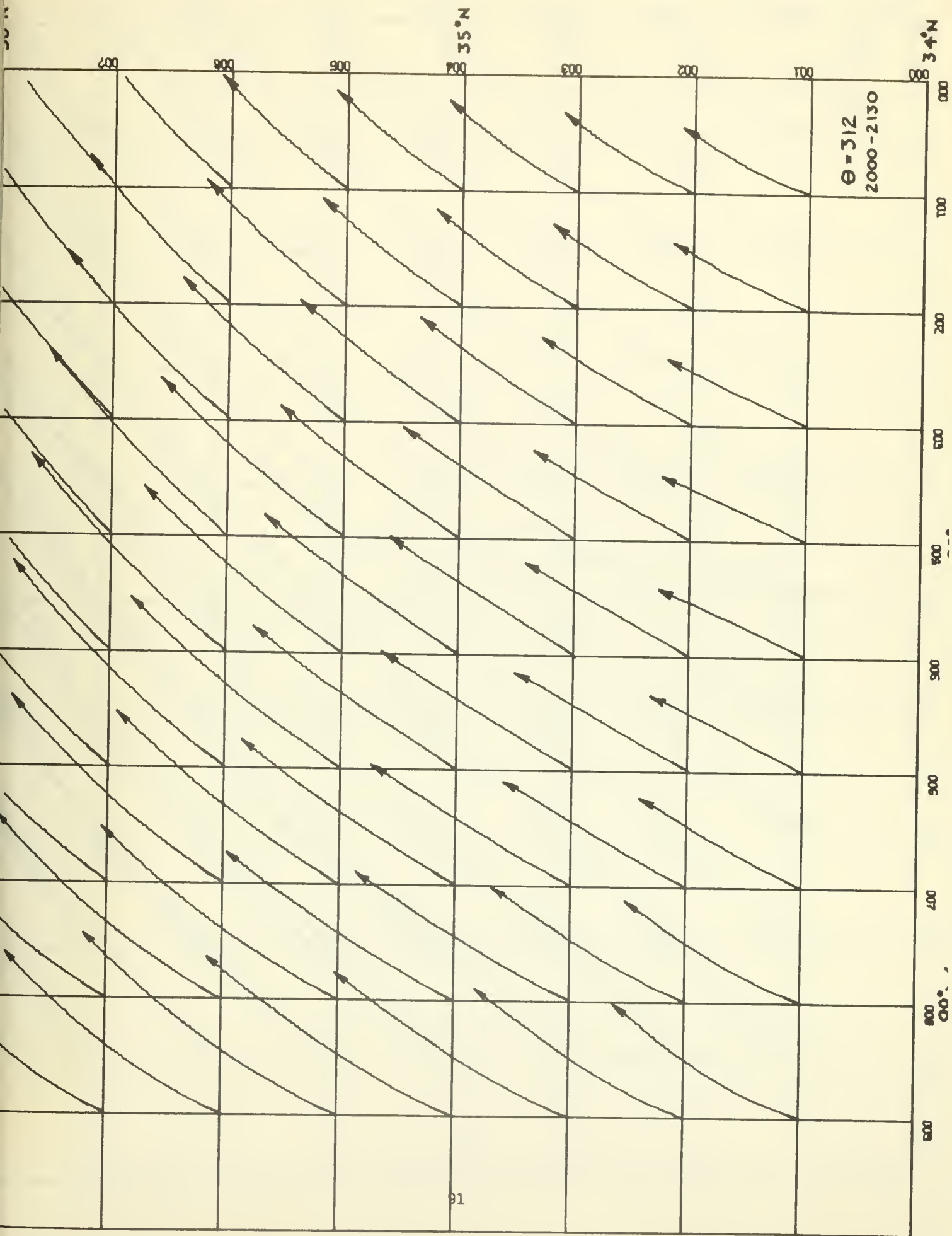
This appendix includes the kinematic trajectories which have been computed for the 308K, 312K, 320K and 332K isentropic surfaces for the time periods 1700-1830, 1830-2000, 2000-2130 and 2130-2300 GMT. They were produced by the objective computer model for the May 28, 1967 severe storm case. The grid is an x, y grid, with equal grid spacing.

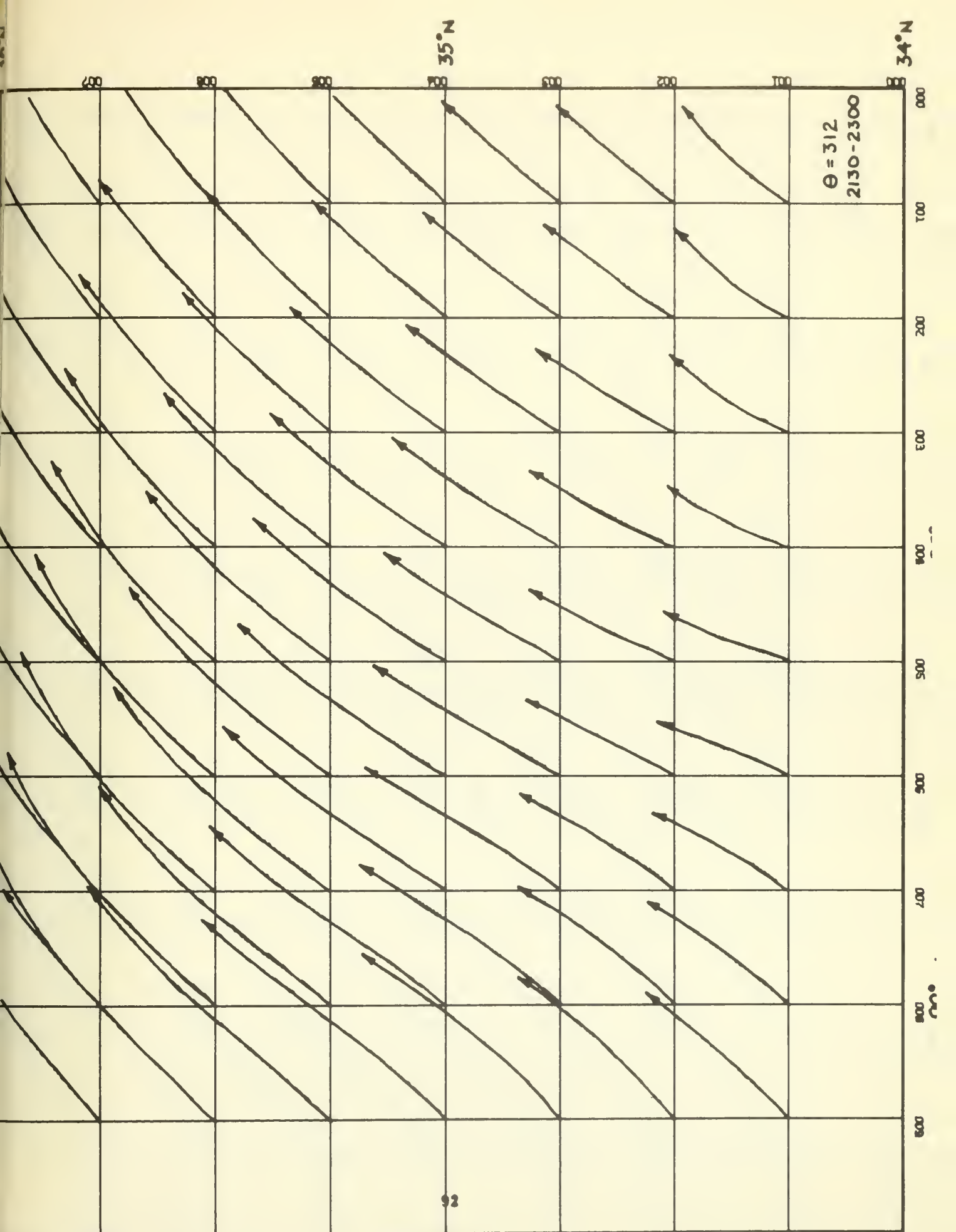


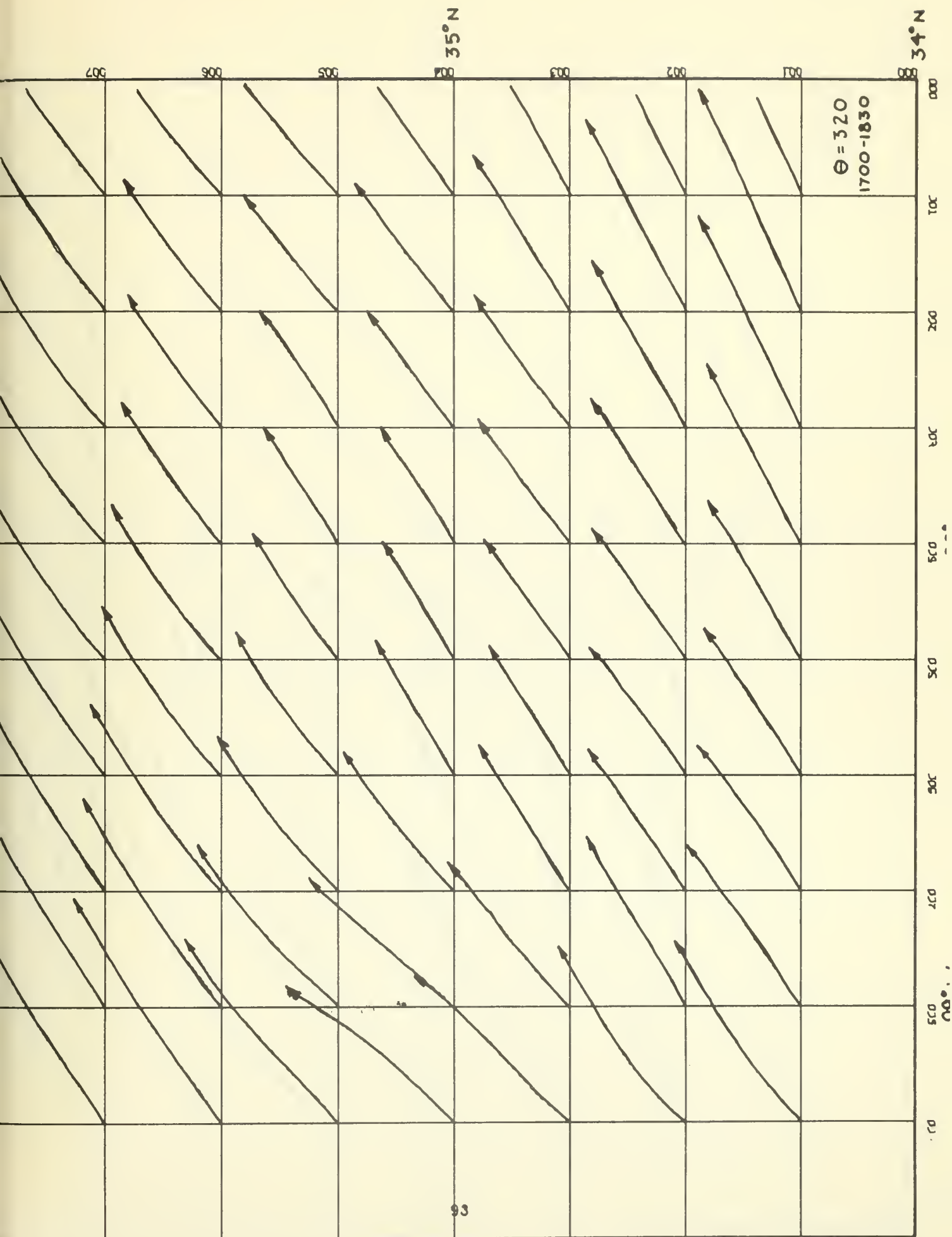


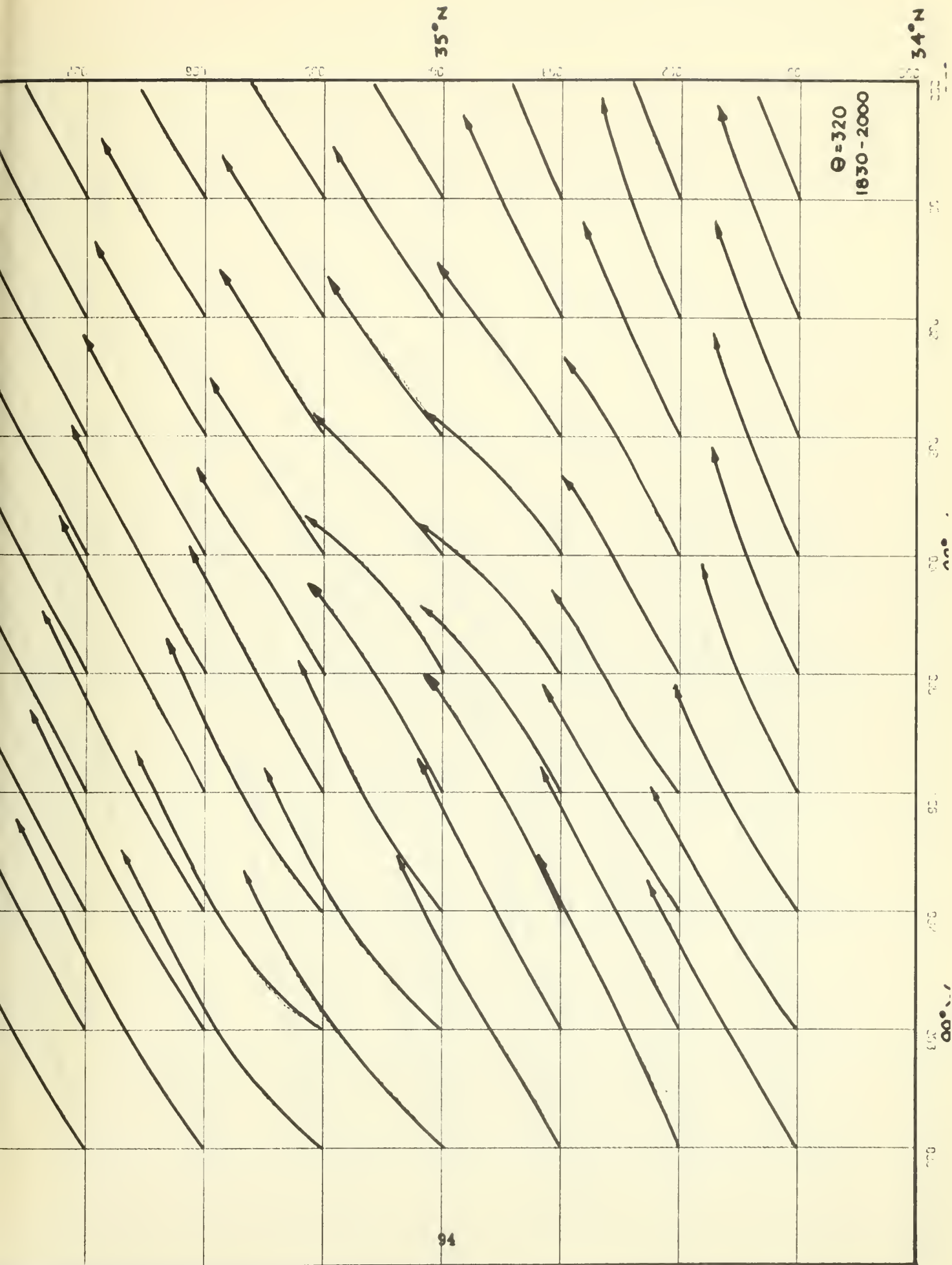


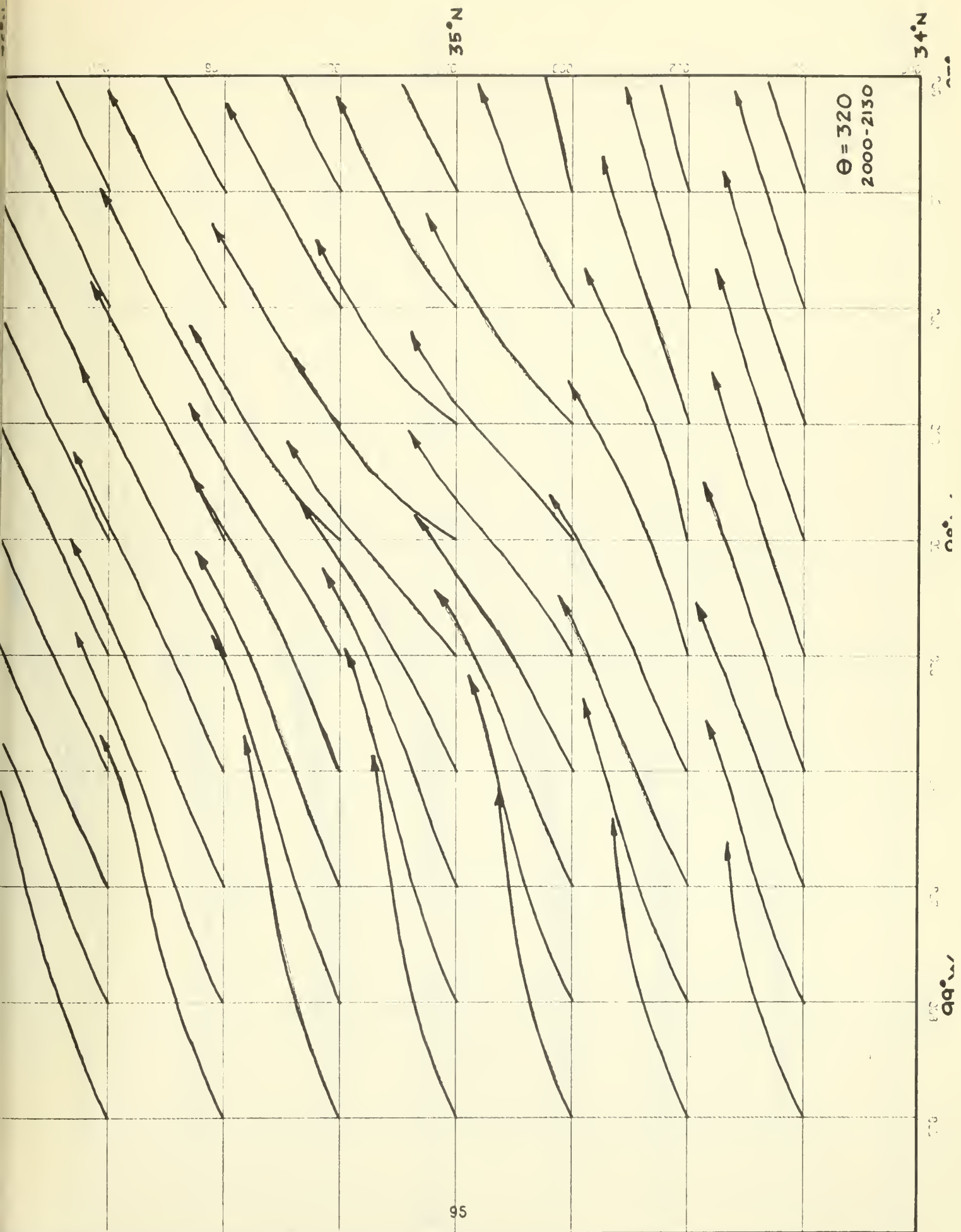


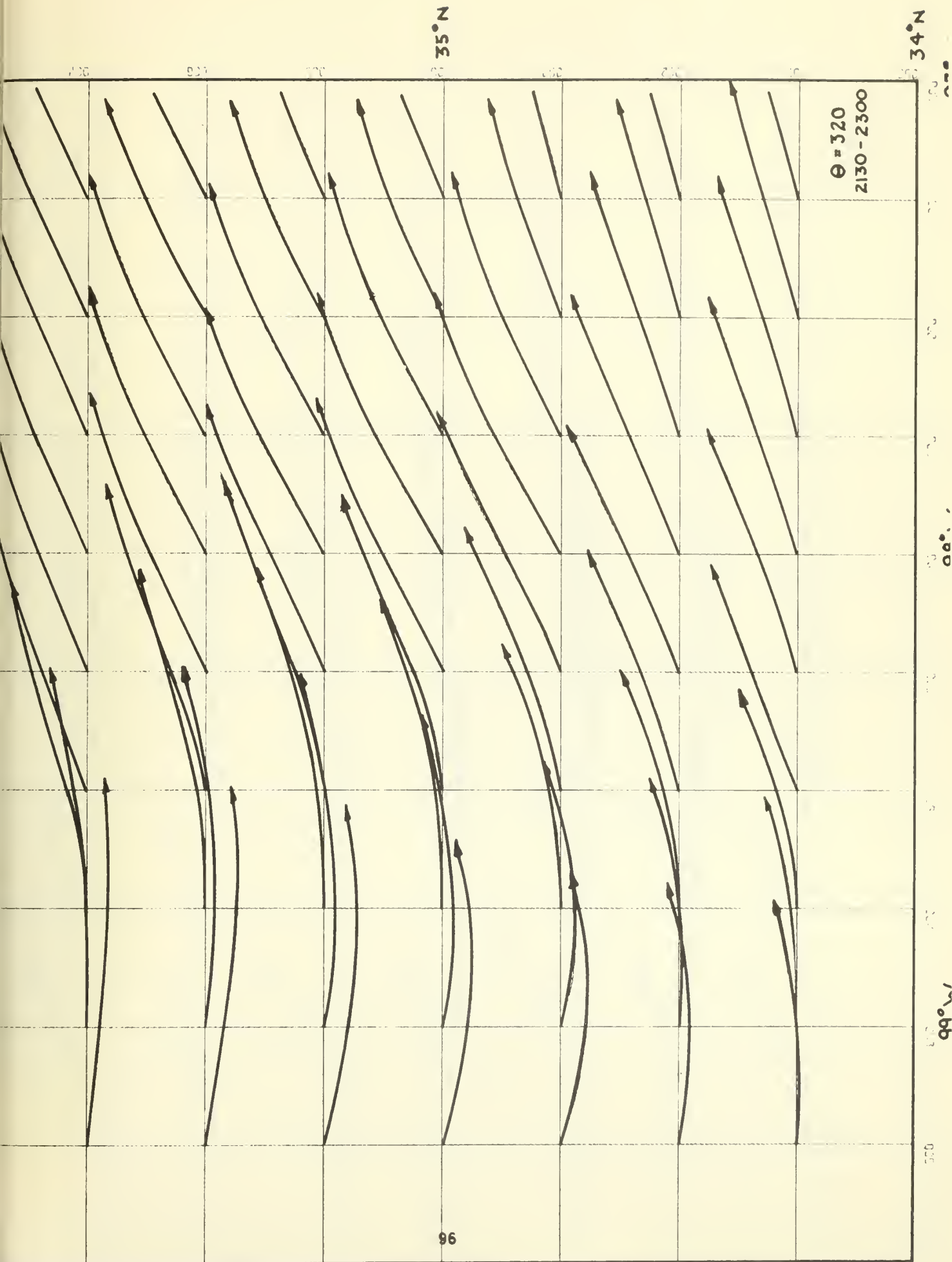


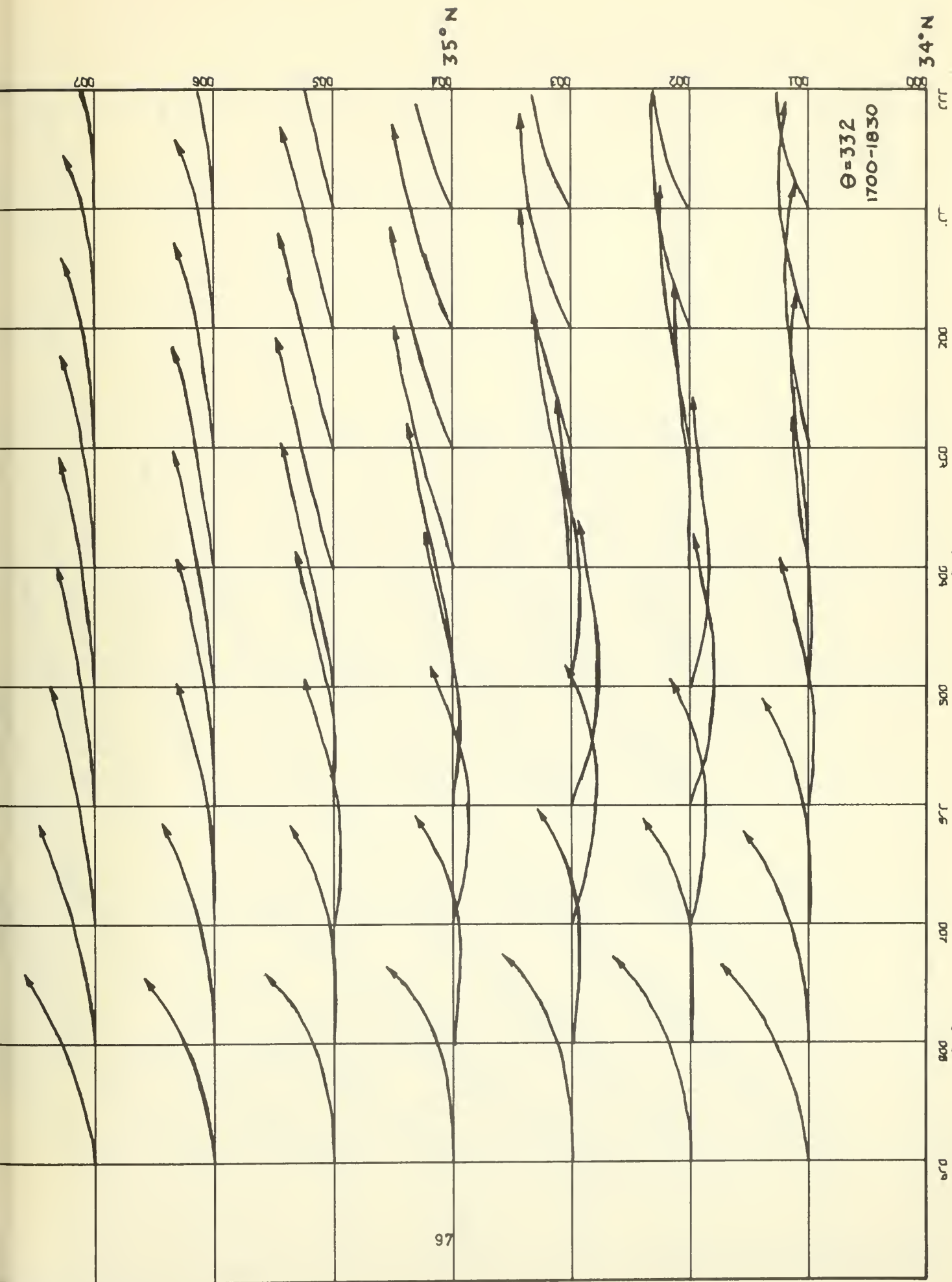


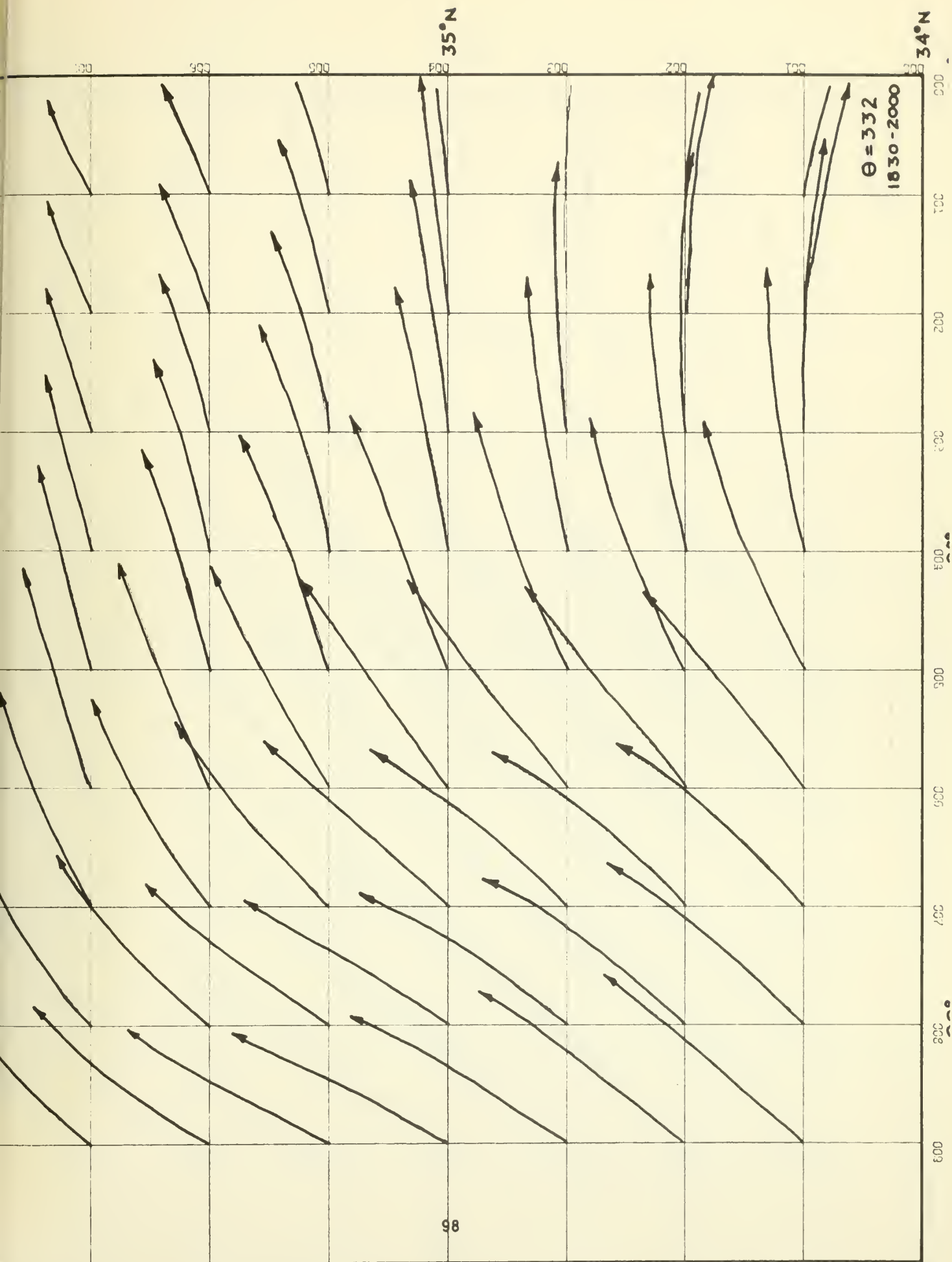


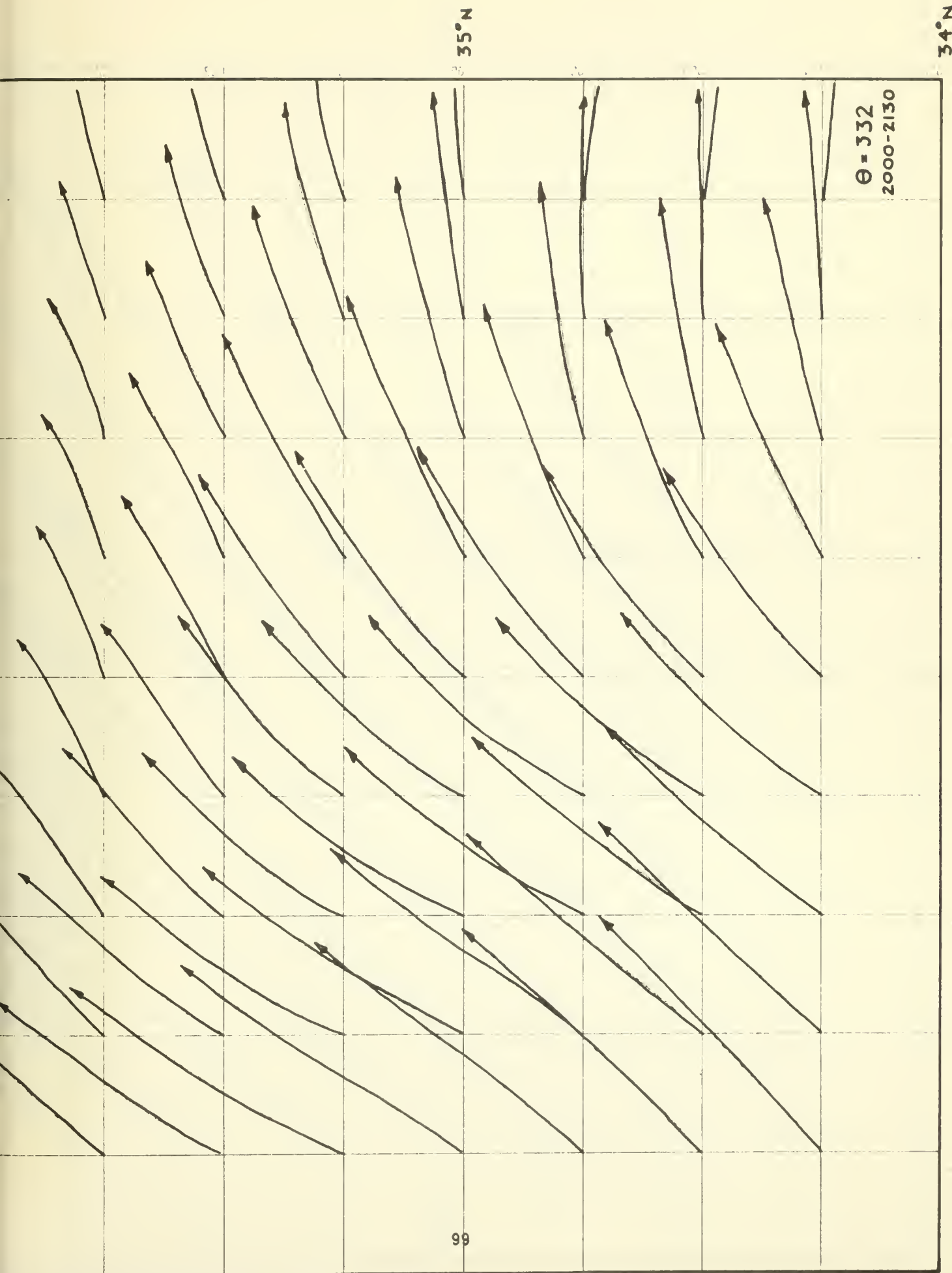


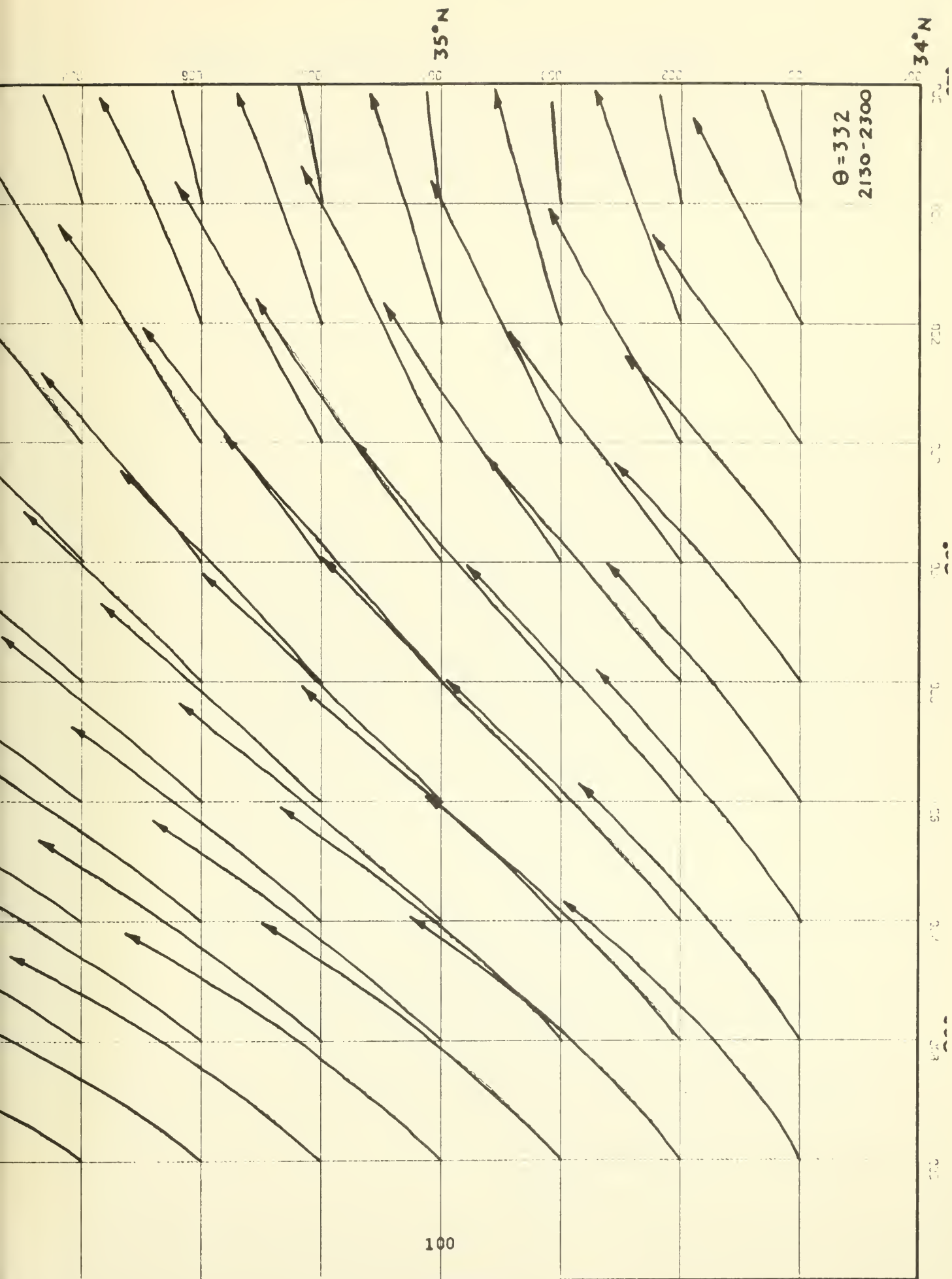












APPENDIX B - ISENTROPIC TRAJECTORY COMPUTER PROGRAM

This appendix includes the objective computer model. The program is written in FORTRAN language. Each routine contains comment cards which explain the routine and each step.


```

C***** ISENTROPIC TRAJECTORY STUDY *****
C
C*****
C      BASIC DESIGN - J. MAHLMAN, PROF., USNPGS
C      MODIFIED BY LT K.L. VAN SICKLE, USN
C*****
C      THIS PROGRAM COMPUTES THREE DIMENSIONAL (KINEMATIC) ISENTROPIC
C      TRAJECTORIES ON AN I, J, K, L LATITUDE-LONGITUDE GRID: I GRID
C      PCINTS ALONG LONGITUDES, J GRID POINTS ALONG LATITUDE
C      LINES, K GRID PCINTS TO BE CONSIDERED. THE PROGRAM AND L ARE THE NO.
C      OF TIME SEQUENCES TO BE CONSIDERED. WIND SPEED (M/SEC), HUMIDITY
C      FIELDS CF: WIND DIRECTION (DEGS), PRESSURE (MB) AND RELATIVE HUMIDITY
C      STREAM FUNCTION (10*7 ERG/GM), PRESSURE (MB) AND RELATIVE HUMIDITY
C      (Z). THE PROGRAM IS BEING RUN ON AN IBM/360 COMPUTER LOCATED AT
C      USNPGS, MONTEREY, CALIF. THE PROGRAM IS CURRENTLY DIMENSIONED FOR
C      A 11,9,2,2 GRID AND WILL OF SEVERE 1.5 HOURS UTILIZING DATA FROM THE
C      SEVERE STORMS USED IN STUDY OF SEVERE 1.5 HOURS UTILIZING DATA FROM THE
C*****
C      REAL*8 ITITL1
C      REAL*8 ITITL2
C
C      COMMON ITITL1(12), ITITL2(12), DD(11,9,2,2), FF(11,9,2,2), F(9), DX(9),
C      1PSIM(11,9,2,2), DMDT2(11,9,2,2), V(11,9,2,2), UO(11,9,2,2), VMDT(11,9,2,2),
C      2DWDT1(11,9,2,2), DMDT1(11,9,2,2), THSFC(2), U1(12), V1(12), DMDT(12), ALAT
C      3(12), ALONG(12), DY, SOULAT, WELONG, NI, NJ, NK, NL, IDATE, DELLAT, DT, DELONG
C      4, ANJ, UL2, VL2, ANK, NNI, NNJ, AI, AJ, AK, INC, SUMXD, SUMYD, SDMDT1, YD, XDI, NLDAY,
C      5AAJ, AAJ, ALAT, ALONG, AI, INC, AI, INC, AI, INC, AI, INC, AI, INC, AI, INC,
C      6II, J, J, FINAL, AMINCO, AMINCO, AMINCO, AMINCO, AMINCO, AMINCO, AMINCO, AMINCO,
C      7, COUNT, X(12), Y(12), Z(12), SHDEF(11,9,2,2), VINIT, VFINAL, ACCEL, I, J, K, L, IZ, JZ, Z1(12), PSAT
C      8, DIV(11,9,2,2), STDEF(11,9,2,2), SMV(2), VORT(11,9,2,2), OSINIT, OSINIT, OSINIT,
C      9CIV(11,9,2,2), STDEF(11,9,2,2), SMV(2), VORT(11,9,2,2), OSINIT, OSINIT, OSINIT,
C      *SPO(12), CRS(2), STDEF(11,9,2,2), SMV(2), VORT(11,9,2,2), OSINIT, OSINIT, OSINIT,
C      1PH(11,9,2,2), Q(11,9,2,2), VOFINL, DFINL, VOFINL, DFINL, VOFINL, DFINL,
C      2T(11,9,2,2), TC(11,9,2,2), E(11,9,2,2), ES(11,9,2,2), Z(11,9,2,2), Z(11,9,2,2),
C      3, STABI, STABF, PVCRIT, PVORIT, POF, POF, POF, POF, POF, POF, POF, POF,
C
C      CALL READ
C      CALL CONST
C      CALL PRAM
C      CALL STABLE
C      CALL MOIST
C      CALL INTERP
C      CALL TRAJ
C
C*****
C      SUBROUTINE ENERGY IS CALLED IN SUBROUTINE TRAJ
C*****
C*****

```


STOP
END

MAIC0470
MAIC0480

```

C****
C      SUBROUTINE READS IN BASIC DATA AND CONVERTS TO U AND V FIELDS
C****
C      REAL*8 IITL1
C      REAL*8 IITL2
C
C      COMMON IITL1(12), IITL2(12), DD(11,9,2,2), FF(11,9,2,2), F(9), DX(9),
1PSIM(11,9,2,2), U(11,9,2,2), V(11,9,2,2), UO(11,9,2,2), VO(11,9,2,2),
2DMDT1(11,9,2,2), DMDT2(11,9,2,2), THSFC(2), U1(12), V1(12), DMDT(12), ALAT
3(12), ALCNG(12), DY, SCULAT, WELONG, NI, NJ, NK, NL, IDATE, DELLAT, DT, DELONG
4, ANJ, U12, V12, NNK, NNI, NNJ, AI, AJ, AK, SUMXD, SUMYD, SDMDT1, YD, XD, NLDAY,
5AAI, AAJ, ALATC, ALONGC, IINC, JINC, AJINC, XDIS, YDIS, T, AAJ, PSAT
6I, JJ, FINALM, AMINIT, AKINIT, FINALK, DELTAM, I, J, K, L, IZ, JZ, Z1(12),
7, PINIT, PFINAL, OMEGA, P(11,9,2,2), VINIT, VFINAL, ACCEL, IMET1, IMET2
8, COUNT, X(12), Y(12), MODCUR, SHDEF(11,9,2,2), STAB(11,9,2,2), ZO(11,9,2,2),
9CIV(11,9,2,2), STDEF(11,9,2,2), VCRIT(11,9,2,2), AVCRT(11,9,2,2), ENGIT
*, SPD(2), CRS(2), SMU(2), SMV(2), OS(11,9,2,2), QSNIT, OFINL, QSFINL,
1FH(11,9,2,2), Q(11,9,2,2), VOFINL, CFINL, VCINT, DINIT, DIFF, QINIT,
2T(11,9,2,2), PD(11,9,2,2), E(11,9,2,2), ES(11,9,2,2), Z(11,9,2,2),
3, STABI, STABF, PVORT1, PVORTF, POTDIF, QDIF
C****
C      READ IN TITLE INFORMATION FOR GRAPHIC DISPLAY
C****
C      READ(5,200)(IITL1(I), I=1,12)
C      READ(5,200)(IITL2(I), I=1,12)
C      FORMAT(6A8)
C****
C      READ IN DISTANCE BETWEEN GRIC PCINTS(METERS); SOUTHERN LAT. OF GRID
C      AND WESTERN LONG. OF GRID; I, J, K, L VALUES
C****
C      READ(5,1) DY, SCULAT, WELONG, NI, NJ, NK, NL
C      FORMAT(5X, F7.0, 3X, F5.2, 3X, F6.2, 3X, I3, 3X, I3, 3X, I3, 13)
C****
C      READ IN DATE INFO(MCNTH, DAY, YEAR); DISTANCE BETWEEN LAT. GRIC POINT
C      (DEGS); INTERVAL BETWEEN TIME STEPS; DISTANCE BETWEEN LONG. PCINTS
C****
C      READ(5,2) IDATE, DELLAT, DT, DELONG
C      FORMAT(5X, I8, 3X, F4.2, 3X, F3.1, 3X, F4.2)
C****
C      1000 FORMAT(1H1)
C      WRITE(6,999)

```



```

999 FORMAT(2X,' DY SOULAT WELONG NI NJ NK NL ',//) REDC0910
WRITE(6,1) DY, SCULAT, WELONG, NI, NJ, NK, NL REDC0920
WRITE(6,998) REDC0930
FORMAT(2X,' IDATE DELLAT DT DELONG',//) REDC0940
WRITE(6,2) IDATE, DELLAT, DT, DELONG REDC0950
C**** REDC0960
C READ IN PCTENTIAL TEMPERATURE SURFACES TO BE USED REDC0970
C**** REDC0980
C READ(5,3) (THSFC(K), K=1, NK) REDC0990
C FORMAT(3X, 2F6.1) REDC1000
C**** REDC1010
C ROUTINE TO OBTAIN TIMES OF DATA FOR OUTPUT DISPLAY REDC1020
C IMET1, ETC. ARE NAMES FOR TIMES OF DATA REDC1030
C**** REDC1040
C READ(5,500) MITE REDC1050
C FORMAT(3X, 11) GO TO 201 REDC1060
C IF(MITE.EQ.1) GO TO 201 REDC1070
C IF(MITE.EQ.2) GO TO 202 REDC1080
C IF(MITE.EQ.3) GO TO 203 REDC1090
C IF(MITE.EQ.4) GO TO 204 REDC1100
C IMET1 = 1700 REDC1110
C IMET2 = 1830 REDC1120
C GO TO 205 REDC1130
C IMET1 = 1830 REDC1140
C IMET2 = 2000 REDC1150
C GO TO 205 REDC1160
C IMET1 = 2000 REDC1170
C IMET2 = 2130 REDC1180
C GO TO 205 REDC1190
C IMET1 = 2130 REDC1200
C IMET2 = 2300 REDC1210
C GO TO 205 REDC1220
C CONTINUE REDC1230
C**** REDC1240
C ROUTINE TO INCLUDE STORM MOVEMENT TO OBTAIN TRAJECTORIES RELATIVE
C TO THE STORM. READ IN AS 000 AND 0.0 IF TRUE TRAJECTORIES ARE
C DESIRED REDC1250
C**** REDC1260
C READ(5,300)(SPD(K), K=1, NK) REDC1270
C FORMAT(2F6.2) REDC1280
C READ(5,300)(CRS(K), K=1, NK) REDC1290
C**** REDC1300
C READ IN BASIC DATA REDC1310
C**** REDC1320
C DO 4 L=1, NL REDC1330
C DO 4 K=1, NK REDC1340
C DO 4 I=1, NI REDC1350
C 4 READ(5,5) (DC(I,J,K,L), J=1, NJ) REDC1360
C REDC1370
C REDC1380

```



```

C
5  FORMAT(20F4.0)
DO 6  L=1,NL
DO 6  K=1,NK
DO 6  I=1,NI
6  READ(5,55) (FF(I,J,K,L),J=1,NJ)
55  FORMAT(20F4.1)
C
DO 7  L=1,NL
DO 7  K=1,NK
DO 7  I=1,NI
7  READ(5,8) (PSIM(I,J,K,L),J=1,NJ)
8  FORMAT(15F5.2)
C
DO 12 L=1,NL
DO 12 K=1,NK
DO 12 I=1,NI
DO 12 J=1,NJ
IF(PSIM(I,J,K,L) .LT. 80.)PSIM(I,J,K,L)=PSIM(I,J,K,L) + 300.
IF(PSIM(I,J,K,L) .LT. 100.)PSIM(I,J,K,L)=PSIM(I,J,K,L) + 200.
12  CONTINUE
C
DO 105 L=1,NL
DO 105 K=1,NK
DO 105 I=1,NI
105  READ(5,106) (P(I,J,K,L),J=1,NJ)
106  FORMAT(19F4.0)
C
DO 107 L=1,NL
DO 107 K=1,NK
DO 107 I=1,NI
107  READ(5,108) (RH(I,J,K,L),J=1,NJ)
108  FORMAT(15F5.1)
C***
C***  COMPUTE U AND V COMPONENTS OF STORM MOTION
C***
DO 301 K=1,NK
SMU(K) = -SPD(K)*SIN(CRS(K)/57.2958)
SMV(K) = -SPD(K)*COS(CRS(K)/57.2958)
301  CONTINUE
C***
C***  COMPUTE U AND V FIELDS
C***
DO 15 L=1,NL
DO 15 K=1,NK
DO 15 J=1,NJ
U(I,J,K,L)=-FF(I,J,K,L)*SIN(DD(I,J,K,L)/57.2958) - SMU(K)

```

```

RED01390
RED01400
RED01410
RED01420
RED01430
RED01440
RED01450
RED01460
RED01470
RED01480
RED01490
RED01500
RED01510
RED01520
RED01530
RED01540
RED01550
RED01560
RED01570
RED01580
RED01590
RED01600
RED01610
RED01620
RED01630
RED01640
RED01650
RED01660
RED01670
RED01680
RED01690
RED01700
RED01710
RED01720
RED01730
RED01740
RED01750
RED01760
RED01770
RED01780
RED01790
RED01800
RED01810
RED01820
RED01830
RED01840
RED01850
RED01860

```



```

15 V(I,J,K,L)=-FF(I,J,K,L)*COS(DD(I,J,K,L)/57.2958) - SMV(K)
C****
C WRITE OUT VARIABLES READ IN
C****
DO 20 L=1,NL
DO 20 K=1,NK
IF(L.EQ.1) IMET = IMET1
IF(L.EQ.2) IMET = IMET2
WRITE(6,1000)
WRITE(6,9) IMET, THSFC(K), IDATE
9 FORMAT(3X, 'WIND DIRECTION FOR TIME =', I4, ' AND FOR THETA =', F7.1, '
1 DATE =', I6, '////)
DO 100 J=1,NJ
DO 100 WRITE(6,10) (DD(I,NJ-J+1,K,L), I=1,NI)
C
WRITE(6,1000)
WRITE(6,13) IMET, THSFC(K), IDATE
13 FORMAT(3X, 'MONTGOMERY STREAM FUNCTION (10**7 ERG/G) FOR TIME =', I4, '
1 AND FOR THETA =', F7.1, ' DATE =', I6, '////)
DO 101 J=1,NJ
DO 101 WRITE(6,14) (PSIM(I,NJ-J+1,K,L), I=1,NI)
C
WRITE(6,1000)
WRITE(6,11) IMET, THSEC(K), IDATE
11 FORMAT(3X, 'WIND SPEED (M/SEC) FOR TIME =', I4, ' AND FOR THETA =', F7.1, '
1 DATE =', I6, '////)
DO 102 J=1,NJ
DO 102 WRITE(6,10) (FF(I,NJ-J+1,K,L), I=1,NI)
C
WRITE(6,1000)
WRITE(6,23) IMET, THSFC(K), IDATE
23 FORMAT(3X, 'PRESSURE (MB) FOR TIME =', I4, ' AND FCR THETA =', F7.1, '
1 DATE =', I6, '////)
DO 24 J=1,NJ
DO 24 WRITE(6,10) (P(I,NJ-J+1,K,L), I=1,NI)
C
C 20 CONTINUE
C****
C THESE FORMAT STATEMENTS ARE SET FOR A ONE INCH BY ONE INCH GRID.
C****
10 FORMAT(2X,11F10.1, '//////)
14 FORMAT(2X,11F10.2, '//////)
C
DO 18 L=1,NL
DO 18 K=1,NK
IF(L.EQ.1) IMET = IMET1
IF(L.EQ.2) IMET = IMET2
WRITE(6,1000)

```

RED01870
 RED01880
 RED01890
 RED01900
 RED01910
 RED01920
 RED01930
 RED01940
 RED01950
 RED01960
 RED01970
 RED01980
 RED01990
 RED02000
 RED02010
 RED02020
 RED02030
 RED02040
 RED02050
 RED02060
 RED02070
 RED02080
 RED02090
 RED02100
 RED02110
 RED02120
 RED02130
 RED02140
 RED02150
 RED02160
 RED02170
 RED02180
 RED02190
 RED02200
 RED02210
 RED02220
 RED02230
 RED02240
 RED02250
 RED02260
 RED02270
 RED02280
 RED02290
 RED02300
 RED02310
 RED02320
 RED02330
 RED02340


```

16 WRITE(6,16) IMET, THSFC(K), IDATE
17 FORMAT(3X, 'U COMPONENT OF WIND (M/SEC) FOR TIME =', I4, ' AND FOR THETA =', I4, '
DO 103 J=1, NJ
103 WRITE(6,14) (U(I, NJ-J+1, K, L), I=1, NI)
C
WRITE(6,1000)
WRITE(6,17) IMET, THSFC(K), IDATE
17 FORMAT(3X, 'V COMPONENT OF WIND (M/SEC) FOR TIME =', I4, ' AND FOR THETA =', I4, '
18 WRITE(6,14) (V(I, NJ-J+1, K, L), I=1, NI)
C
WRITE(6,1000)
WRITE(6,50) IMET, THSFC(K), IDATE
50 FORMAT(3X, 'RELATIVE HUMIDITY(%) FOR TIME =', I4, ' AND FOR THETA =', I4, '
19 WRITE(6,14) (RH(I, NJ-J+1, K, L), I=1, NI)
C
WRITE(6,1000)
WRITE(6,70) (RH(I, NJ-J+1, K, L), I=1, NI)
70 FORMAT(2X, 11F10.3, //)
C
18 CONTINUE
C
WRITE(6,1000)
WRITE(6,302)
302 FORMAT(//, 2X, 'U COMPONENT OF STORM MOVEMENT', //)
303 WRITE(6,303) (SMU(K), K=1, NK)
303 FORMAT(2X, 2F6.2)
304 WRITE(6,304)
304 FORMAT(//, 2X, 'V COMPONENT OF STORM MOVEMENT', //)
C
RETURN
END

```

```

C****
C THIS SUBROUTINE COMPUTES Y-DEPENDENT PARAMETERS FOR THE CARTESIAN
C GRID
C****
C REAL*8 ITITL1
C REAL*8 ITITL2
COMMON ITITL1(12), ITITL2(12), DD(11,9,2,2), FF(11,9,2,2), F(9), DX(9),
1PSIM(11,9,2,2), U(11,9,2,12), V(11,9,2,12), UO(11,9,2), VO(11,9,2),
CSTC2690
CSTC2700
CSTC2710
CSTC2720
CSTC2730
CSTC2740
CSTC2750
CSTC2760
CSTC2770
CSTC2780

```



```

2DMDT1(11,9,2), DMDT2(11,9,2), THSFC(2), U1(12), V1(12), DMDT(12), ALAT-
3(12), ALONG(12), DY, SOULAT, WELONG, NI, NJ, NK, NL, IDATE, DELLAT, DT, DELONG-
4, ANJ, U12, V12, ANK, NNI, NNJ, AI, AJ, AK, SUMXD, SUMYD, SDMDT1, YD, XC, NLDAY,
5AAI, AAJ, ALATO, ALONGO, IINC, AJINC, AJINC, XDI, YDI, ST, YDI, XC, NLDAY,
6II, JJ, FINALM, AMINIT, AKINIT, FINALK, DELTAM, I, J, K, L, IZ, JZ, Z1(12), PSAT-
7, PINIT, PFINAL, OMEGA, P(11,9,2,2), VINIT, VFINAL, ACCEL, I, J, K, L, IZ, JZ, Z1(12), PSAT-
8, COUNT, X(12), Y(12), MODCUR, SHDEF(11,9,2,2), STAB(11,9,2), Z0(11,9,2), ENGI-
9DIV(11,9,2,2), STDEF(11,9,2,2), VORT(11,9,2,2), AVORT(11,9,2,2), ENGI-
* SPD(11,9,2,2), CRS(2), SMU(2), SMV(2), QS(11,9,2,2), QSINIT, QFINL, QSFINL,
1RH(11,9,2,2), Q(11,9,2,2), VOFINL, DFINL, VOINT, DINIT, DIFF, QINIT,
2T(11,9,2,2), TD(11,9,2,2), E(11,9,2,2), ES(11,9,2,2), Z(11,9,2,12)
3, STABI, STABF, PVCRTI, PVORTI, POIDIF, QDIF
C
1000 WRITE(6,1000)
FORMAT(1H1)
SSSLAT = SOULAT
WRITE(6,2)
2 FORMAT(4X, 'LATITUDE', 10X, 'CORIOLIS PARAMETER', 15X, 'DX(J)', //)
DO 1 J=1, NJ
DX(J) = DY * CCS(SOULAT/57.2958)
C***
C*** COMPUTE CORIOLIS PARAMETER
C***
F(J) = 14.58 * SIN(SOULAT/57.2958)
WRITE(6,3) SOULAT, F(J), DX(J)
1 SOULAT = SOULAT + DELLAT
3 FORMAT(6X, F5.2, 18X, F5.2, 15X, F9.1, //)
SOULAT = SSSLAT
C
RETURN
END

```

```

SUBROUTINE PRAM
C***
C THIS SUBROUTINE WILL COMPUTE HCRIZONTAL DIVERGENCE, VORTICITY,
C STRETCHING DEFORMATION AND SHEARING DEFORMATION TERMS.
C***
REAL*8 ITITL1
REAL*8 ITITL2
C
COMMON ITITL1(12), ITITL2(12), DD(11,9,2,2), FF(11,9,2,2), F(9), DX(9),
1PSIM(11,9,2,2), U(11,9,2,12), V(11,9,2,12), UO(11,9,2), VO(11,9,2),
2DMDT1(11,9,2), DMDT2(11,9,2), THSFC(2), U1(12), V1(12), DMDT(12), ALAT,
3(12), ALONG(12), DY, SOULAT, WELONG, NI, NJ, NK, NL, IDATE, DELLAT, DT, DELONG,
4, ANJ, U12, V12, NNI, NNJ, AI, AJ, AK, SUMXD, SUMYD, SDMDT1, YD, XD, NLDAY,
PRMC3090
PRM03100
PRM03110
PRM03120
PRM03130
PRM03140
PRM03150
PRM03160
PRM03170
PRM03180
PRM03190
PRM03200
PRM03210

```



```

C****
C      WRITE OUT FIELDS
C****
      DO 6 L=1,NL
      DO 6 K=1,NK
      IF(L.EQ.1) IMET=IMET1
      IF(L.EQ.2) IMET=IMET2
      WRITE(6,1000)
1000  FORMAT(1H1)
      WRITE(6,7) IMET,THSFC(K),IDATE
      7  FORMAT(3X,'HORIZONTAL DIVERGENCE(10**-4 1/SEC) FOR TIME= ',I4,' AND
10  FOR THETA= ',F7.1,' DATE= ',I6,////)
      DO 8 J=2,MJ
      8  WRITE(6,9) (DIV(I,MJ-J+2,K,L),I=2,MI)
      9  FORMAT(2X,9F10.2,////)
C
      WRITE(6,1000)
      WRITE(6,10) IMET,THSFC(K),IDATE
      10  FORMAT(3X,'HORIZONTAL ABSOLUTE VORTICITY(10**-4 1/SEC) FOR TIME=
11  ,I4,' AND FOR THETA= ',F7.1,' DATE= ',I6,////)
      DO 11 J=2,MJ
      11  WRITE(6,9) (AVORT(I,MJ-J+2,K,L),I=2,MI)
C
      WRITE(6,1000)
      WRITE(6,12) IMET,THSFC(K),IDATE
      12  FORMAT(3X,'STRETCHING DEFORMATION(10**-4 1/SEC) FOR TIME= ',I4,' A
13  ND FOR THETA= ',F7.1,' DATE= ',I6,////)
      DO 13 J=2,MJ
      13  WRITE(6,9) (STDEF(I,MJ-J+2,K,L),I=2,MI)
C
      WRITE(6,1000)
      WRITE(6,14) IMET,THSFC(K),IDATE
      14  FORMAT(3X,'SHEARING DEFORMATION(10**-4 1/SEC) FOR TIME= ',I4,' AND
15  FOR THETA= ',F7.1,' DATE= ',I6,////)
      DO 15 J=2,MJ
      15  WRITE(6,9) (SHDEF(I,MJ-J+2,K,L),I=2,MI)
      6  CONTINUE
C
      RETURN
      END

```

```

PRMC3700
PRM03710
PRM03720
PRM03730
PRM03740
PRM03750
PRM03760
PRM03770
PRM03780
PRM03790
PRM03800
PRM03810
PRM03820
PRM03830
PRM03840
PRM03850
PRM03860
PRM03870
PRM03880
PRM03890
PRM03900
PRM03910
PRM03920
PRM03930
PRM03940
PRM03950
PRM03960
PRM03970
PRM03980
PRM03990
PRMC4000
PRM04010
PRM04020
PRM04030
PRM04050
PRM04060
PRM04070
PRM04080
PRM04090
PRM04100

```



```

SUBROUTINE STABLE
C**** THIS SUBROUTINE COMPUTES STATIC STABILITY GIVEN THE THETA SURFACES
C AND PRESSURES
C****
C
REAL*8 ITITL1
REAL*8 ITITL2
COMMON ITITL1(12), ITITL2(12), DD(11,9,2,2), FF(11,9,2,2), F(9), DX(9),
1PSIM(11,9,2,2), U(11,9,2,2), V(11,9,2,2), V0(11,9,2,2), DMDT(11,9,2,2),
2DMDT1(11,9,2,2), DMDT2(11,9,2,2), THSFC(12), U1(12), V1(12), ALAT
3(12), ALONG(12), DY, SOULAT, WELONG, NI, NJ, NK, NL, IDATE, DELLAT, DT, DELONG
4, ANJ, U12, V12, NNK, NNI, NNJ, AI, AJ, AK, INC, SUMXD, SUMYD, SDMDT1, YD, XDI,
5AAI, AAJ, AAL, AAM, AAN, AAO, AAI, AAK, AAL, AAM, AAN, AAO, AAI, AAK, AAL, AAM,
6II, JJJ, PFINAL, AMINIT, AKINI, AKINC, AFINAL, AFINC, AFINAL, AFINC, AFINAL, AFINC,
7, PINIT, PFINAL, AMINIT, AKINI, AKINC, AFINAL, AFINC, AFINAL, AFINC, AFINAL, AFINC,
8, COUNT, X(12), Y(12), MGDCUR, SHDEF(11,9,2,2), VINIT, VINIT, VINIT, VINIT,
9DIV(11,9,2,2), SMU(2), SMV(2), VORT(11,9,2,2), AVCR(11,9,2,2), QSFINL,
*SPD(11,9,2,2), Q(11,9,2,2), VOFINL, DFINL, VOINT, DINIT, QSFINL,
1RH(11,9,2,2), Q(11,9,2,2), E(11,9,2,2), ES(11,9,2,2), Z(11,9,2,2),
2T(11,9,2,2), D(11,9,2,2), P(11,9,2,2), P(11,9,2,2), P(11,9,2,2),
3, STABI, STABF, PVCRIT, PVORIT, POFIT, QCIF
C
1000 FORMAT(IH1)
DO 5 K=1
DO 5 L=1, NL
DO 5 I=1, NI
DO 5 J=1, NJ
STAB(I,J,L) = -(THSFC(K+1)-THSFC(K))/(P(I,J,K+1,L)-P(I,J,K,L))
5 CONTINUE
C
M = K+1
DO 30 L=1, NL
DO 30 I=1, NI
IF(L.EQ.1) IMET=IMET1
IF(L.EQ.2) IMET=IMET2
WRITE(6,1000)
WRITE(6,10) THSFC(K), THSFC(M), IMET
10 FORMAT(3X, 'STATIC STABILITY( DEG K/MB) FOR THETA SURFACES ', F6.1,
1, ' AND ', F6.1, ' FOR TIME=', I4, '///')
DO 15 J=1, NJ
15 WRITE(6,20) (STAB(I,NJ-J+1,L), I=1, NI)
20 FORMAT(2X, 11F10.3, '///')
30 CONTINUE
C
RETURN
END

```



```

C****
C      SUBROUTINE MOIST
C      THIS SUBROUTINE COMPUTES MOISTURE TERMS TO BE USED IN THE MODEL.
C
REAL*8 ITITL1
REAL*8 ITITL2
COMMON ITITL1(12), ITITL2(12), DD(11,9,2,2), FF(11,9,2,2), VO(11,9,2), V0(11,9,2), F(9), DX(9),
1PSIM(11,9,2,2), U(11,9,2,2), V(11,9,2,2), UO(11,9,2), VMDT(12), V1(12), ALAT
2DMDT1(11,9,2), DMDT2(11,9,2), THSFC(2), UL(12), NL, IDATE, DELLAT, DT, DELONG
3(12), ALONG(12), DY, SOULAT, WELONG, NI, NJ, NK, NL, IDATE, DELLAT, DT, DELONG
4ANJ, UI2, V12, NNK, NNJ, AI, AJ, AK, SUMXD, SUMYD, SCMDT1, YD, XD, NLDAY,
5AAI, AAJ, ALATO, ALONGO, IINC, JINC, AJINC, XDIST, YDIST, AAI, AAJ,
6II, JJ, FINALM, AMINIT, AKINIT, JFINAL, DELTAM, I, J, K, L, IZ, Z1(12), PSA
7, PINIT, PFINAL, OMEGA, P(11,9,2,2), VINIT, VFINAL, ACCEL, I, J, K, L, IZ, Z1(12), PSA
8, COUNT, X(12), Y(12), MODCUR, SHDEF(11,9,2,2), STAB(11,9,2), ZO(11,9,2), ENGI
9DIV(11,9,2,2), STDEF(11,9,2,2), VORT(11,9,2,2), AVORT(11,9,2,2), QSFINL,
*SPD(2), CR$(2), SMU(2), $MV(2), QS(11,9,2,2), QSFINL, QSFINL,
1RH(11,9,2,2), Q(11,9,2,2), VOFINL, DFINL, DFINL, DFINL, QSFINL,
2T(11,9,2,2), TD(11,9,2,2), E(11,9,2,2), ES(11,9,2,2), Z(11,9,2,2)
3, STABI, STABF, PVORTI, PVORTF, POTDIF, QDIF
C
DO 5 L=1,NL
DO 5 K=1,NK
DO 5 I=1,NI
DO 5 J=1,NJ
RH(I,J,K,L) = RH(I,J,K,L)/100.0
C      COMPUTE TEMPERATURE(DEGS C) AT EACH GRID POINT.
C      DEN = (1000.0/P(I,J,K,L))*0.286
T(I,J,K,L) = (THSFC(K)/DEN) - 273.16
C      COMPUTE DEW POINT TEMPERATURE AT EACH GRID POINT.(DEGS C)
C
B = 1.0 - RH(I,J,K,L)
PP1 = (B**7)*(16.65 + .118*T(I,J,K,L))
PP2 = (B**2)*((3.14 + .0246*T(I,J,K,L))**2)
PP3 = B*(13.4 + .103*T(I,J,K,L))
TD(I,J,K,L) = T(I,J,K,L) - (PP1 + PP2 + PP3)
C      COMPUTE VAPOR PRESSURE AT EACH GRID POINT (MB)
C
C = (7.5*TD(I,J,K,L))/(237.3+TD(I,J,K,L))
E(I,J,K,L) = 6.11*(10**C)
C      COMPUTE SPECIFIC HUMIDITY AT EACH GRID POINT(GM/GM)
C

```



```

C**** Q(I,J,K,L) = (0.622*E(I,J,K,L))/(P(I,J,K,L)-0.378*E(I,J,K,L))
C      COMPUTE SATURATION VAPOR PRESSURE AT EACH GRID POINT(MB)
C**** ES(I,J,K,L) = E(I,J,K,L)/RH(I,J,K,L)
C      COMPUTE SPECIFIC HUMIDITY AT SATURATION AT EACH GRID POINT( GM/GM)
C**** QS(I,J,K,L) = (0.622*ES(I,J,K,L))/(P(I,J,K,L)-0.378*ES(I,J,K,L))
C      CONVERT RE. HUMIDITY BACK TC % BEFORE WRITE OUT.
C**** RH(I,J,K,L) = RH(I,J,K,L)*100.0
C      COMPUTE MIXING RATIO
C**** BIXR = (0.622*E(I,J,K,L))/(P(I,J,K,L)-E(I,J,K,L))
C      COMPUTE VIRTUAL TEMPERATURE
C**** TV = (T(I,J,K,L) + 273.16)*(1.0 + 0.61*BIXR)
C      DATA FOR THIS CASE STUDY WAS OBTAINED FOR MONT. STREAM FUNC.
C      FROM THE FORMULA M=CP*TV + G*Z, THUS IT WAS NECESSARY TO
C      COMPUTE THE VIRTUAL TEMP. NOW OBTAIN THE HEIGHT(Z) IN METERS.
C**** Z(I,J,K,L) = ((PSIM(I,J,K,L) - 1.004*TV)/9.797455)*1000.
C      CONTINUE
C**** 5
C      WRITE OUT THE FIELDS COMPUTED
C****
C      DO 90 L=1,NL
C      DO 90 K=1,NK
C      IF(L.EQ.1) IMET = IMET1
C      IF(L.EQ.2) IMET = IMET2
C      WRITE(6,1000)
C      FORMAT(1H1)
C      WRITE(6,50) IMET,THSFC(K),IDATE
C      FORMAT(3X,'RELATIVE HUMIDITY(%) FOR TIME =',I4,' AND FOR THETA =',
1000 1F7.1,' DATE =',I6,////)
C      DO 71 J=1,NJ
C      71 WRITE(6,70) (RH(I,NJ-J+1,K,L),I=1,NI)
C      FORMAT(2X,11F10.3,////)
C      WRITE(6,1000)
C      WRITE(6,51) IMET,THSFC(K),IDATE
C      FORMAT(3X,'TEMPERATURE(DEGREES CENTIGRADE) FOR TIME =',I4,' AND FOR
51 1R THETA =',F7.1,' DATE =',I6,////)
C

```

```

MST05030
MST05040
MST05050
MST05060
MST05070
MST05080
MST05090
MST05100
MST05110
MST05120
MST05130
MST05140
MST05150
MST05160
MST05170
MST05180
MST05190
MST05200
MST05210
MST05230
MST05240
MST05250
MST05260
MST05270
MST05280
MST05290
MST05300
MST05310
MST05320
MST05330
MST05340
MST05350
MST05360
MST05370
MST05380
MST05390
MST05400
MST05410
MST05420
MST05430
MST05440
MST05450
MST05460
MST05470
MST05480
MST05490
MST05500
MST05510

```



```

C
72 DO 72 J=1,NJ
   WRITE(6,70) (T(I,NJ-J+1,K,L),I=1,NI)
   WRITE(6,1000)
   WRITE(6,52) IMET,THSFC(K),IDATE
52 FORMAT(3X,'DEWPOINT TEMPERATURE(DEGREES, CENTIGRADE) FOR TIME =',I4,
1, ' AND FOR THETA =',F7.1, ' DATE =',I6,////)
DO 73 J=1,NJ
73 WRITE(6,70) (TD(I,NJ-J+1,K,L),I=1,NI)
C
   WRITE(6,1000)
   WRITE(6,53) IMET,THSFC(K),IDATE
53 FORMAT(3X,'VAPOR PRESSURE(MB) FOR TIME =',I4, ' AND FOR THETA =',
1,F7.1, ' DATE =',I6,////)
DO 74 J=1,NJ
74 WRITE(6,70) (E(I,NJ-J+1,K,L),I=1,NI)
C
   WRITE(6,1000)
   WRITE(6,54) IMET,THSFC(K),IDATE
54 FORMAT(3X,'SPECIFIC HUMIDITY(GM/GM) FOR TIME =',I4, ' AND FOR THETA
1, =',F7.1, ' DATE =',I6,////)
DO 75 J=1,NJ
75 WRITE(6,80) (Q(I,NJ-J+1,K,L),I=1,NI)
80 FORMAT(2X,11F10.4,////)
C
   WRITE(6,1000)
   WRITE(6,55) IMET,THSFC(K),IDATE
55 FORMAT(3X,'SAT. VAPOR PRESSURE(MB) FOR TIME =',I4, ' AND FOR THETA =
1, =',F7.1, ' DATE =',I6,////)
DO 76 J=1,NJ
76 WRITE(6,70) (ES(I,NJ-J+1,K,L),I=1,NI)
C
   WRITE(6,1000)
   WRITE(6,56) IMET,THSFC(K),IDATE
56 FORMAT(3X,'SAT. SPECIFIC HUMIDITY(GM/GM) FOR TIME =',I4, ' AND FOR T
1, HETA =',F7.1, ' DATE =',I6,////)
DO 77 J=1,NJ
77 WRITE(6,80) (QS(I,NJ-J+1,K,L),I=1,NI)
C
   WRITE(6,1000)
   WRITE(6,85) IMET,THSFC(K),IDATE
85 FORMAT(3X,'HEIGHT(METERS) FOR TIME =',I4, ' AND FOR THETA =',F7.1,
1, ' DATE =',I6,////)
DO 86 J=1,NJ
86 WRITE(6,70) (Z(I,NJ-J+1,K,L),I=1,NI)
C
90 CONTINUE
C

```

```

MST05520
MST05530
MST05540
MST05560
MST05570
MST05580
MST05590
MST05600
MST05610
MST05620
MST05630
MST05640
MST05650
MST05660
MST05670
MST05680
MST05690
MST05700
MST05710
MST05720
MST05730
MST05740
MST05750
MST05760
MST05770
MST05780
MST05790
MST05800
MST05810
MST05820
MST05830
MST05840
MST05850
MST05860
MST05870
MST05880
MST05890
MST05900
MST05910
MST05920
MST05930
MST05940
MST05950
MST05960
MST05970
MST05980
MST05990
MST06000

```


MMST06010
MMST06020

115

INT06460
INT06470
INT06480
INT06490
INT06500
INT06510
INT06520
INT06530
INT06540
INT06550
INT06560
INT06570
INT06580
INT06590
INT06600
INT06610
INT06620
INT06630
INT06640
INT06650
INT06660
INT06670
INT06680
INT06690
INT06700
INT06710
INT06720
INT06730
INT06740
INT06750
INT06760
INT06770
INT06780
INT06790
INT06800
INT06810
INT06820
INT06830
INT06840
INT06850
INT06860
INT06870
INT06880
INT06890
INT06900
INT06910
INT06920
INT06930

```
U(I,J,K,6) = (06./12.)*U0(I,J,K) + (06./12.)*U12
U(I,J,K,7) = (05./12.)*U0(I,J,K) + (07./12.)*U12
U(I,J,K,8) = (04./12.)*U0(I,J,K) + (08./12.)*U12
U(I,J,K,9) = (03./12.)*U0(I,J,K) + (09./12.)*U12
U(I,J,K,10) = (02./12.)*U0(I,J,K) + (10./12.)*U12
U(I,J,K,11) = (01./12.)*U0(I,J,K) + (11./12.)*U12
U(I,J,K,12) = U12
```

C

```
V0(I,J,K) = V(I,J,K,1)
V12 = V(I,J,K,2)
V(I,J,K,1) = (11./12.)*V0(I,J,K) + (01./12.)*V12
V(I,J,K,2) = (10./12.)*V0(I,J,K) + (02./12.)*V12
V(I,J,K,3) = (09./12.)*V0(I,J,K) + (03./12.)*V12
V(I,J,K,4) = (08./12.)*V0(I,J,K) + (04./12.)*V12
V(I,J,K,5) = (07./12.)*V0(I,J,K) + (05./12.)*V12
V(I,J,K,6) = (06./12.)*V0(I,J,K) + (06./12.)*V12
V(I,J,K,7) = (05./12.)*V0(I,J,K) + (07./12.)*V12
V(I,J,K,8) = (04./12.)*V0(I,J,K) + (08./12.)*V12
V(I,J,K,9) = (03./12.)*V0(I,J,K) + (09./12.)*V12
V(I,J,K,10) = (02./12.)*V0(I,J,K) + (10./12.)*V12
V(I,J,K,11) = (01./12.)*V0(I,J,K) + (11./12.)*V12
V(I,J,K,12) = V12
```

C

```
Z0(I,J,K) = Z(I,J,K,1)
Z12 = Z(I,J,K,2)
Z(I,J,K,1) = (11./12.)*Z0(I,J,K) + (01./12.)*Z12
Z(I,J,K,2) = (10./12.)*Z0(I,J,K) + (02./12.)*Z12
Z(I,J,K,3) = (09./12.)*Z0(I,J,K) + (03./12.)*Z12
Z(I,J,K,4) = (08./12.)*Z0(I,J,K) + (04./12.)*Z12
Z(I,J,K,5) = (07./12.)*Z0(I,J,K) + (05./12.)*Z12
Z(I,J,K,6) = (06./12.)*Z0(I,J,K) + (06./12.)*Z12
Z(I,J,K,7) = (05./12.)*Z0(I,J,K) + (07./12.)*Z12
Z(I,J,K,8) = (04./12.)*Z0(I,J,K) + (08./12.)*Z12
Z(I,J,K,9) = (03./12.)*Z0(I,J,K) + (09./12.)*Z12
Z(I,J,K,10) = (02./12.)*Z0(I,J,K) + (10./12.)*Z12
Z(I,J,K,11) = (01./12.)*Z0(I,J,K) + (11./12.)*Z12
Z(I,J,K,12) = Z12
```

C

6 CONTINUE

C****

WRITE OUT U AND V COMPONENT FIELDS

C****

WRITE(6,1000)

FORMAT(IH1)

1000

DO 7 L=1,12

DO 7 K=1,NK

WRITE(6,9) L,THSFC(K)


```

DO 7 J=1,NJ (U(I,NJ-J+1,K,L),I=1,NI)
7 WRITE(6,10) (U(I,NJ-J+1,K,L),I=1,NI)
9 FORMAT(2X,'U COMPONENT OF WIND AT L = ',I2,'THETA=',F6.1,/)
10 FORMAT(2X,'V COMPONENT OF WIND AT L = ',I2,'THETA=',F6.1,/)
DO 8 L=1,12
DO 8 K=1,NK
WRITE(6,11) L,THSFC(K)
DO 8 J=1,NJ
11 WRITE(6,10) (V(I,NJ-J+1,K,L),I=1,NI)
11 FORMAT(2X,'V COMPONENT OF WIND AT L = ',I2,'THETA=',F6.1,/)
C
DO 20 L=1,12
DO 20 K=1,NK
WRITE(6,21) L,THSFC(K)
DO 20 J=1,NJ
21 FORMAT(2X,'HEIGHT(M) AT L = ',I2,'THETA=',F6.1,/)
20 WRITE(6,22) (Z(I,NJ-J+1,K,L),I=1,NI)
22 FORMAT(2X,'11F8.2,/)
C****
C ABOVE ROUTINE ASSUMES NL = 2
C****
C RETURN
C END

```

INT06940
INTC6950
INTC6960
INTC6970
INTC6980
INTC6990
INTC7000
INTC7010
INTC7020
INTC7030
INTC7040
INTC7050
INTC7060
INTC7070
INTC7080
INTC7090
INTC7100
INTC7110
INTC7120
INTC7130
INTC7140
INTC7150
INTC7160

```

SUBROUTINE TRAJ
C****
C THIS SUBROUTINE EVALUATES FIRST GUESS TRAJECTORY WITHOUT ENERGY
C INTEGRAL CORRECTION
C****
REAL*8 ITITL1
REAL*8 ITITL2
REAL*4 LABEL/4H /
C
COMMON ITITL1(12), ITITL2(12), DD(11,9,2,2), FF(11,9,2,2), F(9), DX(9),
1PSIM(11,9,2,2), U(11,9,2,2), V(11,9,2,2), UO(11,9,2,2), VO(11,9,2,2),
2DMDT1(11,9,2,2), DMDT2(11,9,2,2), THSFC(2), U1(12), V1(12), DMDT(12), ALAT
3(12), ALONG(12), DY, SOULAT, WELONG, NI, NJ, AK, NL, ICAFE, DELLAT, DT, DELONG
4AAI, AAJ, ALATC, ALONGC, AI, INC, AI, INC, SUMXO, SUMYO, SCMDT1, YD, XD, NLDAY,
5AAI, AAJ, ALATC, ALONGC, AI, INC, AI, INC, SUMXO, SUMYO, SCMDT1, YD, XD, NLDAY,
6I, J, PFINAL, AMINIT, AKINIT, I, INC, AI, INC, SUMXO, SUMYO, SCMDT1, YD, XD, NLDAY,
7, PINIT, PFINAL, OMEGA, P(11,9,2,2), VORIT(11,9,2,2), IMET1, IMET2, PSAT
8, COUNT, X(12), Y(12), MODCUR, SHDEF(11,9,2,2), STAB(11,9,2,2), Z(11,9,2,2),
9DIV(11,9,2,2), STDEF(11,9,2,2), VORIT(11,9,2,2), AVCR(11,9,2,2), ENGI
*, SPD(2), CRS(2), SMU(2), SMV(2), Q(11,9,2,2), VOFINL, DFINL, VCINT, DINIT,
1RH(11,9,2,2), Q(11,9,2,2), VOFINL, DFINL, VCINT, DINIT,

```

TRJ07170
TRJ07180
TRJ07190
TRJ07200
TRJ07210
TRJ07220
TRJ07230
TRJ07240
TRJ07250
TRJ07260
TRJ07270
TRJ07280
TRJ07290
TRJ07300
TRJ07310
TRJ07320
TRJ07330
TRJ07340
TRJ07350
TRJ07360
TRJ07370


```

2T(11,9,2,2),TD(11,9,2,2),E(11,9,2,2),ES(11,9,2,2),Z(11,9,2,12)
3,STAB1,STABF,PVORT1,PVORTF,PODIF,PODIF
C 1000 FORMAT(1H1)
C****
C SET 85 % DIFFERENCE BETWEEN SPECIFIC HUMIDITY AND SATURATED
C SPECIFIC HUMIDITY
C****
ALFAQ = 0.85
NNK=NK-1
NNI=NI-1
NNJ=NJ-1
DO 99 K=1,NK
5 C****
C COUNTER FOR GRAPHIC DISPLAY
C****
COUNT =1
DO 99 J=2,NAJ
DO 99 I=2,NAI
AI=I
AJ=J
AK=K
SUMXD=0.0
SUMYD=0.0
IZ=I
JZ = J
SDMDT1=0.0
C****
C BEGIN LCOP TO EVALUATE FIRST 1.5 HOUR TRAJECTORIES
C COMPUTE INITIAL DISPLACEMENT IN METERS
C****
XD = U0(I,J,K)*450.
YD = V0(I,J,K)*450.
NLDAY=(NL-1)*12
AAI=AI
AAJ=AJ
ALATO = SOULAT + DELLAT*(AAJ-1.)
ALONG = WELONG - DELCNG*(AAI-1.)
C
WRITE(6,1000)
WRITE(6,19) ALATO,ALONGO,THSFC(K)
19 FORMAT(2X,'KINEMATIC TRAJECTORIES AT 7.5 MINS INTERVALS BEGINNING
1 AT LATITUDE = ',F6.2,' AND AT LONGITUDE = ',F7.2,' FOR THETA = ',
2 F6.1,/,/)
WRITE(6,20)
20 FORMAT(3X,'TIME STEP',5X,'LATITUDE',5X,'LONGITUDE',6X,'U',11X,'V',
114X,/,)
WRITE(6,21) ALATO,ALONGC,U0(I,J,K),V0(I,J,K),ZO(I,J,K)

```

```

TRJ07380
TRJ07381
TRJ07390
TRJ07400
TRJ07410
TRJ07420
TRJ07430
TRJ07440
TRJ07450
TRJ07460
TRJ07470
TRJ07480
TRJ07490
TRJ07500
TRJ07510
TRJ07520
TRJ07530
TRJ07540
TRJ07550
TRJ07560
TRJ07570
TRJ07580
TRJ07590
TRJ07600
TRJ07610
TRJ07620
TRJ07630
TRJ07640
TRJ07650
TRJ07660
TRJ07670
TRJ07680
TRJ07690
TRJ07700
TRJ07710
TRJ07720
TRJ07730
TRJ07740
TRJ07750
TRJ07760
TRJ07770
TRJ07780
TRJ07790
TRJ07800
TRJ07810
TRJ07820
TRJ07830
TRJ07840

```



```

21 FCRMAT(10X,'0',7X,F5.2,7X,F6.2,6X,F6.1,6X,F6.1,9X,F8.2)
C****
C BEGIN DO LOOP TO COMPUTE AND PRINTOUT KINEMATIC TRAJECTORIES
C****
L=1
C****
C COMPUTE INITIAL VALUES FOR VARIOUS PARAMETERS ON THE TRAJECTORY.
C TEMP.,SPECIFIC HUMIDITY,SAT.SPECIFIC HUMIDITY,VORTICITY,DIVERGENCE
C WIND VELOCITY,PRESSURE,MONT.STREAM FUNC., KINETIC ENERGY
C STATIC STABILITY AND POTENTIAL VORTICITY.
C****
TINIT = T(I,J,K,L) + 273.16
QINIT = Q(I,J,K,L)
QSINIT = QS(I,J,K,L)
VOINIT = AVORT(I,J,K,L)
DINIT = DIV(I,J,K,L)
PINIT = P(I,J,K,L)
AMINIT = PSIM(I,J,K,L)
AKINIT = 5*(FF(I,J,K,L))**2
STABI = STAB(I,J,L)
PVORTI = STABI*VOINT*1000.0
DO 98 L=1,NLDAY
SUMXD=SUMXD+XD
SUMYD=SUMYD+YD
C****
C AIINC AND AJINC ARE THE NUMBER OF GRID POINTS THE TRAJECTORIES ARE
C DISPLACED FROM THE ORIGINAL I,J GRID POINT
C****
AIINC = 2.*SUMXD/(DX(J) + DX(JZ))
AJINC=SUMYD/DY
C****
C ROUTINE TO SEE IF TRAJECTORY HAS LEFT THE FIELD
C****
ANJ = NJ
ANI = NI
TESTAI = AAI + AIINC
TESTAJ = AAJ + AJINC
IJZ=TESTAI
IF(TESTAJ .LT. 1.) GO TO 1
IF(TESTAJ .GT. 1.) GO TO 1
IF(TESTAI .LT. 1.) GO TO 1
IF(TESTAI .GT. 1.) GO TO 1
C
3 GO TO 4
1 WRITE(6,2) IZ,JZ,L
2 FORMAT(' TRAJECTORY TERMINATES AT IZ = ',I3,' JZ = ',I3,' ANDTRJ08300
TRJ07850
TRJ07860
TRJ07870
TRJ07880
TRJ07890
TRJ07900
TRJ07910
TRJ07920
TRJ07930
TRJ07931
TRJ07940
TRJ07950
TRJ07960
TRJ07970
TRJ07980
TRJ07990
TRJ08000
TRJ08010
TRJ08020
TRJ08030
TRJ08031
TRJ08032
TRJ08040
TRJ08050
TRJ08060
TRJ08070
TRJ08080
TRJ08090
TRJ08100
TRJ08110
TRJ08120
TRJ08130
TRJ08140
TRJ08150
TRJ08160
TRJ08170
TRJ08190
TRJ08200
TRJ08210
TRJ08220
TRJ08230
TRJ08240
TRJ08250
TRJ08260
TRJ08270
TRJ08280
TRJ08290

```



```

1 AT L = ' , I3)
C****
C THE NEXT CARDS ARE FOR THE CALL DRAW STATEMENT ROUTINE TO PRINT
C OUT THE TRAJECTORIES THAT ARE LESS THAN 12 POINTS. ICK IS JUST
C NAME OF COUNTER TO KEEP TRACK PROGRAM POSITION. SINCE NUMBER OF
C POINTS TO PLOT FOR CURVE IS ONE LESS THAN L COUNTER MUST SUBT. 1.
C****
L = L - 1
ICK = 5
GO TO 49
GO TO 99
CONTINUE
300
4
C****
C XDIST AND YDIST ARE THE DISTANCES CF THE TRAJECTORY POINT FROM THE
C NEW GRID POINTS IINC AND JINC
C****
XDIST = (TESTAI - IZ)*DX(JZ)
YDIST = (TESTAJ - JZ)*DY
C****
C FIND NEW WIND SPEEDS AT END POINT BY INTERPOLATION ROUTINE TO FIND
C GRID POINTS SURROUNDING TRAJECTORY POINT
C****
IF(XDIST .GE. 0. .AND. YDIST .GE. 0.) GO TO 45
IF(XDIST .GE. 0. .AND. YDIST .LT. 0.) GO TO 41
IF(XDIST .LT. 0. .AND. YDIST .GE. 0.) GO TO 42
IF(XDIST .LT. 0. .AND. YDIST .LT. 0.) GO TO 43
C****
C ROUTINE TO PUT THE NEW I AND J POINTS AT THE LOWER LEFT HAND CORNER
C OF BOX SURROUNDING THE TRAJECTORY POINT
C****
41 JZ = JZ - 1
YDIST = DY + YDIST
GO TO 45
C
42 IZ = IZ - 1
XDIST = DX(JZ) + XDIST
GO TO 45
C
43 IZ = IZ - 1
JZ = JZ - 1
YDIST = DY + YDIST
XDIST = DX(JZ) + XDIST
C****
C XDIST AND YDIST ARE NOW THE DISTANCES FROM THE LOWER LEFT GRID POINT
C COMPUTE U, V AND Z FOR END POINT OF TRAJECTORY
C****
45 U1(L) = U(IZ, JZ, K, L) + (U(IZ+1, JZ, K, L) - U(IZ, JZ, K, L))*(XDIST/DX(JZ)
1) + ((U(IZ, JZ+1, K, L) - U(IZ, JZ, K, L))*(DX(JZ) - XDIST))/(DY*DX(JZ)) +

```

TRJ08310
 TRJ08320
 TRJ08330
 TRJ08340
 TRJ08350
 TRJ08360
 TRJ08370
 TRJ08380
 TRJ08390
 TRJ08400
 TRJ08410
 TRJ08420
 TRJ08430
 TRJ08440
 TRJ08450
 TRJ08460
 TRJ08470
 TRJ08480
 TRJ08490
 TRJ08500
 TRJ08510
 TRJ08520
 TRJ08530
 TRJ08540
 TRJ08550
 TRJ08560
 TRJ08570
 TRJ08580
 TRJ08590
 TRJ08600
 TRJ08610
 TRJ08620
 TRJ08630
 TRJ08640
 TRJ08650
 TRJ08660
 TRJ08670
 TRJ08680
 TRJ08690
 TRJ08700
 TRJ08710
 TRJ08720
 TRJ08730
 TRJ08740
 TRJ08750
 TRJ08760
 TRJ08770
 TRJ08780


```

C      2 (U(IZ+1,JZ+1,K,L) - U(IZ+1,JZ,K,L))*(XDIST/(DY*DX(JZ)))*YDIST TRJ08790
      V1(L) = V(IZ,JZ,K,L) + (V(IZ+1,JZ,K,L) - V(IZ,JZ,K,L))*(XDIST/DX(JZ)) TRJ08800
      1Z)) + ((V(IZ,JZ+1,K,L) - V(IZ,JZ,K,L))*(DX(JZ)-XDIST)/(DY*DX(JZ)))* TRJ08810
      2 (V(IZ+1,JZ+1,K,L) - V(IZ+1,JZ,K,L))*(XDIST/(DY*DX(JZ)))*YDIST TRJ08820
      Z1(L) = Z(IZ,JZ,K,L) + (Z(IZ+1,JZ,K,L) - Z(IZ,JZ,K,L))*(XDIST/DX(JZ)) TRJ08830
      1Z)) + ((Z(IZ,JZ+1,K,L) - Z(IZ,JZ,K,L))*(DX(JZ)-XDIST)/(DY*DX(JZ)))* TRJ08840
      2 (Z(IZ+1,JZ+1,K,L) - Z(IZ+1,JZ,K,L))*(XDIST/(DY*DX(JZ)))*YDIST TRJ08850
      DMDT(L) = DMDT1(IZ,JZ,K) + (DMDT1(IZ+1,JZ,K) - DMDT1(IZ,JZ,K))*(XDIST TRJ08860
      1T/DX(JZ)) + ((DMDT1(IZ,JZ+1,K) - DMDT1(IZ,JZ,K))*(DX(JZ) - TRJ08870
      2XDIST)/(DY*DX(JZ)) + (DMDT1(IZ+1,JZ+1,K) - DMDT1(IZ+1,JZ,K))*(XDIST TRJ08880
      3T/(DY*DX(JZ)))*YDIST TRJ08890
      ALAT(L) = SOULAT + DELLAT*(JZ - 1. + YDIST/DY) TRJ08900
      ALONG(L) = WELONG - DELONG*(IZ - 1. + XDIST/DX(JZ)) TRJ08910
      ICK = 2 TRJ08920
      IF(L.EQ.12) GO TO 49 TRJ08930
      GO TO 50 TRJ08940
C**** TRJ08950
C      THIS ROUTINE IS DESIGNED TO MAKE A PLOT OF THE TRAJECTORIES TRJ08960
C      USING SUBROUTINE DRAW. IT WILL PLOT ALL TRAJECTORIES. TRJ08970
C      THE ROUTINE IS GOOD ONLY FOR IBM/360 AT USNPGS TRJ08980
C      DO 55 LL=1,L TRJ09000
      X(LL) = (ALAT(LL)-34.00)*4. TRJ09010
      Y(LL) = (ALONG(LL)-97.00)*4. TRJ09020
      CONTINUE TRJ09030
      IF(CCOUNT.EQ.1)MODCUR=1 TRJ09040
      IF(CCOUNT.EQ.2)MODCUR=2 TRJ09050
      IF(CCOUNT.EQ.63)MODCUR=3 TRJ09060
      IF(K.EQ.2) GO TO 71 TRJ09070
      IF(K.EQ.1) GO TO 70 TRJ09080
      70 CALL DRAW(L,X,Y,MODCUR,0,LABEL,ITITL1,1.0,1.0,0,0,2,2,8,10,1,1, LAST) TRJ09090
      GO TO 72 TRJ09100
      71 CALL DRAW(L,X,Y,MODCUR,0,LABEL,ITITL2,1.0,1.0,0,0,2,2,8,10,1,1, LAST) TRJ09110
      72 COUNT = CCOUNT + 1 TRJ09120
      IF(ICK.EQ.5) GO TO 300 TRJ09130
      CONTINUE TRJ09140
C      WRITE(6,51) L,ALAT(L),ALONG(L),U1(L),V1(L),Z1(L) TRJ09150
      FORMAT(08X,I3,7X,F5.2,7X,F6.1,6X,F6.1,9X,F8.2) TRJ09160
      SDMDT1 = SDMDT1 + DMDT(L) TRJ09170
      XD = U1(L)*450. TRJ09180
      YD = V1(L)*450. TRJ09190
      CONTINUE TRJ09200
C      51 TRJ09210
      TRJ09220
      TRJ09230
      TRJ09240
      TRJ09250
      TRJ09260

```



```

C**** IF(L .LT. 12) GO TO 98
C      COMPUTE FINAL KINETIC ENERGY
C****
C      FINALK = .5*(U1(L)**2 + V1(L)**2)
C
C      DELTAM = SDMOT1/12.
C****
C      COMPUTE FINAL MONT. STREAM FUNC.
C****
C      FINALM = PSIM(IZ,JZ,K,2) + (PSIM(IZ+1,JZ,K,2) -
1      PSIM(IZ,JZ,K,2))*{XDIST/DX(JZ)} + ({PSIM(IZ,JZ+1,K,2) -
2      PSIM(IZ,JZ,K,2)}*(DX(JZ)-XDIST)/(DY*DX(JZ)))+(PSIM(IZ+1,JZ+1,K,2)
3      - PSIM(IZ+1,JZ,K,2))*{XDIST/(DY*DX(JZ))}*YDIST
C****
C      COMPUTE ACCELERATION OF THE AIR PARCEL DURING THE TRAJECTORY
C****
C      VFINAL = SQRT(U1(L)**2 + V1(L)**2)
C      ACCEL = (VFINAL - VINIT)*2./3.
C****
C      COMPUTE FINAL PRESSURE
C****
C      PFINAL = P(IZ,JZ,K,2) + (P(IZ+1,JZ,K,2) -
1      P(IZ,JZ,K,2))*{XDIST/DX(JZ)} + ({P(IZ,JZ+1,K,2) -
2      P(IZ,JZ,K,2)}*(DX(JZ)-XDIST)/(DY*DX(JZ)))+(P(IZ+1,JZ+1,K,2)
3      - P(IZ+1,JZ,K,2))*{XDIST/(DY*DX(JZ))}*YDIST
C****
C      COMPUTE VERTICAL MOTION.
C****
C      OMEGA = (PFINAL - PINIT)* 2./3.
C****
C      COMPUTE FINAL STATIC STABILITY
C****
C      STABF = STAB(IZ,JZ,2) + (STAB(IZ+1,JZ,2) - STAB(IZ,JZ,2))*{XDIST
1/DX(JZ)} + ({STAB(IZ,JZ+1,2) - STAB(IZ,JZ,2)}*(DX(JZ)-XDIST)/
2(DY*DX(JZ)) + (STAB(IZ+1,JZ+1,2) - STAB(IZ+1,JZ,2))*{XDIST/(DY*
3DX(JZ))}*YDIST
C****
C      COMPUTE FINAL SPECIFIC HUMIDITY (GM/GM)
C****
C      QFINL = Q(IZ,JZ,K,2) + (Q(IZ+1,JZ,K,2) - Q(IZ,JZ,K,2))*{XDIST/DX
1(JZ)} + ({Q(IZ,JZ+1,K,2) - Q(IZ,JZ,K,2)}*(DX(JZ)-XDIST)/(DY*DX(JZ))
2) + (Q(IZ+1,JZ+1,K,2) - Q(IZ+1,JZ,K,2))*{XDIST/(DY*DX(JZ))}*YDIST
C****
C      COMPUTE FINAL SATURATED SPECIFIC HUMIDITY (GM/GM)
C****
C      QSFINL = QS(IZ,JZ,K,2) + (QS(IZ+1,JZ,K,2) - QS(IZ,JZ,K,2))*{XDIST
1/DX(JZ)} + ({QS(IZ,JZ+1,K,2) - QS(IZ,JZ,K,2)}*(DX(JZ)-XDIST)/(DY*

```

```

TRJC9270
TRJC9280
TRJC9290
TRJC9300
TRJC9310
TRJC9320
TRJC9330
TRJC9340
TRJC9350
TRJC9360
TRJC9370
TRJC9380
TRJC9390
TRJC9400
TRJC9410
TRJC9420
TRJC9430
TRJC9440
TRJC9450
TRJC9460
TRJC9470
TRJC9480
TRJC9490
TRJC9500
TRJC9510
TRJC9520
TRJC9530
TRJC9540
TRJC9550
TRJC9560
TRJC9561
TRJC9562
TRJC9563
TRJC9564
TRJC9565
TRJC9566
TRJC9567
TRJC9570
TRJC9580
TRJC9590
TRJC9600
TRJC9610
TRJC9620
TRJC9630
TRJC9640
TRJC9650
TRJC9660
TRJC9670

```



```

C *****
C COMPUTE CHANGE IN SPECIFIC HUMIDITY
C QDIF = QFINL - CINIT
C *****
C COMPUTE CHANGE IN DIVERGENCE
C *****
C DIVDIF = DFINL - DINIT
C *****
C COMPUTE CHANGE IN POTENTIAL VORTICITY
C *****
C POTDIF = PVCRTF - PVORTI
C
C WRITE(6,80) PINIT,PFINAL,OMEGA,ACCEL
C FORMAT(//,2X,'INITIAL P =',F5.1,'',FINAL P =',F5.1,'',OMEGA(MB/HR)
C 1=',F5.1,'',ACCELERATION(M/SEC-HR) =',F5.1,//)
C
C WRITE(6,81) QINIT,QFINL,QDIF,QSINIT,QSFINL
C FORMAT(//,2X,'INITIAL Q(GM/GM) =',F9.4,'',FINAL Q =',F9.4,'',CHANGE
C 1=',F9.4,'',INITIAL QS =',F9.4,'',FINAL QS =',F9.4,//)
C
C WRITE(6,82) VQINIT,VQFINL,VORDIF
C FORMAT(//,2X,'INITIAL VORTICITY(10**-4) =',F9.3,'',FINAL VORTICITY
C 1(10**-4) =',F9.3,2X,'CHANGE =',F9.3,//)
C
C WRITE(6,83) DINIT,DFINL,DIVDIF
C FORMAT(//,2X,'INITIAL DIVERGENCE(10**-4) =',F9.3,'',FINAL DIVERGENCE
C 1(10**-4) =',F9.3,2X,'CHANGE =',F9.3,//)
C
C WRITE(6,84) AMINIT,FINALM
C FORMAT(//,2X,'INITIAL MONT. STR. FUNC. =',F9.3,'',FINAL MONT. STR.
C 1FUNC. =',F9.3,//)
C
C WRITE(6,85) AKINIT,FINALK
C FORMAT(//,2X,'INITIAL KINETIC ENERGY =',F9.3,'',FINAL KINETIC ENERG
C 1Y =',F9.3,//)
C
C WRITE(6,87) PSAT,TIMSAT
C FORMAT(//,2X,'SATURATED PRESSURE =',F8.2,2X,'TIME OF SATURATION
C 1 =',F7.3,//)
C
C WRITE(6,88) ENGIT,ENGFL,ENGDF
C FORMAT(//,2X,'INITIAL ENERGY(10**7 ERG/GM) =',F9.3,2X,'FINAL ENERG
C 1Y =',F9.3,2X,'CHANGE =',F9.3,//)
C
C WRITE(6,89) STABI,STABF
C FORMAT(//,2X,'INITIAL STABILITY =',F9.3,'',FINAL STABILITY =',
C 1F9.3,//)

```

```

TRJ1010102
TRJ1010103
TRJ1010104
TRJ1010110
TRJ1010120
TRJ1010130
TRJ1010140
TRJ1010141
TRJ1010142
TRJ1010143
TRJ1010144
TRJ1010150
TRJ1010160
TRJ1010170
TRJ1010180
TRJ1010190
TRJ1010200
TRJ1010210
TRJ1010220
TRJ1010230
TRJ1010240
TRJ1010250
TRJ1010260
TRJ1010270
TRJ1010280
TRJ1010290
TRJ1010300
TRJ1010310
TRJ1010320
TRJ1010340
TRJ1010350
TRJ1010360
TRJ1010370
TRJ1010380
TRJ1010390
TRJ1010400
TRJ1010410
TRJ1010420
TRJ1010430
TRJ1010440
TRJ1010450
TRJ1010460
TRJ1010470
TRJ1010480
TRJ1010481
TRJ1010482
TRJ1010483
TRJ1010484

```



```

      C
      90      WRITE(6,9C) PVCRTI,PVCRIFF,POTDIF
      1F9.3,' FINAL POT. VORT.= ',F9.3,' CHANGE= ',F9.3,/)
      C
      86      WRITE(6,86) LAST
      98      FORMAT(//,2X,'LAST =',I2,/)
      CONTINUE
      C****
      C      IF IT IS DESIRED TO ADJUST THE KINEMATIC TRAJECTORIES FROM THE
      C      TOTAL ENERGY EQUATION, "CALL ENERGY" WOULD BE INSERTED AT THIS
      C      POINT.
      C****
      99      CONTINUE
      C
      C      RETURN
      C      END

```

TRJ10485
 TRJ10486
 TRJ10487
 TRJ10488
 TRJ10490
 TRJ10500
 TRJ10510
 TRJ10520
 TRJ10530
 TRJ10540
 TRJ10550
 TRJ10560
 TRJ10580
 TRJ10590
 TRJ10600
 TRJ10610
 TRJ10620

```

      C****
      C      SUBROUTINE ENERGY
      C      THIS SUBROUTINE ITERATIVELY ADJUSTS THE KINEMATIC TRAJECTORIES
      C      FROM THE TOTAL ENERGY EQUATION EXPRESSED IN ISENTROPIC
      C      COORDINATE SYSTEM.
      C****
      C      REAL*8 ITITL1
      C      REAL*8 ITITL2

```

ENG10630
 ENG10640
 ENG10650
 ENG10660
 ENG10670
 ENG10680
 ENG10690
 ENG10700
 ENG10710
 ENG10720
 ENG10730
 ENG10740
 ENG10750
 ENG10760
 ENG10770
 ENG10780
 ENG10790
 ENG10800
 ENG10810
 ENG10820
 ENG10830
 ENG10840
 ENG10850
 ENG10860
 ENG10870
 ENG10880

```

      COMMON ITITL1(12), ITITL2(12), DD(11,9,2,2), FF(11,9,2,2), F(9), DX(9),
      1PSIM(11,9,2,2), U(11,9,2,12), V(11,9,2,12), UO(11,9,2,1), VO(11,9,2,1),
      2DMDT1(11,9,2,2), DMDT2(11,9,2,2), THSFC(2), U1(12), V1(12), DMDT(12), ALAT
      3(12), ALONG(12), CY, SCULAT, WELONG, NI, NJ, NK, NL, IDATE, DELCAT, DT, DELONG
      4, ANJ, U12, V12, NNK, NNI, NNJ, AI, AJ, AK, SUMXD, SUMYD, SDMDT1, YD, XD, NLDAY,
      5AAI, AAJ, ALATC, ALONGC, AIINC, AJINC, XDI, YDI, XDI, YDI, XDI, YDI, XDI, YDI,
      6II, JI, JI, JI, JI, JI, JI, JI, JI, JI, JI, JI, JI, JI, JI, JI, JI, JI, JI, JI,
      7, PINIT, PFINIT, AMINIT, AKINIT, FINALK, DELTAM, I, J, K, L, Z, Z1(12), PSAT
      8, COUNT, X(12), Y(12), MODCUR, P(11,9,2,2), VINIT, VFINAL, ACCEL, IMET1, IMET2
      9CIV(11,9,2,2), STDEF(11,9,2,2), VORI(11,9,2,2), STAR(11,9,2,2), ZO(11,9,2,2),
      * SPD(2), CRS(2), SMU(2), SMV(2), QS(11,9,2,2), QSINIT, QFINL, QSFINL,
      1RH(11,9,2,2), Q(11,9,2,2), VOFINL, DFINL, VCINT, DINIT, DIFF, QINIT,
      2T(11,9,2,2), TD(11,9,2,2), E(11,9,2,2), ES(11,9,2,2), Z(11,9,2,2),
      3, STABI, STABF, PVCRTI, PVCRIFF, POTDIF, QCIF

```

```

      C****
      C      EVALUATE ENERGY INTEGRAL FOR KINEMATIC TRAJECTORY
      C****
      C****
      C****

```

C****
 C****
 C****


```
C*****  
C      COEFFICIENT FOR OPTIMUM FIRST GUESS.  
C  
C      ALPHA = .6  
  
C      NCOUNT = 0  
L=12  
AKINIT = .001*AKINIT  
FINALK = .001*FINALK  
EPSPM = AMINIT - FINALM - (FINALK - AKINIT) + DELTAM  
C****  
C      COMPUTE FRGM EPSPM THE DISTANCE TO CORRECT TRAJECTORY  
C      FOLLOWING DELTA QUANTITIES ARE IN METERS  
C  
C      DELTAN = (-EPSPM/(F(J)*SQRT(U1(L)**2+ V1(L)**2))*10**8)*ALPHA  
24  
C****  
C      DELTAX IS IN THE SAME DIRECTION AS DELLAM AS GIVEN HERE  
C  
C      DELTAX = DELTAN*V1(L)/SQRT(U1(L)**2 + V1(L)**2)  
DELTAY = DELTAN*U1(L)/SQRT(U1(L)**2 + V1(L)**2)  
C****  
C      COMPUTE DISPLACEMENT IN DEGREES LATITUDE AND LONGITUDE  
C  
C      DELLAM={DELTAX/(6.371*10**6*COS(ALAT(L)/57.2958))}*57.2958  
DELPHI=(DELTAY/(6.371*10**6))*57.2958  
C  
WRITE(6,501)  
FORMAT(2X,'EPSPM          FINAL M    INITIAL M    DELTAM',//)  
501 WRITE(6,502) EPSPM,FINALM,AMINIT,DELTAM  
502 FORMAT(1X,F7.2,6X,F7.2,6X,F7.2,6X,F7.2,//)  
WRITE(6,503)  
503 FORMAT(2X,'DELTAN        DELTAX       DELTAY     DELLAM   DELPHI' ,//)  
WRITE(6,504) DELTAN,DELTAX,DELTAY,CELLAM,DELPHI  
504 FORMAT(2X,3F9.0,2F8.2//)  
IF(ABS(EPSM).LT. .05) GO TC 78  
IF(FINALK.LT. .0045) GO TO 78  
  
C      XSUM=0.0  
YSUM=0.0  
  
C****  
C      SSUM IS THE TOTAL DISPLACEMENT DETERMINED BY THE INTERPOLATED WIND  
FIELD FROM THE ENERGY ITERATION AT THE NEW POINTS.  
C  
C      SSUM = 0.0  
  
C****  
C      BEGIN LOOP TO ADJUST TRAJECTORIES FROM ABOVE ENERGY EQUATION  
RESULTS.  
C  
C      DO 80 L=1,NLDAY
```



```

C***      AL=L
C          ALAT(L) = ALAT(L) + (AL/12.)*DELPHI
C          ALONG(L) = ALONG(L) + (AL/12.)*DELLAM
C
C          ROUTINE TO CCNVERT LATITUDES AND LONGITUDES BACK INTO I,J FIELD.
C          ZJ AND ZI ARE RELATIVE GRID POINT DISTANCES FROM THE ORIGIN, IZ
C          AND JZ ARE THE COORDINATES OF THE LOWER LEFT HAND CORNER OF THE
C          BOX SURROUNDING THE PARCEL, XDIST AND YDIST ARE DEFINED AS BEFORE.
C***
C          ZJ = (ALAT(L) - SOULAT + DELLAT)/DELLAT
C          ZI = (WELONG - ALONG(L) + DELONG)/DELONG
C          ANI = NI
C          ANJ = NJ
C          JZ = ZJ
C          AJZ = JZ
C          YDIST = (ZJ - AJZ)*DY
C
C          IZ = ZI
C          AIZ = IZ
C          XDIST = (ZI - AIZ)*DX(JZ)
C
C          IF(AIZ .LT. 1.) GO TO 76
C          IF(AIZ .GT. ANI) GO TO 76
C          IF(AJZ .GT. ANJ) GO TO 76
C          IF(AJZ .LT. 1.) GO TO 76
C          GO TO 555
C          WRITE(6,77) IZ,JZ,L
C          FORMAT(2X,'TRAJECTORY TERMINATES AT IZ = ',I3,' JZ = ',I3,' AND
C          1  IAT L= ',I3,')
C          GO TO 78
C          CONTINUE
C          555
C***
C          COMPUTATION OF WIND SPEEDS AT NEW TRAJECTORY POINTS
C***
C          U1(L)=U(IZ,JZ,K,L) + (U(IZ+1,JZ,K,L) - U(IZ,JZ,K,L))*(XDIST/DX(JZ)
C          1) + ((U(IZ,JZ+1,K,L) - U(IZ,JZ,K,L))*(DX(JZ)-XDIST)/(DY*DX(JZ)) +
C          2 (U(IZ+1,JZ+1,K,L) - U(IZ+1,JZ,K,L))*(XDIST/(DY*DX(JZ)))*YDIST
C
C          V1(L) = V(IZ,JZ,K,L) + (V(IZ+1,JZ,K,L) - V(IZ,JZ,K,L))*(XDIST/DX(J
C          1Z)) + ((V(IZ,JZ+1,K,L) - V(IZ,JZ,K,L))*(DX(JZ)-XDIST)/(DY*DX(JZ)) +
C          2 (V(IZ+1,JZ+1,K,L) - V(IZ+1,JZ,K,L))*(XDIST/(DY*DX(JZ)))*YDIST
C
C          XINC = 450.*U1(L)
C          YINC = 450.*V1(L)
C          XSUM=XSUM+XINC
C          YSUM = YSUM + YINC
C          SSUM = SSUM + SQRT(XINC**2 + YINC**2)
C

```



```

80 CONTINUE
C***
C ROUTINE TO MAKE DISTANCE CORRECTION
C SMEAS IS THE STREAMLINE DISPLACEMENT DETERMINED FROM THE
C COORDINATES OF THE ENERGY EQUATION ITERATED TRAJECTORY.
C***
      L=1
      SMEAS = 0.0
      DSTRAJ = SQRT((6371000.*(ALAT(L)-ALATO)/57.2958)**2 +
1 (6371000.*COS(ALAT(L)/57.2958)*(ALONG(L)-ALONGO)/57.2958)**2)
C
      DO 809 L=2,NLDAY
      SMEAS = SMEAS + DSTRAJ
      DSTRAJ = SQRT((6371000.*(ALAT(L)-ALAT(L-1))/57.2958)**2 +
1 (6371000.*COS(ALAT(L)/57.2958)*(ALONG(L)-ALONG(L-1))/57.2958)**2)
      SMEAS = SMEAS + DSTRAJ
C***
C COMPUTE DIFFERENCE BETWEEN DISPLACEMENT AT THE NEW ITERATION
C COMPUTED FROM THE WIND FIELD AND FROM THE GEOMETRICALLY DETERMINED
C POINTS.
C***
      DELS = (SSUM - SMEAS)*ALPHA
      L=L+1
C***
C SIGN HAS BEEN CHANGED TO MINUS IN DELLAM EXPRESSION FOR A CHECK.
C***
      DELLAM=(57.2958*DELS*U1(L)/SQRT(U1(L)**2 + V1(L)**2))/(6371000.*
1 COS(ALAT(L)/57.2958))*(-1.)
      DELPHI=(57.2958*DELS*V1(L)/SQRT(U1(L)**2+V1(L)**2))/6371000.
C
      WRITE(6,806)
      FORMAT(2X,1 DELS SSUM SMEAS DELLAM DELPHI)
      WRITE(6,807) DELS,SSUM,SMEAS,DELLAM,DELPHI
      FORMAT(2X,3F10.0,2F6.2)
C
      SDMDT1 = 0.0
      DO 81 L=1,NLDAY
      AL=L
      ALAT(L)=ALAT(L) + (AL/12.)*DELPHI
      ALONG(L) = ALONG(L) + (AL/12.)*DELLAM
C***
C TERM IS MINUS IN ALONG EXPRESSION BECAUSE LONG INCREASES WITH
C DECREASING I VALUES.
C
      ROUTINE TO CONVERT LAT + LONG BACK TO I,J FIELD
C***
      ZJ=(ALAT(L) - SOULAT + DELLAT)/DELLAT
      JZ=ZJ

```

ENGL11860
 ENGL11870
 ENGL11880
 ENGL11890
 ENGL11900
 ENGL11910
 ENGL11920
 ENGL11930
 ENGL11940
 ENGL11950
 ENGL11960
 ENGL11970
 ENGL11980
 ENGL11990
 ENGL12000
 ENGL12010
 ENGL12020
 ENGL12030
 ENGL12040
 ENGL12050
 ENGL12060
 ENGL12070
 ENGL12080
 ENGL12090
 ENGL12100
 ENGL12110
 ENGL12120
 ENGL12130
 ENGL12140
 ENGL12150
 ENGL12160
 ENGL12170
 ENGL12180
 ENGL12190
 ENGL12200
 ENGL12210
 ENGL12220
 ENGL12230
 ENGL12240
 ENGL12250
 ENGL12260
 ENGL12270
 ENGL12280
 ENGL12290
 ENGL12300
 ENGL12310
 ENGL12320
 ENGL12330


```

C
YDIST = (ZJ - JZ)*DY
ZI = (WELONG - ALONG(L) + DELONG)/DELONG
IZ=ZI
XDIST = (ZI - IZ)*DX(JZ)
IF (IZ .LT. 1) GO TO 76
IF (IZ .GT. NN1) GO TO 76
IF (JZ .LT. 1) GO TO 76
IF (JZ .GT. NNJ) GO TO 76
C
U1(L)=U(IZ,JZ,K,L) + (U(IZ+1,JZ,K,L) - U(IZ,JZ,K,L))*(XCIST/DX(JZ)
1) + ((U(IZ,JZ+1,K,L) - U(IZ,JZ,K,L))*(CX(JZ)-XDIST)/(DY*DX(JZ)) +
2 (U(IZ+1,JZ+1,K,L) - U(IZ+1,JZ,K,L))*(XDIST/(DY*DX(JZ)))*YDIST
C
V1(L) = V(IZ,JZ,K,L) + (V(IZ+1,JZ,K,L) - V(IZ,JZ,K,L))*(XDIST/DX(J
1Z)) + ((V(IZ,JZ+1,K,L) - V(IZ,JZ,K,L))*(DX(JZ)-XDIST)/(DY*DX(JZ)) +
2 (V(IZ+1,JZ+1,K,L) - V(IZ+1,JZ,K,L))*(XDIST/(DY*DX(JZ)))*YDIST
C
DMDT(L) = DMDT1(IZ,JZ,K) + (DMDT1(IZ+1,JZ,K) - DMDT1(IZ,JZ,K))*(XDIS
1T/DX(JZ)) + ((DMDT1(IZ,JZ+1,K) - DMDT1(IZ,JZ,K))*(DX(JZ) -
2XDIST)/(DY*DX(JZ)) + (DMDT1(IZ+1,JZ+1,K) - DMDT1(IZ+1,JZ,K))*(XDIS
3T/(DY*DX(JZ)))*YDIST
C
SDMDT1 = SDMDT1 + DMDT(L)
C
81 CONTINUE
C
L=NLDAY
NCOUNT = NCCUNT + 1
DELTAM = SDMDT1/12.
C****
ITERATION TO ADJUST TRAJECTORY IS NOW COMPLETE FOR STREAM FUNCTION
AND FOR DISTANCE. CHECK ENERGY INTEGRAL FOR CONVERGENCE.
C****
FINALM = PSIM(IZ,JZ,K,2) + (PSIM(IZ+1,JZ,K,2) -
1 PSIM(IZ,JZ,K,2))*(XDIST/DX(JZ)) + ((PSIM(IZ,JZ+1,K,2) -
2 PSIM(IZ,JZ,K,2))*(DX(JZ)-XDIST)/(DY*DX(JZ)) + (PSIM(IZ+1,JZ+1,K,2)
3 - PSIM(IZ+1,JZ,K,2))*(XDIST/(DY*DX(JZ)))*YDIST
C
FINALK = .0005*(U1(L)**2 + V1(L)**2)
C
EPSM = AMINIT - FINALM - (FINALK - AKINIT) + DELTAM
C
WRITE(6,8880) EPSM,AMINIT,FINALM,FINALK,AKINIT,DELTAM
8880 FORMAT('/',',',*DIAGNOSTIC*,6F12.2,/)
C
IF(ABS(EPSM) .LT. .05) GO TO 88

```

ENG12340
 ENG12350
 ENG12360
 ENG12370
 ENG12380
 ENG12390
 ENG12400
 ENG12410
 ENG12420
 ENG12430
 ENG12440
 ENG12450
 ENG12460
 ENG12470
 ENG12480
 ENG12490
 ENG12500
 ENG12510
 ENG12520
 ENG12530
 ENG12540
 ENG12550
 ENG12560
 ENG12570
 ENG12580
 ENG12590
 ENG12600
 ENG12610
 ENG12620
 ENG12630
 ENG12640
 ENG12650
 ENG12660
 ENG12670
 ENG12680
 ENG12690
 ENG12700
 ENG12710
 ENG12720
 ENG12730
 ENG12740
 ENG12750
 ENG12760
 ENG12770
 ENG12780
 ENG12790
 ENG12800
 ENG12810


```

C      IF(NCCUNT .GT. 9) GO TO 88
C      GO TO 24
C      88 CONTINUE
C      VFINAL = SQRT(U1(L)**2 + V1(L)**2)
C      ACCEL = (VFINAL - VINIT)*2./3.
C
C      PFINAL = P(IZ,JZ,K,2) + (P(IZ+1,JZ,K,2) -
1 P(IZ,JZ,K,2))*XDIST/DX(JZ)) + ((P(IZ,JZ+1,K,2) -
2 P(IZ,JZ,K,2))*DX(JZ)-XDIST)/(DY*DX(JZ)) + (P(IZ+1,JZ+1,K,2) -
3 - P(IZ+1,JZ,K,2))*XDIST/(DY*DX(JZ)))*YDIST
C      OMEGA = (PFINAL - PINIT)* 2./3.
C
C      STABF = STAB(IZ,JZ,2) + (STAB(IZ+1,JZ,2) - STAB(IZ,JZ,2))*(XDIST
1/DX(JZ)) + ((STAB(IZ,JZ+1,2) - STAB(IZ,JZ,2))*(DX(JZ)-XDIST)/
2(DY*DX(JZ)) + (STAB(IZ+1,JZ+1,2) - STAB(IZ+1,JZ,2))*(XDIST/(DY*
3DX(JZ)))*YDIST
C
C      QFINL = Q(IZ,JZ,K,2) + (Q(IZ+1,JZ,K,2) - Q(IZ,JZ,K,2))*(XDIST/DX
1(JZ)) + ((Q(IZ,JZ+1,K,2) - Q(IZ,JZ,K,2))*(DX(JZ)-XDIST)/(DY*DX(JZ))
2) + (Q(IZ+1,JZ+1,K,2) - Q(IZ+1,JZ,K,2))*(XDIST/(DY*DX(JZ)))*YDIST
C
C      QSFINL = QS(IZ,JZ,K,2) + (QS(IZ+1,JZ,K,2) - QS(IZ,JZ,K,2))*(XDIST
1/DX(JZ)) + ((QS(IZ,JZ+1,K,2) - QS(IZ,JZ,K,2))*(DX(JZ)-XDIST)/(DY*
2DX(JZ)) + (CS(IZ+1,JZ+1,K,2) - CS(IZ+1,JZ,K,2))*(XDIST/(DY*DX(JZ)
3))*YDIST
C
C      VOFINL = AVORT(IZ,JZ,K,2) + (AVORT(IZ+1,JZ,K,2) - AVORT(IZ,JZ,K,2)
1)*(XDIST/DX(JZ)) + ((AVORT(IZ,JZ+1,K,2) - AVORT(IZ,JZ,K,2))*(DX(JZ)-
2XDIST)/(DY*DX(JZ)) + (AVORT(IZ+1,JZ+1,K,2) - AVORT(IZ+1,JZ,K,2)
3)*(XDIST/(DY*DX(JZ)))*YDIST
C
C      DFINL = DIV(IZ,JZ,K,2) + (DIV(IZ+1,JZ,K,2) - DIV(IZ,JZ,K,2))*
1(XDIST/DX(JZ)) + ((DIV(IZ,JZ+1,K,2) - DIV(IZ,JZ,K,2))*(DX(JZ)-
2XDIST)/(DY*DX(JZ)) + (DIV(IZ+1,JZ+1,K,2) - DIV(IZ+1,JZ,K,2))*
3(XDIST/(DY*DX(JZ)))*YDIST
C
C      PVORTF = STABF*VOFINL*1000.0
C
C      TIMSAT = ((PSAT-PINIT)/(PFINAL-PINIT))*1.5
C
C      ENGFL = FINALM + 1111.48*QFINL + FINALK/1000.
C
C      DIVDIF = DFINL - DINIT
C      VORDIF = VOFINL - VINIT
C      ENGDF = ENGFL - ENGIT
C      QDIF = QFINL - QINIT

```



```

C
  98 WRITE(6,98) ENGIT,ENGFL,ENGDIFF
    1Y =',F9.3,2X,'INITIAL ENERGY(10**7 ERG/GM) =',F9.3,2X,'FINAL ENERGY(10**7 ERG/GM) =',F9.3,2X,','
C
  66 WRITE(6,66) STABI,STABF
    1F9.3,2X,'INITIAL STABILITY= ',F9.3,2X,'FINAL STABILITY= ',F9.3,2X,','
C
  89 WRITE(6,89) PVORTI,PVORTF,POTDIF
    1F9.3,2X,'INITIAL POT. VORT=(10**10 DEG. K SEC CM/GM)= ',F9.3,2X,'FINAL POT. VORT.= ',F9.3,2X,'CHANGE= ',F9.3,2X,','
C****
C    THIS SUBROUTINE RETURNS TO THE END OF TRAJ, NOT MAIN
C****
  78 CONTINUE
    RETURN
  END
ENG13690
ENG13700
ENG13710
ENG13720
ENG13721
ENG13722
ENG13723
ENG13724
ENG13725
ENG13726
ENG13727
ENG13728
ENG13730
ENG13740
ENG13750
ENG13760
ENG13770

```


DISTRIBUTION

Agency	No. of Copies
Naval Weapons Center China Lake, California Code 602	5
Defense Documentation Center Cameron Station, Bldg. 5 Alexandria, Virginia 22314	20
Library Naval Postgraduate School Monterey, California	2
Dean of Research Administration Naval Postgraduate School Monterey, California	2
Professor R. L. Alberty Department of Meteorology Naval Postgraduate School Monterey, California	71

DOCUMENT CONTROL DATA - R & D

(Security classification of title, body of abstract and indexing annotation must be entered when the overall report is classified)

1. ORIGINATING ACTIVITY (Corporate author) Naval Postgraduate School Monterey, California		2a. REPORT SECURITY CLASSIFICATION Unclassified	
		2b. GROUP	
3. REPORT TITLE AN ANALYSIS OF A SEVERE LOCAL STORM USING ISENTROPIC TRAJECTORIES			
4. DESCRIPTIVE NOTES (Type of report and, inclusive dates) Technical Report 1969			
5. AUTHOR(S) (First name, middle initial, last name) Ronnie L. Alberty Kenneth Lee Van Sickle			
6. REPORT DATE 15 August 1969		7a. TOTAL NO. OF PAGES 138	7b. NO. OF REFS 24
8a. CONTRACT OR GRANT NO. b. PROJECT NO. 80143 c. d.		9a. ORIGINATOR'S REPORT NUMBER(S) NPS-51A19081A 9b. OTHER REPORT NO(S) (Any other numbers that may be assigned this report)	
10. DISTRIBUTION STATEMENT This document has been approved for public release and sale; its distribution is unlimited.			
11. SUPPLEMENTARY NOTES This project funded by: Naval Weapons Center China Lake, California, Code 602		12. SPONSORING MILITARY ACTIVITY Naval Postgraduate School Monterey, California	
13. ABSTRACT One and one-half hour isentropic trajectories obtained from an objective computer technique for the 308K, 312K, 320K and 332K isentropic surfaces are investigated for the May 28, 1967, severe local storm case in the National Severe Storm Laboratory (NSSL) network. In conjunction with the trajectories, air parcel properties of vertical motion, acceleration, divergence, vorticity, static stability and total energy have been studied with respect to development, growth, movement and decay of the storm system. Basic assumptions are that the flow is frictionless and adiabatic over the entire grid. The results show that the observed winds do provide some skill in formulating isentropic trajectories which demonstrate the presence of storm activity in the specific region. The investigation of a mesoscale inertial-gravity wave having a wave length of 150 KM, period of 3 hours and phase speed of 14 m sec^{-1} is also presented, with its possible correlation to the onset of the severe storm.			

14

KEY WORDS

LINK A

LINK B

LINK C

ROLE

WT

ROLE

WT

ROLE

WT

Isentropic Trajectories
Severe Storm
Mesoscale Analysis

DUDLEY KNOX LIBRARY



3 2768 00396456 0